ANALYSIS AND DESIGN OF HIGH STRENGTH CONCRETE COLUMNS SUBJECTED TO COMPRESSION AND BIAXIAL BENDING

BY

NIZAR ABDUL-HAMID YOUSEF ASSI

A Thesis Presented to the
DEANSHIP OF GRADUATE STUDIES

KING FAHD UNIVERSITY OF PETROLEUM & MINERALS

DHAHRAN, SAUDI ARABIA

In Partial Fulfillment of the
Requirements for the Degree of

MASTER OF SCIENCE

In

CIVIL ENGINEERING

MAY 2015

KING FAHD UNIVERSITY OF PETROLEUM & MINERALS

DHAHRAN- 31261, SAUDI ARABIA

DEANSHIP OF GRADUATE STUDIES

This thesis, written by **Nizar Abdul-Hamid Yousef Assi** under the direction his thesis advisor and approved by his thesis committee, has been presented and accepted by the Dean of Graduate Studies, in partial fulfillment of the requirements for the degree of **MASTER OF SCIENCE IN CIVIL ENGINEERING.**

26/4/15

Prof. Husain Al-Gahtani
(Advisor)

Dr. Omar A. Al-Swailem
Department Chairman (A)

26/4/2015

Prof. Shamsad Ahmad
(Member)

Prof. Salam A. Zummo
Dean of Graduate Studies

26/4/15

Dr. Mohammed Al-Osta
(Member)

30/4/15

Date

Dedication

To

My parents and family

For their support and help

ACKNOWLEDGMENTS

All praise and glory to ALLAH for giving me the good health, courage and patience to complete this work. I would like to express my heartfelt love and gratitude to my parents and family in Palestine for their support and help in overcoming the challenges I have faced during my study. Also, I would like to thank my Brother Eng. Sami Assi for his motivation and support in my MS study.

I would like to express my deep appreciation to my MS Thesis advisor, Dr. Husain Jubran AL-Gahtani, for his efficient and continuous help, support, motivation, guidance, enthusiasm and immense knowledge. I would like to extend my appreciation to my Thesis Committee Members, Dr. Shamsad Ahmad and Dr. Mohammed Al-Osta, for their support, insightful comments and hard questions.

I would like to thank KFUPM for providing the financial support. Special thanks to the Chairman of Civil & Environmental Eng. Department Dr. Nedal T. Ratrout, and all other faculty and staff members for their support during my study at KFUPM.

TABLE OF CONTENTS

LIST OF TABLES

LIST OF FIGURES

LIST OF ABBREVIATIONS

The clear definitions of the symbols and abbreviations are listed below:

fy	:	Yielding stress of reinforcement steel
Es	:	Modulus of elasticity of reinforcement steel
ϵ_y	:	Yielding strain of reinforcement steel
NSC	:	Normal strength concrete
HSC	:	High strength concrete
NSRC	:	Normal strength reinforced concrete
HSRC	:	High strength reinforced concrete
ρ	:	Steel bars percentage
f'c	:	Concrete compressive strength at 28 days
γ	:	Ratio of the distance between extreme steel fibers
b	:	width of the rectangular cross section
h	:	Depth of rectangular cross section
D	:	Diameter of circular cross section
$\mathbf{A_g}$	:	Gross sectional area of column
$\mathbf{A_s}$	:	Sectional area of steel rebar

fc	:	Stress in concrete as a function of concrete strain
$\boldsymbol{\varepsilon_c}$	:	Stain in concrete
$\boldsymbol{\varepsilon_{cu}}$	:	Crushing strain of concrete
n1	:	Number of points in region one for Mathematica code
n2	:	Number of points in region two for Mathematica code
n3	:	Number of points in region three for Mathematica code
λ	:	The angle between biaxial and uniaxial interaction diagrams
α_1	:	Stress block intensity factor
β_1	:	Stress block depth factor
c	:	Distance from extreme compression fiber to neutral axis
x, y	:	dummy variable for the integrations
$\mathbf{M_{nxo}}$	:	Nominal bending moment capacity of a column with compression and uniaxial bending moment about x principal axis

$\mathbf{M_{nyo}}$	:	Nominal bending moment capacity of a column with compression and uniaxial bending moment about y principal axis
$\mathbf{M_n}$	:	Nominal bending moment capacity of a column with compression and biaxial bending moment about general axis
$\mathbf{P_{nx}}$	:	Nominal axial load capacity of the column with compression and bending moment about x principal axis
$\mathbf{P_{ny}}$	:	Nominal axial load capacity of the column with compression and bending moment about y principal axis
$\mathbf{P_n}$	:	Nominal axial load capacity of the column with compression and biaxial bending moment about general axis
$\mathbf{P_o}$	:	Nominal axial load capacity of the concentric column
$\mathbf{P_b}$	:	Nominal balanced axial load capacity of the column

		subjected to compression and uniaxial bending moment
$\mathbf{M_b}$	:	Nominal balanced bending moment capacity of the column subjected to compression and uniaxial bending moment
$\mathbf{\Phi}$	:	Strength reduction factor
$\mathbf{f_s}$	:	Stress in steel rebar as a function strain
$\boldsymbol{\varepsilon_{s1}}$	:	Strain in steel at the extreme tensile fiber
$\boldsymbol{\varepsilon_{s2}}$	:	Strain in steel at the extreme compression fiber
θ_1	:	Angle that locates the neutral axis
θ_2	:	Angle that locates the depth of the equivalent rectangular stress block of the concrete under compression on the outer surface of column
θ_3	:	Angle that locates the point at which yielding starts in the steel under compression

θ_4	:	Angle that locates the point at which yielding starts in the steel under tension
θ_5	:	Angle that locates the depth of the equivalent rectangular stress block of the concrete under compression on the steel boundary
$\mathbf{F_c}$	:	Force provided by concrete
$\mathbf{M_c}$	:	Moment provided by concrete
$\mathbf{F_s}$	:	Force provided by rebar
$\mathbf{M_s}$	:	Moment provided by rebar
$\mathbf{F_f}$	:	Correction factor for force due to overlap between steel and Concrete
$\mathbf{M_f}$	:	Correction factor for moment due to overlap between steel and concrete
P	:	Sum of all forces
M	:	Sum of all moments
y	:	Distance measured form extreme tensile steel
y_1	:	locates the end of yielding in the steel under tension

y_2	:	locates the start of yielding in the steel under compression

ABSTRACT

Full Name : Nizar Abdul-Hamid Yousef Assi

Thesis Title : Analysis and Design of High Strength Concrete Columns Subjected to Compression and Biaxial Bending

Major Field : Civil Engineering

Date of Degree : May 2015

The use of high strength concrete for major construction projects has become popular due to in the advancement in concrete technology and the development of new types of mineral and chemical admixtures. High-strength concrete could lead to smaller member sizes for compression members and therefore provide considerable savings associated with material costs and reduction of dead loads. Moreover, due to the superior durability of high-strength concrete, considerable reduction of the maintenance efforts and an increase in the service life of the structure can be attained. However, most of the current design codes are still based on analytical or numerical models and experimental tests conducted using normal strength concrete. Recent studies indicate that the behavior of columns with high-strength concrete is different from that of normal-strength concrete.

The main objective of this research is to investigate the behavior of high strength concrete columns subjected to compression and biaxial bending which will ultimately help in developing design aids for the analysis and design of such columns. Although, the developed design aids are based on analytical and computational analysis, they have been validated against the experimental data found in literature and against the results obtained from PCA software.

ملخص الرسالة

الاسم الكامل: نزار عبد الحميد يوسف عاصي

عنوان الرسالة: تحليل وتصميم الأعمدة الخرسانية عالية القوة التي تتعرض للضغط و الانحناء ذو محورين

التخصص: الهندسة المدنية

تاريخ الدرجة العلمية: أيار 2015م

لقد أصبح لاستخدام الخرسانة عالية القوة في مشاريع البناء الكبرى شعبية عالية بسبب التقدم في تكنولوجيا الخرسانة وأيضا لتطوير أنواع جديدة من المعادن والمواد الكيميائية و الخلطات. حيث يؤدي هذ النوع من الخرسانة عالية القوة إلى أحجام أصغر للعناصر الانشائية التي تتعرض للقوى والاحمال الضاغطة وبالتالي تؤدي الى تقليل التكاليف المادية والحد من الأحمال الميتة التي اصبح بالامكان الغنى عنها. وعلاوة على ذلك، المتانة المتفوقة للخرسانة عالية القوة، والحد من الصيانة المطلوبة وزيادة الحياة التشغيلية للابنية الخرسانة. ومع ذلك، إلا ان معظم كودات التصميم العالمية والحالية لا تزال تستند إلى النماذج التحليلية و العددية والفحوصات التجريبية التي تجري للخرسانة عادية التحمل. وتشير الدراسات الأخيرة إلى أن سلوك الأعمدة ذات الخرسانة عالية القوة يختلف عن ذلك للخرسانة عادية القوة.

الهدف الرئيسي من هذا البحث هو دراسة سلوك الأعمدة الخرسانية عالية القوة التي تتعرض للضغط والانحناء حول محورين، والذي سوف يساعد في تطوير أدوات التصميم و التحليل لهذا النوع من الأعمدة. وعلى الرغم من انه سيتم تطوير الادوات النظرية التصميمة بناءعلى التحليل والعمليات الحسابية، إلا انه سيتم التحقق من صحة النتائج النظرية من خلال النتائج التجريبة والعملية من خلال البحث في الادب الهندسي فقط،وايضا سيتم تأكييد النتائج من خلال استحدام البرامج الهندسية ذات الشأن.

CHAPTER ONE

INTRODUCTION

1.1 General

Column is one of the most critical members of a framed structure, the failure of which could lead to a catastrophic failure of the whole structure. In recent years, high strength concrete (HSC) columns have been widely used in major construction projects, especially, in high-rise buildings. The advancement in concrete technology and the development of new types of mineral and chemical admixtures have enabled the production of concrete with compressive strength exceeding 150 MPa. HSC could lead to smaller member sizes for compression members and therefore provide considerable savings associated with material costs and reduction of dead loads. Moreover, due to the superior durability of HSC, considerable reduction of the maintenance efforts and an increase in the service life of the structure can be attained as compared to the normal strength concrete (NSC).

The increasing use of HSC has led to concern over the applicability of current design codes and standards. Although the latest ACI code provides uniaxial bending interaction curves for up to f ’c = 12 ksi (82.7 MPa), the curves are based on the stress block for normal concrete. Recent research indicates that the behavior of HSC is different

from NSC in many aspects. The shape of the stress–strain relation of HSC differs from that of NSC [1].

It is the aim of this research to revise and extend the current code design charts for HSC columns. The study will be concluded with a computer code capable of performing the analysis and design of concrete columns made of HSC and subjected to compression and biaxial bending. The developed code will also have the capability of generating design charts similar to the one provided by ACI for NSC.

1.2 Problem Statement

Concrete columns subjected to biaxial bending are frequently encountered in practice. A typical interaction diagram for bi-axially loaded column is shown in Figure 1.1 Case (a) and Case (b) are the uniaxial bending about the principal directions, y and x respectively. The interaction curve represent the failure envelop for different combinations of the axial load and bending moments. The analyses of such cases are easy to handle since the neutral axis can be obtained directly from equilibrium. On the other hand, Case (c) is difficult because a trial and adjustment procedure is necessary to find the inclination and depth of the neutral axis satisfying equilibrium conditions. If the depth and inclination of the neutral axis are determined, the corresponding interaction curve can be easily established. By solving the interaction curve for different values of λ, the failure surface for biaxial bending may be constructed. It is intended in this study to use the symbolic software 'Mathematica' for formulating and programming the problem such that the contour lines are generated at constant axial compressive force using load contour method as proposed in literature.

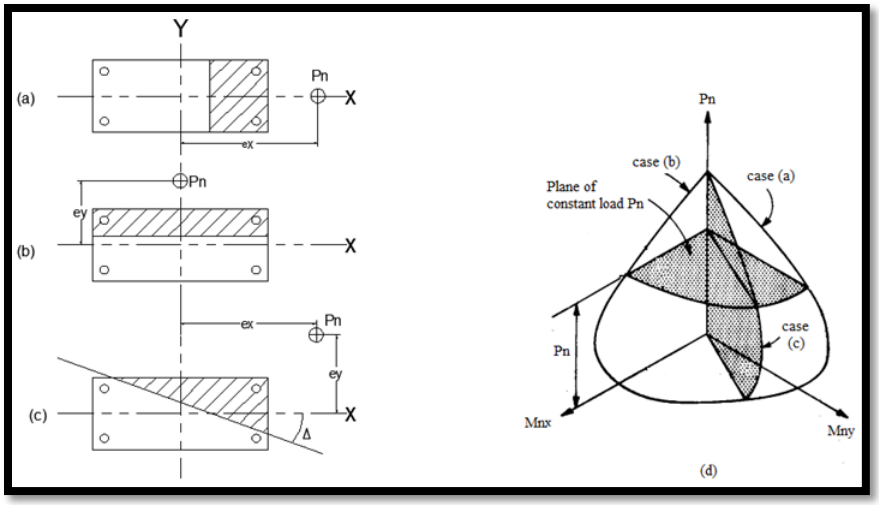

Figure 1.1: Interaction surface for reinforced concrete column with compression and biaxial bending.

The study is limited to the analysis of reinforced concrete columns with rectangular and circular cross-sections having symmetrical and uniform reinforcement. The concrete strength considered ranges from 3 ksi (21 MPa) to 18 ksi (124 MPa) and the range of the steel ratio is from 1% to 8%. The investigated columns are considered to be short and therefore, the slenderness effect is neglected.

1.3 Motivation and Objectives

1.3.1 Motivation

The use of HSC in construction has noticeably increased over the past two decades. Numerous studies have demonstrated the advantages of the material in terms of long-term economy and durability. However, most of the provisions in the current concrete codes and standards are based on NSC behavior. Although the latest ACI code provides uniaxial bending interaction curves for up to f'c = 12 ksi (82.7 MPa), the curves are based on the stress block for normal concrete. The applicability of these curves for

HSC is questionable for the following two reasons: i) as mentioned later in the literature, the stress block parameters for HSC are different from those assumed for NSC, ii) the capacity of high strength concrete columns are overestimated using the NSC stress block parameters.

Furthermore, the majority of the available procedures for biaxial bending are based on approximate interpolation of those uniaxial bending curves which already have a questionable adequacy for HSC. As an example, for an HSC (f'_c = 90 MPa; ρ = 2.8%) column subjected to biaxial bending, Bresler's method overestimates the capacity of the column by 30% [2].

Therefore, there is a need for new methods that offer more accurate and convenient procedure and take into account the properties of this new material. The powerful symbolic software, Mathematica, will be utilized to implement the analytical formulation of the problem and produce interaction curves and contours. The achievement of such symbolic relationships will enable to study the effect of various geometric and mechanical properties on the ultimate capacity of the columns.

1.3.2 Objectives

The main objective of this study is to develop computational and graphical aids for the analysis and design of concrete columns made of high strength concrete and subjected to compression and biaxial bending. The specific objectives are:

1. Develop a Mathematica code capable of computing and generating the current ACI interaction diagrams for NSC columns subjected to compression and uniaxial bending.
2. Reformulate the ACI method taking into account the new stress block based on the stress-strain relationship for HSC.
3. Encode the above formulation and generate new interaction diagrams for the high strength concrete columns subjected to compression and uniaxial bending.
4. Extend the above formulation and coding to generate contour lines for the general case of compression and biaxial bending.
5. Validate the developed codes and interaction curves /contours against the experimental data available in the literature, ACI interaction diagrams and PCA software.

1.4 Thesis Outline

The thesis consists of 8 chapters. Chapter 1 contains the introduction, describes the problem and states the objectives. Chapter 2 gives a comprehensive literature review about analysis and design of reinforced concrete columns subjected to compression and biaxial bending. The review includes: stress-strain relationships for NSC, stress-strain relationships for HSC, equivalent rectangular stress block for NSC, equivalent rectangular stress block for HSC, NSRC columns subjected to compression and uniaxial bending, NSRC columns subjected to compression and biaxial bending, HSRC columns subjected to compression and uniaxial bending and HSRC columns subjected to compression and biaxial bending.

Chapter 3 is devoted to the generation of ACI interaction curves for NSRC columns. This chapter contains the basic assumptions, NSC stress block parameters, formulation of the column capacity, key-points on the interaction diagram, MATHEMATICA code and the validation of the generated ACI-interaction diagrams.

Chapter 4 focuses on the development of interaction curves for HSRC columns. It contains stress-strain models, computation of stress block parameters, MATHEMATICA code, validation using PCA software and comparison with previous experimental work.

Chapter 5 contains the formulation and the results validation for the contour lines of HSRC columns. Some numerical applications are summarized in chapter 6.

The thesis is concluded with Chapter 7 which contains conclusions and recommendations followed by references and appendices.

CHAPTER TWO

LITERATURE REVIEW

2.1 General

Review of previous research on normal and high strength concrete columns subjected to concentric and eccentric loading conditions is presented in the following section. The emphasis is placed on those that were conducted with high strength concrete. The stress blocks are discussed first due to their importance in performing the analysis for both uniaxial and biaxial bending. The literature review is made for the following subjects:

- Stress-strain relationships for NSC.
- Stress-strain relationships for HSC.
- Equivalent rectangular stress block for NSC.
- Equivalent rectangular stress block for HSC.
- NSRC columns subjected to compression and uniaxial bending.
- NSRC columns subjected to compression and biaxial bending.
- HSRC columns subjected to compression and uniaxial bending.
- HSRC columns subjected to compression and biaxial bending.

2.2 Stress-strain relationships for NSC

The following references proposed the analytical relationship for NSC stress strain diagram, based on which analysis and design can be performed without using the equivalent stress block. Literature review shows that the stress strain relationship does not have an exact pattern, therefore some researchers assumed linear, parabolic, polynomial or any combination of those mathematical functions. The following is the summary of the literature review for those relationships.

Hognestad, 1951[3]

A common representation of stress strain diagram for concrete is established by Hognestad. In this representation it is assumed that the stress strain curve consists of two parts. The ascending part is parabolic while the descending part is liner relation. They are defined by:

$$fc = fc'' \left[\frac{2\varepsilon_c}{\varepsilon_0} - \left(\frac{\varepsilon_c}{\varepsilon_0}\right)^2\right], 0 \le \varepsilon_c \le \varepsilon_0$$

$$fc = fc'' \left[1 - 0.15\left(\frac{\varepsilon_0 - \varepsilon_c}{\varepsilon_0 - 0.0038}\right)\right], \varepsilon_0 \le \varepsilon_c \le \varepsilon_{cu}$$

Where

$fc'' = 0.9f'c$,

$$\varepsilon_0 = \frac{1.8\, fc''}{Ec}$$

$$Ec = 4700\sqrt{f'c(\text{MPa})}$$

Todeschini, 1964[4]

Stress strain curve is represented by a single parabola valid up to 6000 psi concrete strength. It is given by:

$$\text{fc} = \frac{2\text{fc}''(\varepsilon_c/\varepsilon_0)}{1+(\varepsilon/\varepsilon_0)^2}, 0 \le \varepsilon \le \varepsilon_{ult}$$

Where

fc''=0.9 f'c

$$\varepsilon_0 = \frac{1.71\, f'c}{Ec}$$

Desayi and Krishnan, 1964[5]

They proposed a stress strain relationship for NCS as follows:

$$fc = f'c\left(\frac{2\frac{\varepsilon}{\varepsilon_m}}{1+\left(\frac{\varepsilon}{\varepsilon_m}\right)^2}\right)$$

Where:$\varepsilon_m$is the strain corresponding to the maximum concrete stress, and f'c in MPa.

Popovics Relation, 1973[6]

Popovics proposed a stress strain relation for NSC (f'c<55 MPa) as follows:

$$fc = \frac{\varepsilon}{\varepsilon_m} * \frac{n\, f'c}{(n-1)+\left(\frac{\varepsilon}{\varepsilon_m}\right)^2}$$

$$\frac{Eci}{f'c/\varepsilon_m} = \frac{n}{n-1}$$

n = k f'c +1

k = 0.058 MPa^{-1}

Where:

f'c in MPa.

Thorenfeldt, Tomaszewicz, and Jensen, 1987[7]

They generalized two formulations to find the stress strain diagram which can be applied for concrete strength from 15 MPa to 125 MPa.

$$\frac{fc}{f'c} = \frac{n\,(\frac{\varepsilon_c}{\varepsilon_0})}{n-1+(\frac{\varepsilon_c}{\varepsilon_0})^{nk}}$$

Where:

f'c = concrete strength from cylinder test.

ε_0=strain when fc reaches f'c =$\frac{f'_c}{Ec}(\frac{n}{n-1})$

n = a curve-fitting factor equal to Ec/(Ec-E'c)

Ec= initial tangent modulus.

E'c =$\frac{f'_c}{\varepsilon_0}$

K= controlling slope factor equal to 1.0 for $\frac{\varepsilon_c}{\varepsilon_0} \leq 1.0\ or\ to\ 0.67 + \frac{f'c}{9000} \geq 1.0$ for $\frac{\varepsilon_c}{\varepsilon_0} > 1$

2.3 Stress-strain relationships for HSC

The following references proposed the analytical relationships for HSC stress strain diagram, based on which analysis and design can be performed without using the equivalent stress block. The following is the summary of the literature review for those relationships.

Carreira and Chu, 1985[8]

They proposed the following stress-strain model for concrete under compression:

$$k = 32.4$$

$$\epsilon 0 = (0.71 f_c' + 168) * 10^{-5}$$

$$n = \left(\frac{f_c'}{k}\right)^3 + 1.55$$

$$\sigma_c = \frac{\epsilon_c}{\epsilon_0} \frac{n f_c'}{(n-1) + (\frac{\epsilon_c}{\epsilon_0})^n}$$

Kumar, Collins et. al., 1993[9]

The following stress-strain model has been proposed:

$$E_{ci} = 3320\sqrt{f_c'} + 6900$$

$$n = 0.8 + \frac{f_c'}{17}$$

$$\epsilon_0 = \frac{n f_c'}{(n-1) E_{ci}}$$

$$k = \begin{bmatrix} \mathrm{k} = 1 & \epsilon_c \leq \epsilon_0 \\ k = 0.67 + \frac{\mathrm{f}_c'}{62} & \epsilon_c > \epsilon_0 \end{bmatrix}$$

$$\sigma_c = \frac{\epsilon_c}{\epsilon_0}(n\mathrm{f}_c')/((n-1) + (\frac{\epsilon_c}{\epsilon_0})^{nk})$$

Wee et al., 1996[10]

A research was conducted for HSC to find a model for the stress-strain relationships. The proposed relationship consists of ascending and descending parts. The equation for the ascending branch is:

$$f_c = f_c' \left[\frac{\beta \left(\frac{\epsilon}{\epsilon_0}\right)}{\beta - 1 + \left(\frac{\epsilon}{\epsilon_0}\right)^{\beta}} \right]$$

$$\beta = \frac{1}{1 - (\frac{f_c'}{\epsilon_0 E_{it}})}$$

And for the descending branch the same equation is used with two correction factors k_1 and k_2:

$$f_c = f_c' \left[\frac{k_1\, \beta \left(\frac{\epsilon}{\epsilon_0}\right)}{k_1\, \beta - 1 + \left(\frac{\epsilon}{\epsilon_0}\right)^{k_2\, \beta}} \right]$$

For concrete strength ranging from 7.25 ksi to 17.4 ksi, k_1 and k_2 are found as follow:

$$k_1 = \left(\frac{7252}{f_c'(psi)}\right)^{3.0}$$

$$k_1 = \left(\frac{7252}{f_c'(psi)}\right)^{1.3}$$

For concrete strength below 7.25 ksi, k_1 and k_2 are taken as unity.

$$E_{it} = 281571(f_c'(psi))^{(\frac{1}{3})}$$

$$\epsilon_0 = 0.000225(f_c'(psi))^{(\frac{1}{4})}$$

Van Gysel and Taerwe, 1996[11]

Van Gysel and Taerwe suggested a stress-strain relationship for HSC. This relationship consists of ascending and descending branches. For the ascending the following relationship was proposed:

$$\frac{f_c}{f_c'} = \frac{\frac{E_{c0}}{E_{c1}}\frac{\epsilon_c}{\epsilon_{c1}} - \left(\frac{\epsilon_c}{\epsilon_{c1}}\right)^2}{1 + \left(\frac{E_{c0}}{E_{c1}} - 2\right)\frac{\epsilon_c}{\epsilon_{c1}}} \quad \text{for } \epsilon_c < \epsilon_{c1}$$

$$\epsilon_{c1} = 0.00015\, f_c'^{0.31}(psi) \;\; for\; f_c' > 5831\; psi$$

$$\epsilon_{c1} = 0.0022 \;\; for\; f_c' \leq 5831\; psi$$

For the descending branch, the following relation was proposed:

$$\frac{f_c}{f_c'} = \frac{1}{1 + \left(\frac{\frac{\epsilon_c}{\epsilon_{c1}} - 1}{\epsilon_{c1} + \frac{t}{\epsilon_{c1}}} - 2\right)}$$

With corresponding t values as proposed in the table below:

Table 2.1: Values of t vs. concrete strength.

f'c (ksi)	7252	8702	10153	11603	13053	14504
t (%)	0.807	0.579	0.388	0.221	0.07	0.015

Oztekin et al., 2003[12]

Oztekin et al. used the stress-strain model which was proposed by Hognestad et al (1951) to obtain a modified model for HSC. The following relation was proposed:

$$f_c = f'_c\left(k\frac{\epsilon_c}{\epsilon_{cu}} - (k-1)\left(\frac{\epsilon_c}{\epsilon_{cu}}\right)^2\right)$$

Where k is a modification parameter as follow:

$$k = 2 - \frac{f'_c(psi) - 5800}{10153}\ for\ 8700\ psi \le f'_c \le 13633\ psi$$

$$\epsilon_{cu} = [2.2 + 1.034 \times 10^{-4}(f'_c - 5800)\ ] \times 10^{-3}\ for\ 8700\ psi \le f'_c \le 13633\ psi$$

Halit Cenan Mertol, 2006[13]

He proposed the following stress-strain diagram for concrete:

$$n = 0.310 * 0.145fc + 0.78$$

$$k = 0.10 * 0.145fc + 1.2$$

$$\epsilon_{c0} = 0.0033 - 2 * 0.145f'_c * 10^{-5}$$

$$\epsilon_{cu} = 0.0038 - 4 * 0.145f'_c * 10^{-5}$$

$$\sigma_c = \frac{\epsilon_c}{\epsilon_{c0}}\frac{nf'_c}{(n-1) + (\frac{\epsilon_c}{\epsilon_{c0}})^{n*k}}$$

2.4 Equivalent rectangular Stress block for both NSC & HSC

There are many references that propose the equivalent rectangular stress block for concrete under compression to simplify the analysis and design of concrete members subjected to axial compression and flexure. This equivalency varies throughout the literature review which is shown below. Some of those references distinguish between NSC and HSC, whereas others do not. The following is a summary of the review:

Whitney, 1937[14]

Whitney proposed the equivalent rectangular stress block for the normal concrete under compression with $\alpha 1 f c'$ width and $\beta 1 * c$ hight

$\alpha 1 = 0.85$

$\beta 1 = 0.85 - 0.05(f'c - 4) \rightarrow 0.65 \leq \beta 1 \leq 0.85$

There are no specifications in this study regarding the concrete strength.

Ertekin Oztekin, SelimPul, Metin Husem, 2003[12]

This study proposed an equivalent stress block similar to the one used for the normal concrete to simplify analysis and design, as shown in the figure below:

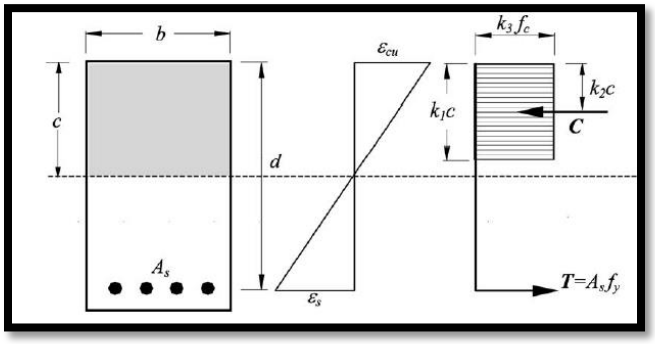

Figure 2.1: High strength concrete section with stress – strain variations.

Where:

K_1 = - 0.0012 fc + 0.805

K_3 = - 0.002 fc + 0.964

$K_1 k_3$ = - 0.0024 fc + 0.762

K_1= $2k_2$

Togay Ozbakkaloglu and Murat Saatcioglu, 2004[15]

According to this study, it was shown that concrete with 40 MPa or higher is considered high strength concrete, and the HSC ascending part of the stress-strain diagram is approximately linear with steeper slope than normal concrete. This study proposes the use of an equivalent stress block similar to the one used for normal concrete, but with some changes in the parameters as shown below.

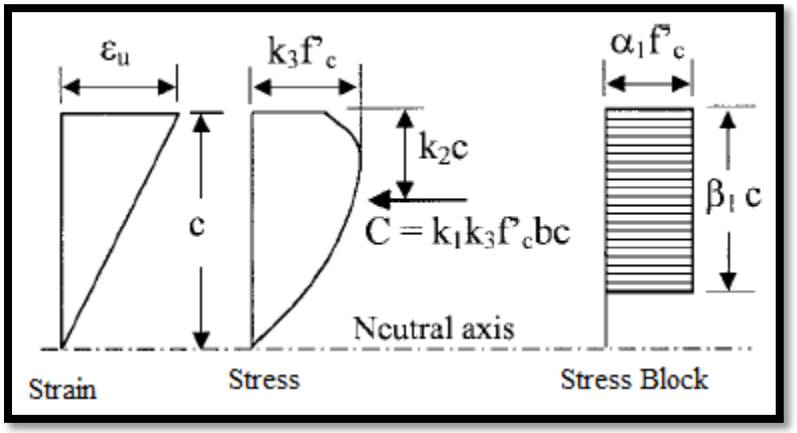

Figure 2.2: Stress-strain for HSC [15].

Where:

α1 and β1 can be determined using the following relations:

for $f'c \leq 4000$ psi

$\alpha 1 = 0.85$

$\beta 1 = 0.85$

for $f'c \geq 4000$ psi

$\alpha 1 = 0.85 - (f'c - 4000) * 10^{-5} \geq 0.72$

$\beta 1 = 0.85 - 1.3(f'c - 4000) * 10^{-5} \geq 0.67$

where:

$\alpha 1$: is the stress intensity factor.

$\beta 1$: is the stress block depth factor.

The above relations were verified experimentally.

National Cooperative Highway Research Program (NCHRP), 2007[16]

This program proposed the use of the equivalent rectangular stress block for both normal and high strength concrete with limits on upper strength to be 18 Ksi, the proposed parameters are:

$$\alpha 1 = \begin{cases} 0.85 & f'c \leq 10\ Ksi \\ 0.85 - 0.02(f'c - 10) \geq 0.75 & f'c > 10\ Ksi \end{cases}$$

$$\beta 1 = \begin{cases} 0.85 & f'c \leq 4\ Ksi \\ 0.85 - 0.05(f'c - 4) \geq 0.65 & f'c > 4\ Ksi \end{cases}$$

Peng et al., 2011[17]

They have studied the characteristics of the equivalent rectangular stress block of concrete by investigating effects other than concrete strength. An experimental study was carried on concrete columns which were divided into two groups where each group has the same properties but one is concentrically loaded while the other is eccentrically loaded. The equivalent rectangular stress block was modified based on this study to consider other effects like strain gradient. They proposed the following parameters:

$\beta 1 = 0.8$

$$\alpha 1 = \begin{cases} 0.85 & for\ 0 \leq \frac{d}{c} < 1.3 \\ 0.815\left(\frac{d}{2}\right) - 0.21 & for\ 1.3 \leq \frac{d}{c} < 2 \\ 1.42 & for\ 2 \leq \frac{d}{c} \end{cases}$$

In the following two tables contain a summary of the literature review regarding the concrete building codes and other published journals. Based on that review it is noticed that most of the available codes and published researches propose the use of the equivalent rectangular stress block for concrete under compression and the rectangular stress depth is $\beta_1 c$ with height of $\alpha_1 f'c$. However, those codes do not specify the limits of strength of concrete for that proposed simplification of stress block i.e. the same parameters α_1 and β_1 can be used for both normal and high concrete strength as in Table 2.2.

Table 2.2: Equivalent rectangular stress block for concrete in different codes.

Code	α_1 (Stress intensity factor)	β_1(Stress block depth factor)	ε_{cu}
LRFD and ACI 318-(2011),[18,1]	0.85	0.85 for f'c≤ 4ksi 0.85-0.05(f'c-4)≥0.65 for f'c>4 ksi	0.003
NZS 3101 (1995)[19] (see Li, Park and Tanaka 1994)[20]	0.85 for f'c≤8ksi 0.85-0.02758(f'c-8) ≥0.72 for f'c>8ksi	0.85 for f'c≤4.35ksi 0.85-0.05516(f'c-4.35) ≥0.65 for f'c>4.35ksi	0.003
CSA A23.3 (1994)[21]	0.85-0.01034f'c ≥0.67	0.97-0.01724f'c≥0.67	0.0035
CEB-FIB (1990)[22]	$0.85(1-\frac{f'c}{36.3})$	1	$0.004-0.002\frac{f'c}{14.5}$
AFREM (1995)[23]	0.85	$1.0-\frac{0.7}{4.5-0.1724\,f'c}$	0.003
ACI 441-R96 (1996)[24]	0.85-0.05033(f'c-10) ≥0.6 for f'c>10ksi	0.67 for f'c≥10 ksi	0.003

Table 2.3 shows various proposals by researchers for α1 and β_1 parameters.

Table 2.3: Equivalent rectangular stress blocks for concrete in different research publications.

Publication	α_1 (Stress intensity factor)	β_1(Stress block depth factor)	ε_{cu}
Azizinamini et al. (1994)[25]	0.85 for f'c ≤10ksi 0.85-0.05(f'c-10) ≥0.6 for f'c>10 ksi	0.85 for f'c≤4.35ksi 0.85-0.05516(f'c-4.35) ≥0.65 for f'c>4.35ksi	0.003
Ibrahim and MacGregor (1997)[26]	$0.85-\frac{f'c}{116}\geq 0.725$	$0.95-\frac{f'c}{58}\geq 0.70$	0.003
Pendyala and Mendis (1998)[27]	0.85-0.01724(f'c-8.7) for 8.7ksi≤f'c≤14.5 ksi	0.65-0.00862(f'c-8.7) for 8.7ksi≤f'c≤14.5 ksi	0.003
Attard and Stewart (1998)[28]	$1.2932(\frac{f'c}{0.145})^{-0.0998}\geq 0.71$ for Dagbone tests $0.6470(\frac{f'c}{0.145})^{0.0324}\geq$	$1.0948(\frac{f'c}{0.145})^{-0.091}\geq 0.67$	0.003

	0.58 for Sustain load test		
Bae and Bayrak (2003)[29]	0.85 for f'c≤10.2 ksi 0.85-0.02758(f'c-10.2)≥0.67 for f'c>10.2 ksi	0.85 for f'c≤4.35 ksi 0.85-0.02758(f'c-4.35)≥0.67 for f'c>4.35	0.003 for f'c≤8ksi 0.0025 for f'c≥ 8ksi
Ozbakkaloglu and Saatcioglu (2003)[15]	0.85 for f'c≤ 4ksi 0.85-0.01(f'c-4)≥0.72 for f'c>4 ksi	0.85 for f'c ≤4ksi 0.85-0.014(f'c-4) ≥0.67 for f'c>4ksi	0.003
Mertol et al. (2006)[13]	0.85 for f'c ≤69 MPa 0.85-0.0058(f'c-69)≥0.65 for f'c>69MPa	0.85 for f'c≤27.6 MPa 0.85-0.00725(f'c-27.6) ≥0.65 for f'c>27.6 MPa	0.003
Ali Al-Ghalib, 2007[30]	0.95 for f'c≤17 MPa 0.95-0.0021(f'c-17) ≥0.775 for f'c>17MPa	0.87 for f'c≤17 MPa 0.87-0.0024(f'c-17) ≥0.67 for f'c>17MPa	

2.5 NSRC columns subjected to compression and uniaxial bending

ACI Design Handbook, 1964[31]

This hand book contains the interaction diagrams for normal concrete columns with compression and uniaxial bending. Those diagrams were plotted by Dr. Mohsen A. Issa and Alfred A. Yousif. FORTRAN software was available at that time and the equations used to develop the solutions data were derived by Dr. Everard in 1963. Steel was considered as a thin rectangular or circular layer based on the column shape.

Noel J.Everard, 1997[32]

Computerized equations are derived for the development of the interaction diagrams for reinforced concrete columns with steel distributed uniformly and continuously in a circular pattern.

Ramon V. Jarquio, 2004[33]

An analytical method was proposed to find the column capacity based on the use of parabolic stress strain diagram for concrete under compression. External and internal equilibrium was utilized in this approach. Equivalent stress block was avoided in this approach, and interaction diagrams for circular cross section were generated as a sample on this approach.

ACI-318, 2011[1]

Section 9.3.2 in the ACI code proposed to use the proper strength reduction factor (Φ) for the concrete sections that are subjected to axial compression and bending moment. (Φ) Can be found based on the strain (εt) in the steel at the extreme fiber in tension. The proposed values of (Φ) are:

Φ=0.65 for tied columns and $\varepsilon_t<0.002$

Φ=0.75 for spiral columns and $\varepsilon_t<0.002$

Φ=0.9 for tied columns and $\varepsilon_t>0.005$

However, in the transition zone, the code permits to use linear interpolation for getting the actual or proper strength reduction factor. Based on the strength reduction factor (Φ), Figure 2.3 shows the modification on the interaction diagram in the region where the strain in the tensile steel at the extreme fiber is in the range $0.002\leq\varepsilon_t\leq0.005$.

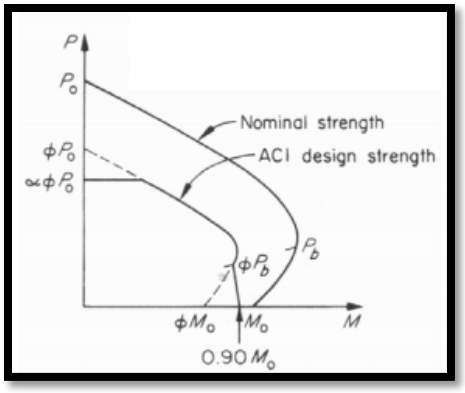

Figure 2.3: Nominal strength curve vs. ACI design strength curve after modification.

2.6 NSRC columns subjected to compression and biaxial bending

Bresler, 1960[34]

This study is considered as the most famous approach for biaxial bending analysis. Bresler developed two methods for biaxial loaded columns: reciprocal load method and load contour method. The reciprocal load method was developed by approximation the curve surface into plane surface, which is more conservative, and then derived the following formula:

$$\frac{1}{P_n} = \frac{1}{P_{nx}} + \frac{1}{P_{ny}} - \frac{1}{P_0}$$

Where:

P_n: is the nominal axial capacity of the column with compression and biaxial bending.

P_{nx}: is the nominal axial capacity of the column with compression and uniaxial bending about x axis.

P_{ny}: is the nominal axial capacity of the column with compression and uniaxial bending about y axis.

P_0: is the nominal axial capacity of the column with concentric load.

Moreover, he developed a graphical solution for his equation and it is also available in the ACI design handbook.

The load contour method:

$$\left(\frac{M_x}{M_{xo}}\right)^{\alpha} + \left(\frac{M_y}{M_{yo}}\right)^{\alpha} = 1$$

Where:

M_x=moment component in direction of major axis.

M_y=moment component in direction of minor axis.

M_{xo}=moment capacity when the load acts along the major axis.

M_{yo}=moment capacity when the load acts along the minor axis.

Weber, Donald C., 1966[35]

This study proposed charts for analysis and design of biaxial reinforced concrete columns. Those charts are only for one case which is square column with symmetrical steel reinforcement.

Warner, 1969[36]

Warner developed finite method through which the column capacity can be found. That method is based on dividing the columns sections into finite discrete parts and the finding the force corresponding to that discrete part as well as moment, and summing all forces and moment for all discrete parts to obtain the columns capacity. That method is also applicable for irregular column sections.

Furlong, 1979[37]

He proposed a design method for reinforced concrete columns subjected to compression and biaxial bending. He employed a parabola trapezoidal stress strain function of the concrete in the compression zone instead of using the rectangular stress block, and observed that the obtained results were more accurate than other methods.

Yen, 1991[38]

In this study, an iterative approach was used to design columns under both uniaxial and biaxial bending using computer. This approach starts with assumptions for the neutral axis such as location and orientation and then the column capacity was found. Several examples were given to illustrate the procedure for the design of columns subjected to uniaxial and biaxial bending based on this approach.

Hsu, 1994[39]

He proposed the following interaction equation which is similar to the load contour method proposed by Bresler:

$$\frac{P_n - P_{nb}}{P_o - P_{nb}} + \left(\frac{M_{nx}}{M_{nbx}}\right)^{1.5} + \left(\frac{M_{ny}}{M_{nby}}\right)^{1.5} = 1.0$$

Where:

P_n = nominal axial compression or tension.

M_{nx}, M_{ny} = nominal bending moments about x and y axis.

P_o = maximum nominal axial compression or tension.

P_{nb} = nominal axial compression at balanced condition.

M_{nbx}, M_{nby} = nominal bending moments about x and y axis at balanced strain condition.

A Najmi, 1997[22]

A new technique was proposed to design short columns under biaxial bending using the principle of section transformation at the ultimate load. The method was in the flexure formula instead of the equilibrium equations. Different design curves with different eccentricities were presented.

M.Y. Rafiq, C. Southcombe, 1998[40]

Optimization approach was used to get an optimal design for reinforced concrete columns under biaxial bending using the principles of genetic algorithm. The design of columns under biaxial bending using genetic algorithm approach is considered safe and accurate compared with those approximate methods.

Fafitis, 2001[41]

In this study the interaction surfaces for reinforced concrete columns under biaxial bending are developed using the green's theorem which was used in this study to convert the equilibrium double integration into the line integral, resulting in a computationally efficient approach.

Bonet et al., 2004[42]

He proposed an analytical approach for interaction surfaces for reinforced concrete rectangular section with concrete strength ranging from 25MPa to 80MPa, i.e. normal and high strength concrete. That approach is obtained using the mean of reference

generatrices which lie on two directrices and on the ultimate axial loads corresponding to a situation of pure axial tension and compression. Moreover, that approach was verified by numerical test and experimental results from the literature.

L. Cedolin, G. Cusatis, S. Eccheli, M. Roveda, 2006[43]

A numerical solution was proposed to find the interaction surfaces for reinforced concrete columns under biaxial bending based on the use of equivalent dimensionless square with unit side. Although, the solution is based on approximation but it yielded accurate results.

L. Pallarés, Pedro F. Miguel, Miguel A. Fernández-Prada, 2009[44]

An iterative approach was proposed to design concrete sections subjected to compression and biaxial based on the principle of ultimate strain method which was already used in the uniaxial case. This approach is considered effectively and it was verified with the experimental data.

Marinella Fossetti, Maurizio Papia, 2012[45]

A numerical approach was proposed to provide ultimate moment curvature relation for rectangular concrete sections subjected to axial compression and biaxial bending, this approach was performed in a dimensionless manner.

2.7 HSRC columns subjected to compression and uniaxial bending

Ibrahim and MacGregor (1996a, 1996b)[46, 47]

An experiment research was conduct on high strength concrete columns with compression and uniaxial load. It was found that the ratio between the maximum compression stresses to the cylinder strength was 0.92, which indicated that the use of rectangular stress block, for concrete under compression, was considered unsafe in the design of HSC columns.

Foster and Attard, 1997[48]

Experimental research was carried out on eccentric columns with normal and high strength concrete, and based on the test results it was shown that the use of equivalent rectangular stress for concrete, as proposed by ACI code, was considered good prediction for the column capacities at failure. However, for high strength it gave a lower prediction for the column capacity

Lee and Son, 2000[49]

A set of eccentric columns with concrete strength 5.1 to 13.5 ksi was tested experimentally. Based on these tests it was shown that the rectangular stress block was overestimating the column capacity. Whereas the trapezoidal stress block and the modified rectangular stress block, as suggested by Ibrahim and MacGergor, were considered as a lower bound conservative.

Togay Ozbakkaloglu and Murat Saatcioglu, 2004[15]

Experimental results for HSC eccentric columns with different concrete strengths are summarized. Those results were plotted on the uniaxial interaction diagrams for the columns. Those diagrams were developed based on different stress block model for the concrete in order to find the best model for the concrete in case of high strength that will fit the experimental results.

Tan and Nguyen, 2005[50]

Experiment investigation was carried out on columns with uniaxial bending with concrete strength range from 6.7 to 14.6 ksi. It was found that the use of rectangular stress block which as proposed by ACI is not conservative for expecting the column capacity.

S. Kim, H. C. Mertol, S. Rizkalla, P. Zia, 2006[16]

Interaction diagrams for uniaxial eccentric columns were plotted using data from the experimental work, and those diagrams were also generated using the equivalent rectangular stress block theoretically. It was found that the use of equivalent stress block was conservative. In this study the following parameters (AASHTO-LRFD) were used and based on which the interaction diagrams were plotted.

$$\alpha 1 = 0.85$$

$$\beta 1 = \begin{cases} 0.85 & f'c \leq 27.6\ \text{MPa} \\ 0.85 - 0.00725(f'c - 27.6) \geq 0.65 & f'c > 27.6\ \text{MPa} \end{cases}$$

However, $\alpha 1$ from AASHTO did not work properly for concrete strength beyond 69 MPa. Mertol has modified the parameter ($\alpha 1$) for high strength concrete, as follows:

$$\alpha 1 = \begin{cases} 0.85 & f'c \leq 69 \text{ MPa} \\ 0.85 - 0.0058(f'c - 69) \geq 0.65 & f'c > 69 \text{ MPa} \end{cases}$$

Hany A. Kottb, Nasser F. El-Shafey, Akram A. Torkey, 2014[51]

An experimental study was conducted on columns of high strength concrete and the test data was used to derive the relationships between the load and the moment at failure. The study concluded that ACI diagrams are not convenient for high strength concrete.

2.8 HSRC columns subjected to compression and biaxial bending

Wang and Hong, 2002[2]

The reciprocal load method was used to interpolate the capacity of biaxial column from uniaxial column capacity for both NCS and HCS. A numerical assessment of this method was made on the adequacy of concrete short columns with NCS and HCS by comparing the capacities obtained by reciprocal load method with those obtained from equilibrium and taking into account the nonlinearity of stress stain relationships for both steel and concrete. This method showed that Bresler's method overestimates the capacity of the column by 30%.

Bonet et al., 2004[52]

He proposed an analytical approach for interaction surfaces for reinforced concrete rectangular section with concrete strength ranging from 25MPa to 80MPa. That approach is obtained using the mean of reference generatrices which lie on two directrices and on the ultimate axial loads corresponding to a situation of pure axial

tension and compression. Moreover, that approach was verified by numerical test and experimental results from the literature done by him.

J.L. Bonet, P.F. Miguel, M.A. Fernandez, M.L. Romero, 2004[42]

A simplified method was suggested for designing biaxial slender columns with rectangular cross section and doubly symmetric reinforcement for both normal and high strength concrete. This method is based on the moment magnifier method and for columns with the same buckling length in the two directions.

Amarjit Singh Bajaj and P. Mendis, 2005[53]

A computer program was developed to find the interaction surfaces for rectangular and square biaxial columns for both NSC and HSC. This program used the ACI 2002 equivalent rectangular stress block for NCS and the modified stress block by Ibrahim and Macgregor [26] for the HSC. The main task in this program is to assume neutral axis and try to satisfy the equilibrium equations iteratively. The obtained interaction surface was compared with the Bresler surface.

Pallarés et al., 2008[54]

In this study an experimental research has been conducted on high strength concrete columns subjected to compression and uniaxial and biaxial bending. The column cross section was rectangular cross section. Based on this research it was observed that the failure in columns happened due to either columns instability or ultimate capacity failure.

CHAPTER THREE

GENERATION OF ACI COLUMN INTERACTION CURVES FOR NSRC COLUMNS

3.1 Basic Assumptions

As per ACI, the nominal column capacity is based on the following assumptions:

- Plane section remains plane before and after bending, which is the basic assumption for the beam theory and based on which linear strain is compatible after deformation has happened.
- Concrete and steel are assumed to be homogenous and isotropic with the same modulus of elasticity and resistance for each material in all directions.
- The normal strain in the reinforcement steel is exactly the same of the strain in the surrounding concrete; this implies the perfect bond between steel and concrete.
- Steel is assumed to behave as full elastic-plastic, where the stress in the steel remains constant after the yielding stress.
- Concrete resistance to tensile stress below the neutral axis is neglected.
- Reinforcement Steel is assumed to be distributed uniformly and continuously around the cross section perimeter in order to follow the ACI basic assumptions.
- Force in concrete is found using the equivalent rectangular stress block as defined by the ACI code.

- Crushing strain for the concrete is assumed to be 0.003 as defined by ACI code.
- NSC is considered in this MS Thesis when concrete strength is less than 12 ksi (82.5MPa).

3.2 Stress block parameters

Different stress-strain relationships have been proposed in the literature and also different stress block parameters. The equivalent rectangular stress block which was used in this research is the ACI code's model, and it was used for the purpose of generating ACI interaction diagrams for NSRC columns. The equivalent rectangular stress block for the normal concrete under compression has $\alpha_1 f_c{}'$ stress intensity and $\beta_1 * c$ depth, where:

$\alpha_1 = 0.85$

$\beta_1 = 0.85 - 0.05(f_c'(\text{ksi}) - 4), \text{where } 0.65 \leq \beta_1 \leq 0.85$

Where:

α_1: is the stress intensity factor.

β_1: is the stress block depth factor.

The modified Hognestad [3] and Todeschini [4] stress-strain models for concrete under compression are used to find the equivalent rectangular stress block parameters for NSC as follow:

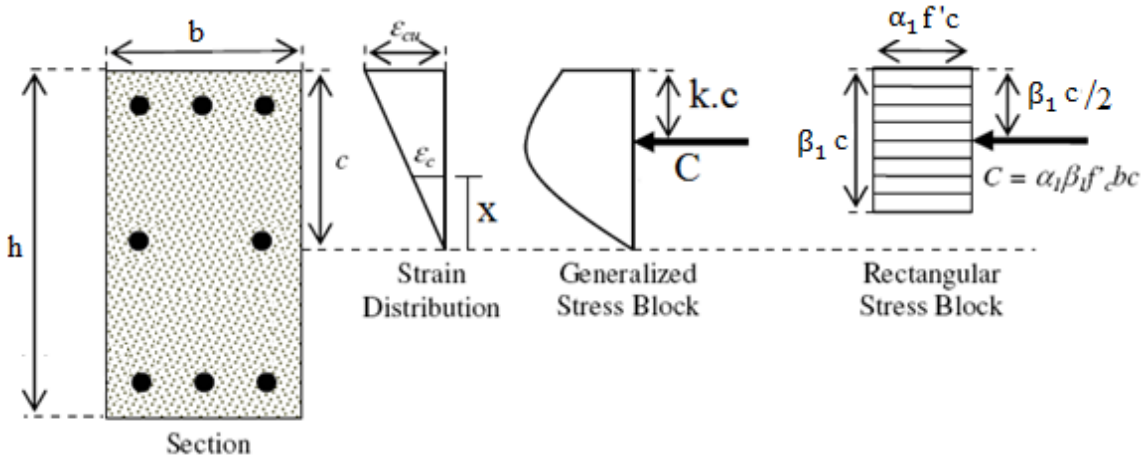

Figure 3.1: Stress distribution in concrete over compression zone.

Modified Hognestad stress-strain model:

Figure 3.2 shows the proposed stress-strain relationship for f'c=4000 psi, and it is drawn based on the following proposed equations:

$$\epsilon_{cu} = 0.0038$$

$$E_c = 57000\sqrt{f'_c(psi)}$$

$$f''_c = 0.9f'_c$$

$$\epsilon_0 = \frac{1.8f''_c}{E_c}$$

$$f_c = f''_c\left(\frac{2\epsilon_c}{\epsilon_0} - \left(\frac{\epsilon_c}{\epsilon_0}\right)^2\right) \quad \text{for } 0 \le \epsilon_c \le \epsilon_0$$

$$f_c = \frac{0.15f''_c}{\epsilon_0 - \epsilon_{cu}}(\epsilon_c - \epsilon_0) + f''_c \quad \text{for } \epsilon_0 \le \epsilon_c \le \epsilon_{cu}$$

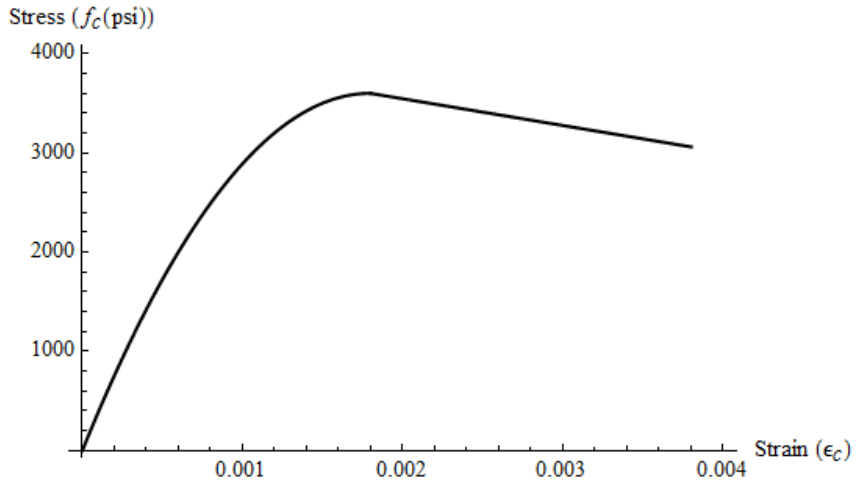

Figure 3.2: Modified Hognestad stress-strain model for f'c=4000 psi.

Todeschini model:

Figure 3.3 shows the proposed stress-strain relationship for f'c=40 MPa and it is drawn based on the following proposed equations:

$$f_c'' = 0.9f_c'$$

$$E_c = 4700\sqrt{f_c'}$$

$$\epsilon_0 = \frac{1.71f_c'}{E_c}$$

$$\sigma_c = \frac{2f_c''\frac{\epsilon_c}{\epsilon_0}}{1 + (\frac{\epsilon_c}{\epsilon_0})^2}$$

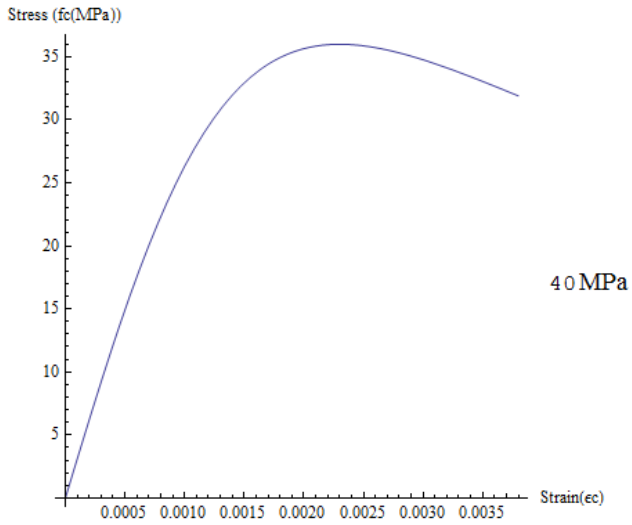

Figure 3.3: Todeschini stress-strain model for f'c=40 MPa.

Stress block parameters (α_1 and β_1) are derived based on proposed stress-strain relationships by Hognestad and Todeschini. Figure 3.1 shows the generalized and equivalent stress block, and based upon which the following two equations are derived:

$$\int_0^{\epsilon_{cu}} f_c \, d\epsilon_c = \alpha \, f'_c \, \beta_1 \, \epsilon_{cu}$$

$$\int_0^{\epsilon_{cu}} f_c \, \epsilon_c \, d\epsilon_c = \alpha \, f'_c \, \beta_1 (1 - 0.5\beta) \epsilon_{cu} \, \epsilon_{cu}$$

The following two tables (Table 3.1 and Table 3.2) summarize the results for stress block parameters based on the previous two models for NSC, by solving the above two equations for α_1 and β_1:

Table 3.1: Stress blocks parameters based on different model for NSC.

f'_c(MPa)	Hognestad		Todeschini	
	α_1	β_1	α_1	β_1
15	0.841	0.867	0.734	0.960
20	0.840	0.846	0.776	0.926
25	0.839	0.828	0.804	0.900
30	0.837	0.812	0.823	0.880

35	0.834	0.798	0.836	0.863
40	0.830	0.786	0.844	0.849

Table 3.2: Stress blocks parameters relationships.

Model	α_1 and β_1Relationships
Hognestad	$\alpha_1 = 0.8489 - 0.000437f_c'$
	$\beta_1 = 0.91162 - 0.00323f_c'$
Todeschini	$\alpha_1 = 0.685 + 0.00428f_c'$
	$\beta_1 = 1.0167 - 0.00437f_c'$

Figure 3.4 and Figure 3.5 show that β_1 parameter is linearly changing with concrete strength and this variation is expected.

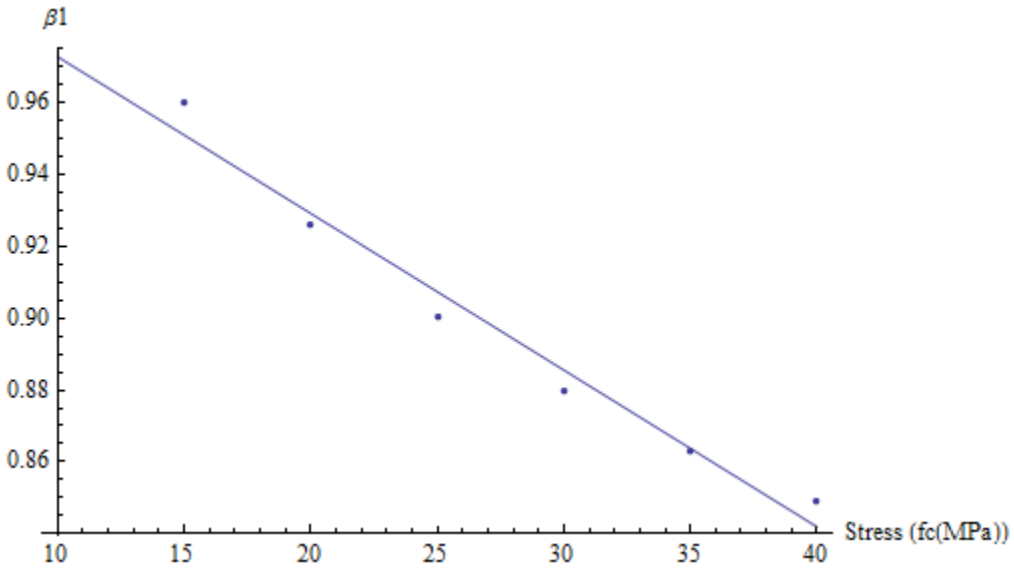

Figure 3.4: Developed β_1 parameter based on Todeschini stress-strain model.

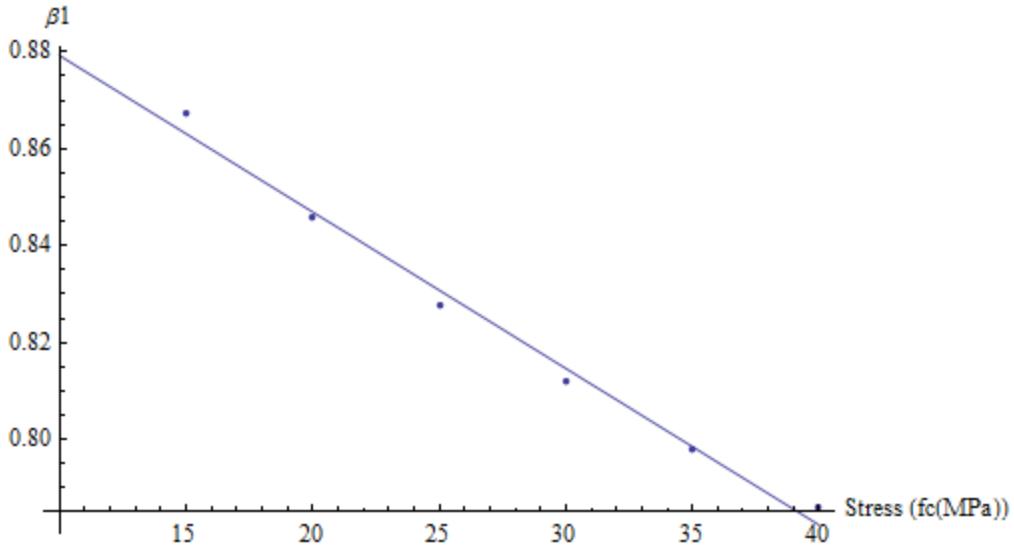

Figure 3.5: Developed β_1 parameter based on Hognestad stress-strain model.

3.3 Formulation of the Column Capacity

Based upon the earlier assumptions, the neutral axis depth is assumed and then equilibrium is used to find the corresponding nominal column capacity (P_n, M_n) which represents a point on the interaction diagram. The procedure is repeated for more points, until the complete diagram is obtained.

Two columns cross sections are considered in this Thesis: circular and rectangular. Each cross section has its own properties and formulations. The formulations of the nominal column capacity for both sections are given below.

3.4 Circular column

The formulation is based on the procedure given by Noel J. Everard [32]. To simplify the derivations, it is better to use polar coordinate system instead of the

rectangular Cartesian coordinate system. The following definitions are used in the derivations of the interaction diagrams of circular cross section (Figure 3.6).

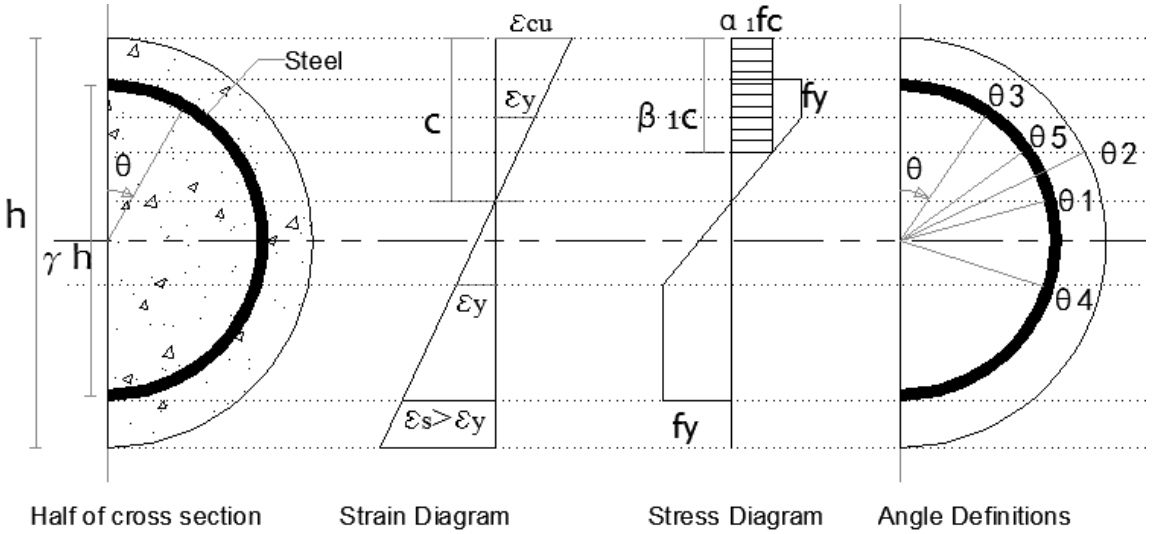

Figure 3.6: Basic definitions for circular column section.

$$\theta_1 = \arccos[\frac{1}{\gamma}\left(1 - 2\frac{c}{h}\right)]$$

$$\theta_2 = \arccos[1 - \frac{2\,\beta_1\,c}{h}]$$

$$\theta_3 = \arccos[\frac{1}{\gamma}\left(1 - \frac{2c}{h}(1 - \frac{\varepsilon_y}{\varepsilon_{cu}})\right)]$$

$$\theta_4 = \arccos[\frac{1}{\gamma}\left(1 - \frac{2c}{h}(1 + \frac{\varepsilon_y}{\varepsilon_{cu}})\right)]$$

$$\theta_5 = \arccos[\frac{1}{\gamma} - \frac{2\,\beta_1\,c}{\gamma h}]$$

Where:

θ_1: Angle that locates the neutral axis.

θ_2: Angle that locates the depth of the equivalent rectangular stress block of the concrete under compression on the outer surface of column.

θ_3: Angle that locates the point at which yielding starts in the steel under compression.

θ_4: Angle that locates the point at which yielding starts in the steel under tension.

θ_5: Angle that locates the depth of the equivalent rectangular stress block of the concrete under compression on the steel boundary.

In order to generate the interaction diagrams, the neutral axis depth is assumed to be in the following ranges:

1) $\mathbf{c = \infty}$

$P_o = (A_g - \rho\, A_g)\alpha_1\, f'_c + \rho\, A_g\, f_y$

P_o: Nominal capacity of the concentric axial reinforced concrete column under compression.

A_g: Concrete gross section area.

ρ: Steel percentage.

f'_c: Concrete strength in compression.

f_y: Steel yielding strength.

α_1: Stress intensity factor for concrete under compression.

2) $\mathbf{c = 0}$

$t = -\rho\, A_g\, f_y$

t: Nominal capacity of the concentric axial reinforced concrete column under tension.

3) $\mathbf{\frac{h}{2}(1+\gamma) \le c \le \infty}$

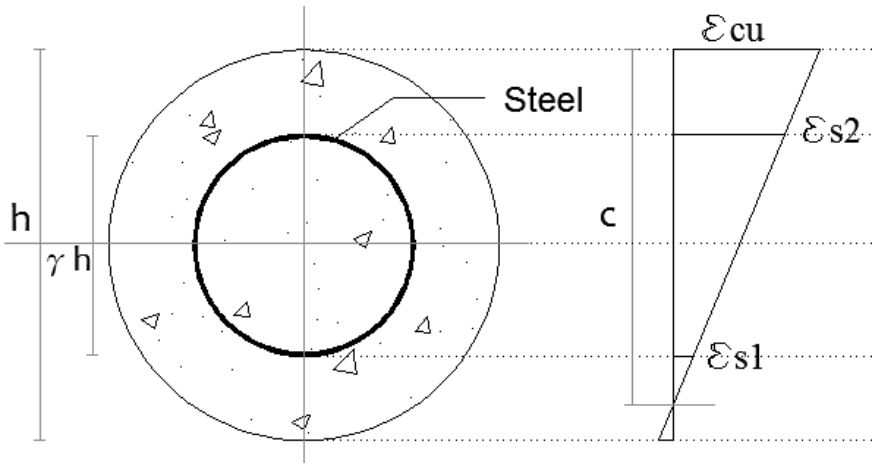

Figure 3.7: Strain distribution in circular section when $\frac{\mathbf{h}}{\mathbf{2}}(\mathbf{1}+\boldsymbol{\gamma}) \leq \mathbf{c} \leq \infty$.

The strain in the steel at the extreme fibers is:

$$\epsilon_{s1} = \frac{\epsilon_{cu}}{c}\left(c - \frac{h}{2}(1+\gamma)\right)$$

$$\epsilon_{s2} = \frac{\epsilon_{cu}}{c}\left(c - \frac{h}{2}(1-\gamma)\right)$$

Force and moment provided by concrete are:

$$\mathrm{F_c} = \begin{cases} \alpha_1\, \mathrm{f'_c}\, \mathrm{A_g}, & \beta_1\, c > h \\ -\alpha_1 \dfrac{\mathrm{f'_c}}{2} h^2 \displaystyle\int_{\theta 2}^{0} (\mathrm{Sin}[\theta])^2 d\theta\,, & \beta_1\, c \leq h \end{cases}$$

$$\mathrm{M_c} = \begin{cases} 0, & \beta_1\, c > h \\ -\alpha_1 \dfrac{\mathrm{f'_c}}{4} h^3 \displaystyle\int_{\theta 2}^{0} (\mathrm{Cos}[\theta])(\mathrm{Sin}[\theta])^2 d\theta\,, & \beta_1\, c \leq h \end{cases}$$

Steel stress is:

$$\mathrm{f_s} = \frac{\mathrm{E_s}\, \epsilon_{\mathrm{cu}}}{c}\left(c - \frac{h}{2}(1 - \gamma\, \mathrm{Cos}[\theta])\right) \leq \mathrm{f_y}$$

Force and moment provided by steel are:

$$F_s = \frac{A_s}{\pi}\int_0^{\pi} f_s \, d\theta$$

$$M_s = \frac{\gamma h \, A_s}{2\pi}\int_0^{\pi} \mathrm{Cos}[\theta]\, f_s \, d\theta$$

Force and moment correction due to the overlap between steel and concrete are:

$$F_f = \begin{cases} -\alpha_1 \, f'_c \, \rho \, A_g, & \beta_1 \, c \geq \dfrac{h}{2}(1+\gamma) \\ \dfrac{-\alpha_1 \, f'_c \, \rho \, A_g}{\pi}\theta_5, & \beta_1 \, c < \dfrac{h}{2}(1+\gamma) \end{cases}$$

$$M_f = \begin{cases} 0, & \beta_1 \, c \geq \dfrac{h}{2}(1+\gamma) \\ -\dfrac{\alpha_1 \, f'_c \, \rho \, A_g \, \gamma \, h \, \mathrm{Sin}[\theta_5]}{2\pi}, & \beta_1 \, c < \dfrac{h}{2}(1+\gamma) \end{cases}$$

The resultant force and moment:

$$P = \sum \text{forces}$$

$$M = \sum \text{moments}$$

4) $\frac{h}{2}(1-\gamma) \leq c \leq \frac{h}{2}(1+\gamma)$

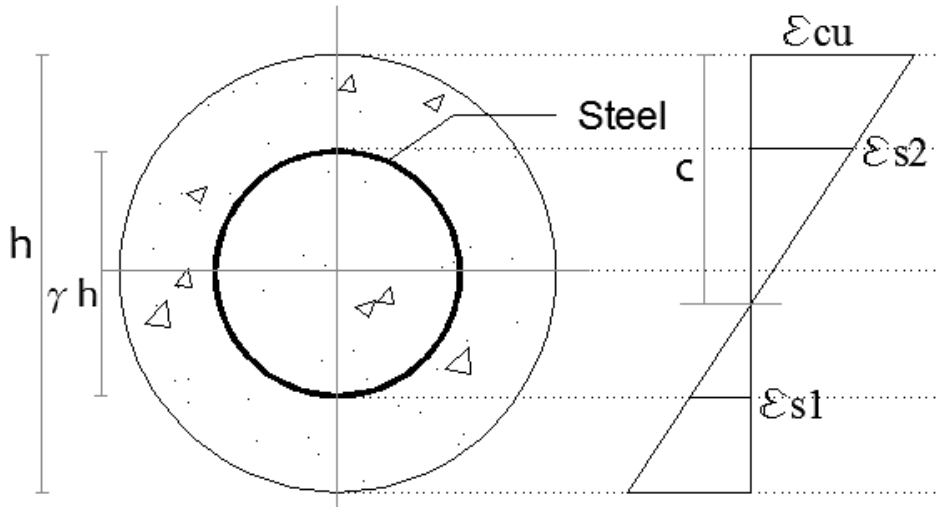

Figure 3.8: Strain distribution in circular section when $\frac{h}{2}(1-\gamma) \leq c \leq \frac{h}{2}(1+\gamma)$.

Strain in steel at the extreme fibers is:

$$\epsilon_{s1} = \frac{\epsilon_{cu}}{c}\left(\frac{h}{2}(1+\gamma) - c\right)$$

$$\epsilon_{s2} = \frac{\epsilon_{cu}}{c}\left(c - \frac{h}{2}(1-\gamma)\right)$$

Stress in steel is:

$$f_s = \frac{f_y\ \gamma}{2\left(\frac{c}{h}\right)\left(\frac{\varepsilon_y}{\varepsilon_{cu}}\right)}(\cos[\theta] - \cos[\theta_1]) \leq f_y$$

Force and moment provided by steel:

$$\frac{F_s}{2} = \int_0^{\theta_3} f_y\, dA_s + \int_{\theta_3}^{\theta_1} f_s\, dA_s - \int_{\theta_1}^{\theta_4} f_s\, dA_s - \int_{\theta_4}^{\pi} f_y\, dA_s$$

$$\frac{M_s}{2} = \frac{f_y\,\rho\,A_g\,\gamma\,h}{4\pi}\left\{\int_0^{\theta_3}\cos[\theta]\,d\theta + \frac{\gamma}{2\left(\frac{c}{h}\right)\left(\frac{\varepsilon_y}{\varepsilon_{cu}}\right)}\int_{\theta_3}^{\theta_4}(\cos[\theta]-\cos[\theta_1])\,\cos[\theta]\,d\theta - \int_{\theta_4}^{\pi}\cos[\theta]\,d\theta\right\}$$

Force and moment provided by concrete:

$$F_c = \frac{-0.85f_c'\,h^2}{2}\int_{\theta_2}^{0}\sin^2[\theta]\,d\theta$$

$$M_c = \frac{-0.85f_c'\,h^3}{4}\int_{\theta_2}^{0}\sin^2[\theta]\cos[\theta]\,d\theta$$

Correction force and moment due to overlap of steel and concrete:

$$F_f = \frac{-0.85f_c'\,\rho\,A_g}{\pi}\theta_5$$

$$M_f = \frac{-0.85f_c'\,\rho\,A_g\gamma\,h}{2\pi}\mathrm{Sin}[\theta_5]$$

The resultant force and moment:

$$P = \sum \text{forces}$$

$$M = \sum \text{moments}$$

5) $\mathbf{0 < c \leq \frac{h}{2}(1-\gamma)}$

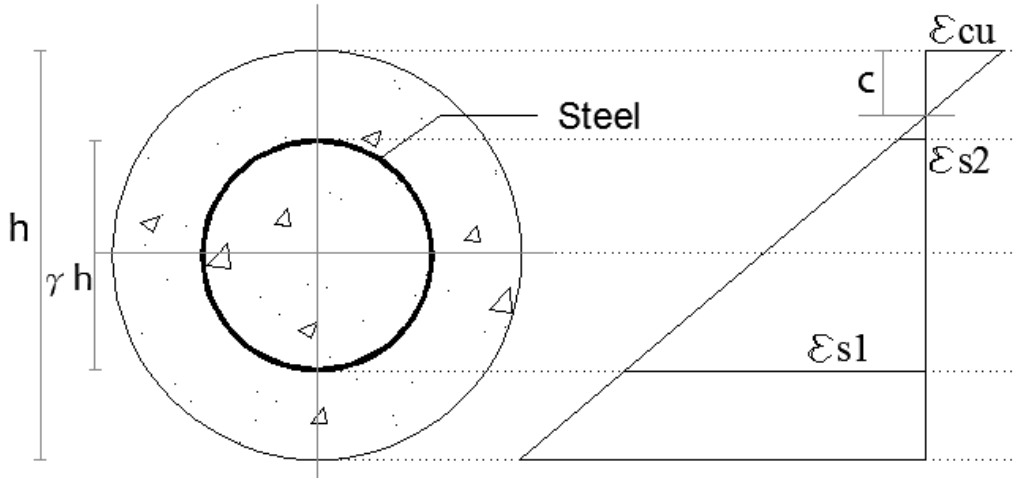

Figure 3.9: Strain distribution in circular section when $\mathbf{0 < c \leq \frac{h}{2}(1-\gamma)}$.

Strain in steel at extreme fibers:

$$\epsilon_{s1} = \frac{\epsilon_{cu}}{c}\left(c - \frac{h}{2}(1+\gamma)\right)$$

$$\epsilon_{s2} = \frac{\epsilon_{cu}}{c}\left(c - \frac{h}{2}(1-\gamma)\right)$$

Force and moment provided by concrete:

$$F_c = \frac{-\alpha_1 f_c' h^2}{2}\int_{\theta_2}^{0} \sin^2[\theta]\, d\theta$$

$$M_c = \frac{-\alpha_1 f_c' h^3}{4}\int_{\theta_2}^{0} \sin^2[\theta]\, cos[\theta]\, d\theta$$

Stress in steel:

$$f_s = \frac{E_s \epsilon_{cu}}{c}\left(-c + \frac{h}{2}(1 - \gamma\, Cos[\theta])\right) \leq f_y$$

Force and moment provided by steel are:

$$F_s = \frac{A_s}{\pi} \int_0^{\pi} f_s \, d\theta$$

$$M_s = \frac{\gamma h \, A_s}{2\pi} \int_0^{\pi} Cos[\theta] \, f_s \, d\theta$$

Correction force and moment due to overlap between steel and concrete:

$$M_f = 0$$

$$F_f = 0$$

The resultant force and moment:

$$P = \sum forces$$

$$M = \sum moments$$

Where:

F_f: Force correction due to overlap of concrete and steel stresses.

M_f: Moment correction due to overlap of concrete and steel stresses.

F_c: Total force provided by concrete.

M_c: Total moment provided by concrete.

f_s: Stress in steel.

F_s: Total force provided by steel.

M_s: Total moment provided by steel

3.4.1 Rectangular column

Rectangular Cartesian coordinate system is used to find the column capacities. The following definitions are used in the derivations of the interaction diagrams for rectangular cross section.

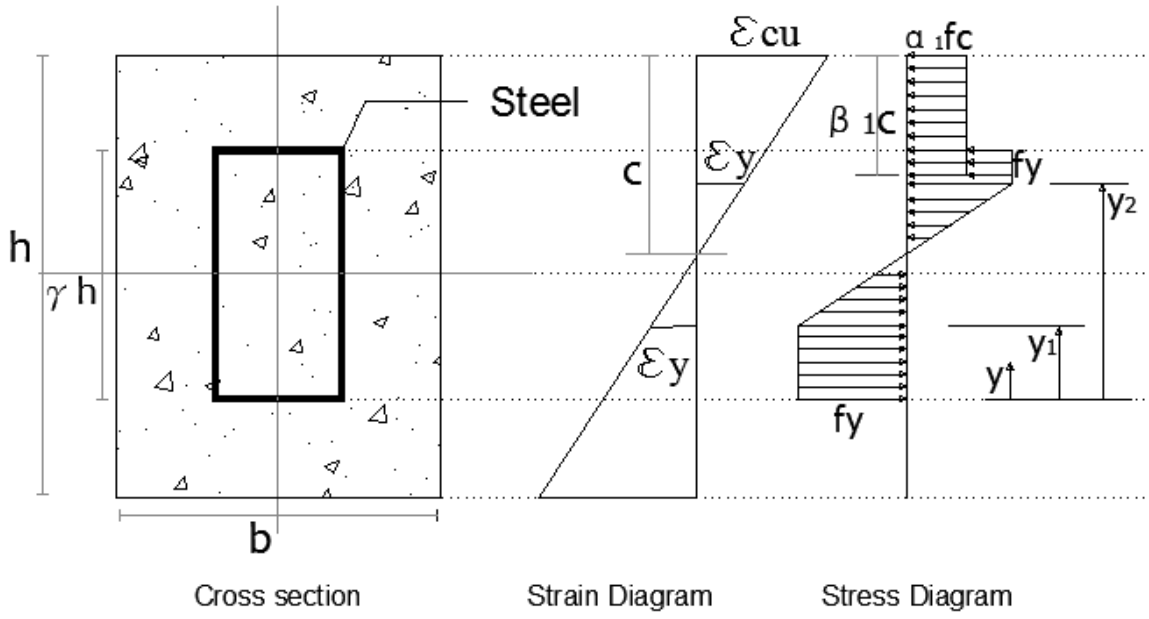

Figure 3.10: Basic sketch and definitions for rectangular column section.

Where:

y: Distance measured form extreme tensile steel.

y_1: locates the end of yielding in the steel under tension.

y_2: locates the start of yielding in the steel under compression.

In order to find the interaction diagrams, the neutral axis depth is assumed to be in the following ranges:

1) $\mathbf{c = \infty}$

$$P_o = (A_g - \rho\, A_g)\alpha_1 f'_c + \rho\, A_g f_y$$

2) $\mathbf{c = 0}$

$$t = -\rho\, A_g f_y$$

3) $\mathbf{\frac{h}{2}(1+\gamma) \le c \le \infty}$

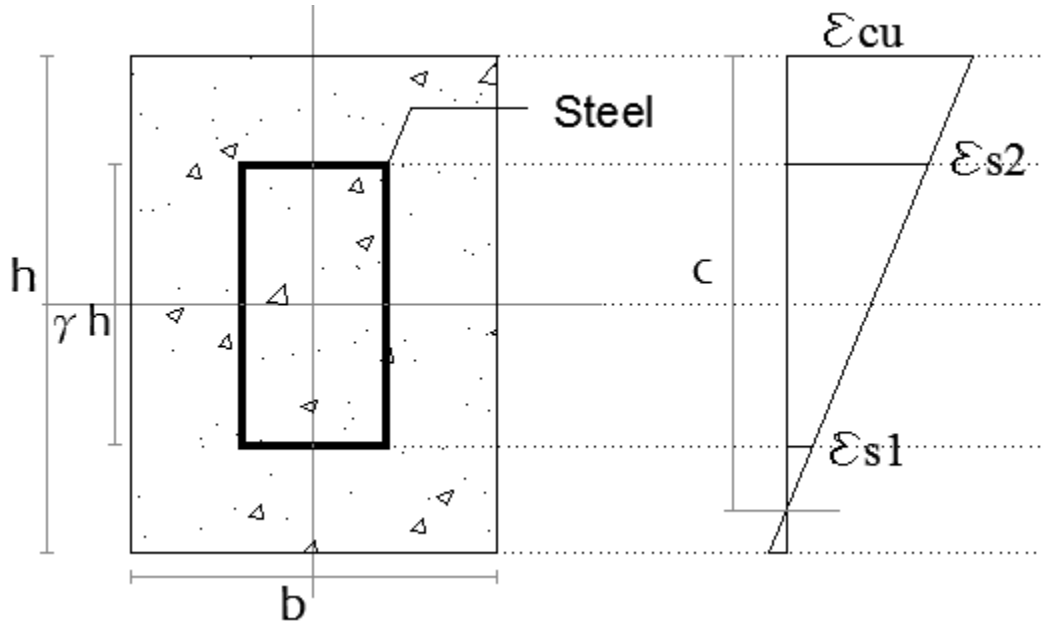

Figure 3.11: strain distribution in rectangular cross section when $\frac{h}{2}(1+\gamma) \le c \le \infty$.

Strain in steel at the extreme fibers is:

$$\epsilon_{s1} = \frac{\epsilon_{cu}}{c}\left(c - \frac{h}{2}(1+\gamma)\right)$$

$$\epsilon_{s2} = \frac{\epsilon_{cu}}{c}\left(c - \frac{h}{2}(1-\gamma)\right)$$

Strain at distance x from compression fiber is:

$$\epsilon = \frac{\epsilon_{cu}}{c}(c - x)$$

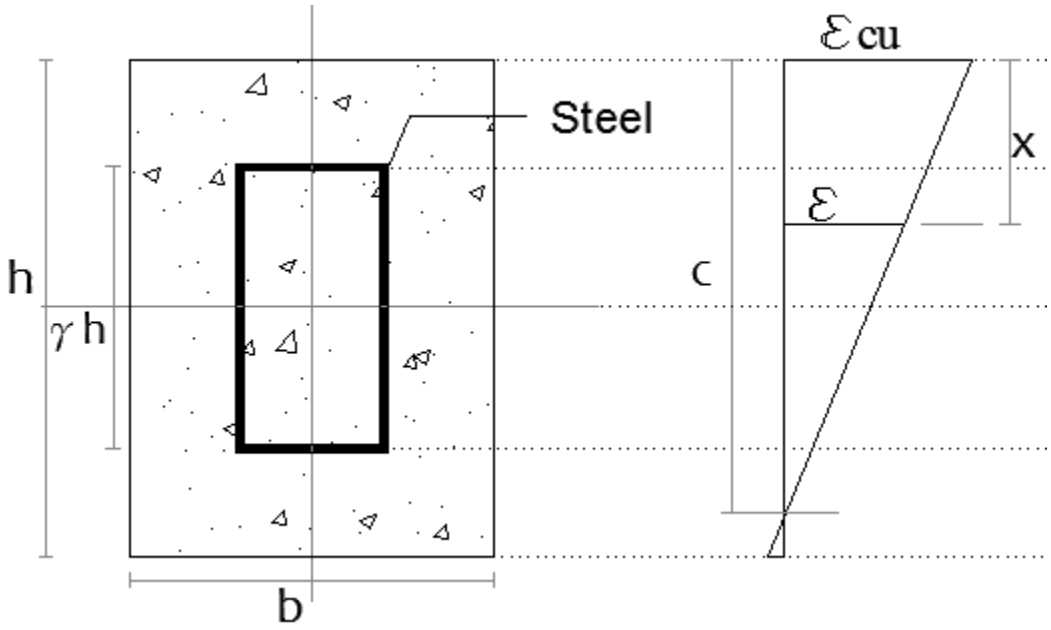

Figure 3.12: Strain at distance x from compression fiber when $\frac{h}{2}(1+\gamma) \leq c \leq \infty$.

Force and moment provided by concrete are:

$$F_c = \begin{cases} \alpha_1 f'_c \, b \, h, & \beta_1 \, c > h \\ \alpha_1 f'_c \, b \, \beta_1 c, & \beta 1 \, c \leq h \end{cases}$$

$$M_c = \begin{cases} 0, & \beta_1 \, c > h \\ \alpha_1 f'_c \, b \, \beta_1 \, c \left(\frac{h - \beta_1 \, c}{2}\right), & \beta_1 \, c \leq h \end{cases}$$

Stresses in steel:

$$f_{s1} = \epsilon_{s1} E_s \leq f_y$$

$$f_{s2} = \epsilon \, E_s \leq f_y \ , \ \text{where } \frac{h}{2}(1-\gamma) \leq x \leq \frac{h}{2}(1+\gamma)$$

$$f_{s3} = \epsilon_{s2} E_s \leq f_y$$

Forces and moments provided by steel:

$$F_{s1} = A_{s1}(f_{s1} - \alpha_1 f'_c)$$

$$F_{s2} = \frac{A_s}{\gamma h}\int_{\frac{h}{2}(1-\gamma)}^{\gamma h}(f_{s2} - \alpha_1\, f'_c)dx$$

$$F_{s3} = A_{s3}\,(f_{s3} - \alpha_1 f'_c)$$

$$M_{s1} = F_{s1} * \frac{\gamma\, h}{2}$$

$$M_{s2} = \frac{A_s}{\gamma h}\int_{\frac{h}{2}(1-\gamma)}^{\gamma h}(\frac{h}{2} - x)(f_{s2} - \alpha_1\, f'_c)\, dx$$

$$M_{s3} = F_{s3} * \frac{\gamma\, h}{2}$$

The resultant force and moment:

$$P = \sum \text{forces}$$

$$M = \sum \text{moments}$$

4) $\mathbf{\frac{h}{2}(1-\gamma) \le c \le \frac{h}{2}(1+\gamma)}$

Strain in steel at the extreme fibers is:

$$\epsilon_{s1} = \frac{\epsilon_{cu}}{c}\left(\frac{h}{2}(1+\gamma) - c\right)$$

$$\epsilon_{s2} = \frac{\epsilon_{cu}}{c}(c - \frac{h}{2}(1-\gamma))$$

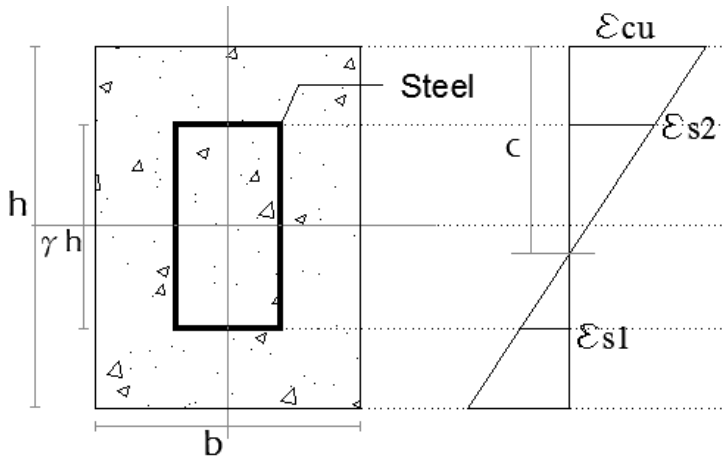

Figure 3.13: Strain distribution for rectangular cross section when $\frac{h}{2}(1-\gamma) \leq c \leq \frac{h}{2}(1+\gamma)$.

Strain at distance x from compression fiber is:

$$\epsilon = \frac{\epsilon_{cu}\,(x - \frac{h}{2}(1+\gamma))}{c} + \epsilon_{cu}$$

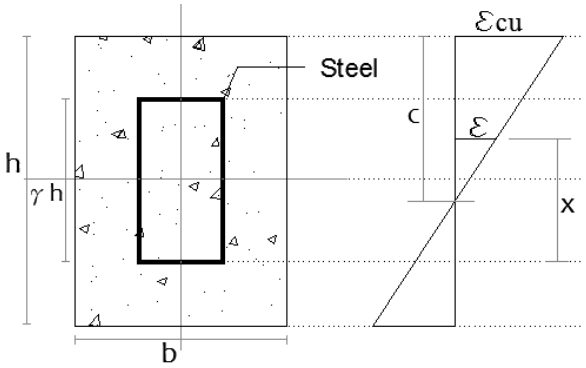

Figure 3.14: Strain at distance x from the tensile steel face when $\frac{h}{2}(1-\gamma) \leq c \leq \frac{h}{2}(1+\gamma)$.

Force and moment provided by concrete are:

$$F_c = \alpha_1\, f'_c\, b\, \beta_1\, c$$

$$M_c = F_c(\frac{h - \beta_1\, c}{2})$$

Stresses in steel:

$$f_{s1} = \epsilon_{s1}\, E_s \leq f_y$$

$$f_{s2} = \epsilon\, E_s \leq f_y \ , \ \text{where } 0 \leq x \leq \gamma h$$

$$f_{s3} = \epsilon_{s2}\, E_s \leq f_y$$

Forces and moments provided by steel:

$$F_{s1} = A_{s1} f_{s1}$$

$$F_{s2} = \frac{A_s}{\gamma h} \int_0^{\frac{h}{2}(1+\gamma)-c} f_{s2}\, dx + \frac{A_s}{\gamma h} \int_{\frac{h}{2}(1+\gamma)-c}^{\gamma h} f_{s2} - \alpha_1\, f_c\, dx$$

$$F_{s3} = A_{s3}\, (f_{s3} - \alpha\_1 f_c)$$

$$M_{s1} = F_{s1} * \frac{\gamma\, h}{2}$$

$$M_{s2} = \frac{A_s}{\gamma h} \int_0^{\frac{h}{2}(1+\gamma)-c} (\frac{h}{2} - x)(f_{s2})dx + \frac{A_s}{\gamma h} \int_{\frac{h}{2}(1+\gamma)-c}^{\gamma h} (\frac{h}{2} - x)(f_{s2} - \alpha_1 f_c)dx$$

$$M_{s3} = F_{s3} * \frac{\gamma\, h}{2}$$

The resultant force and moment:

$$P = \sum \text{forces}$$

$$M = \sum \text{moments}$$

5) $\mathbf{c \leq \frac{h}{2}(1-\gamma)}$

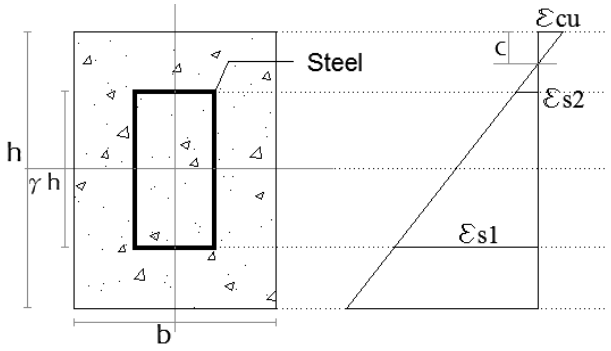

Figure 3.15: Strain distribution for rectangular cross section when $\mathbf{c \leq \frac{h}{2}(1-\gamma)}$.

Strain in steel at the extreme fibers is:

$$\epsilon_{s1} = \frac{\epsilon_{cu}}{c}\left(\frac{h}{2}(1+\gamma) - c\right)$$

$$\epsilon_{s2} = \frac{\epsilon_{cu}}{c}\left(\frac{h}{2}(1-\gamma) - c\right)$$

Strain at distance x from compression fiber is:

$$\epsilon = \frac{\epsilon_{cu}\left(\frac{h}{2}(1+\gamma) - x - c\right)}{c}$$

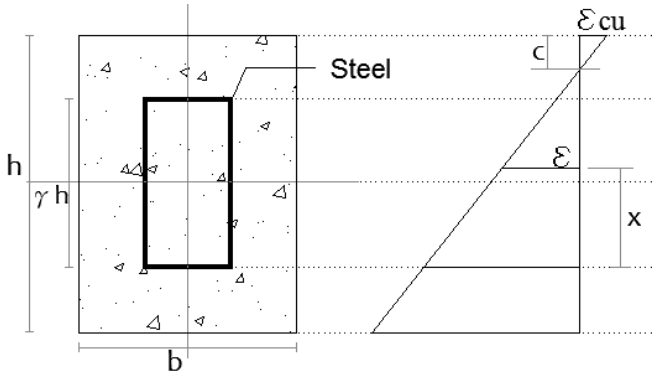

Figure 3.16: Strain at distance x from the tensile steel face when $\mathbf{c \leq \frac{h}{2}(1-\gamma)}$.

Force and moment provided by concrete are:

$$F_c = \alpha_1 f_c' \, b \, \beta_1 \, c$$

$$M_c = F_c\left(\frac{h - \beta_1 \, c}{2}\right)$$

Stresses in steel:

$$f_{s1} = \epsilon_{s1} \, E_s \leq f_y$$

$$f_{s2} = \epsilon \, E_s \leq f_y \ , \ \text{where } 0 \leq x \leq \gamma h$$

$$f_{s3} = \epsilon_{s2} \, E_s \leq f_y$$

Forces and moments provided by steel:

$$F_{s1} = A_{s1} f_{s1}$$

$$F_{s2} = \frac{A_s}{\gamma h} \int_0^{\gamma h} (f_{s2}) dx$$

$$F_{s3} = A_{s3} \, (f_{s3})$$

$$M_{s1} = F_{s1} * \frac{\gamma \, h}{2}$$

$$M_{s2} = \frac{A_s}{\gamma h} \int_0^{\gamma h} \left(\frac{h}{2} - x\right)(f_{s2}) dx$$

$$M_{s3} = F_{s3} * \frac{\gamma \, h}{2}$$

The resultant force and moment:

$$P = \sum \text{forces}$$

$$M = \sum \text{moments}$$

The above procedure can be used to obtain nominal capacity of the column with steel distributed on two faces only by setting $A_{s2} = 0$ in all equations.

3.5 MATHEMATICA Code

The procedure explained in section 3.3 for generating the interaction curves has been implemented in a Mathematica code. The code is capable of generating interaction curves for any arbitrary values for f'_c, f_y and γ assuming that steel is uniformly distributed.

The algorithm of the code can be represented by the flow chart given in Figure 3.17.

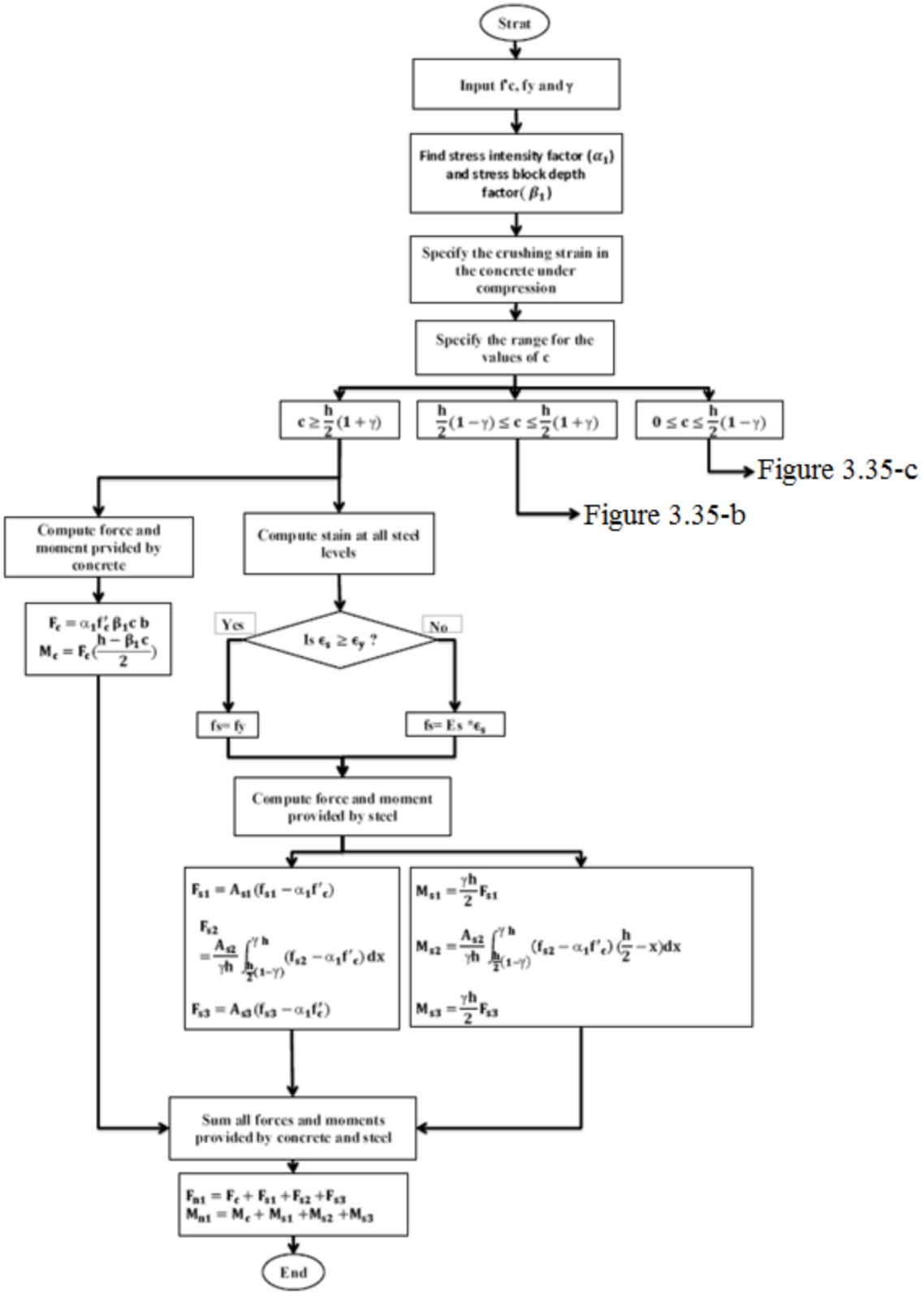

Figure 3.17-a: Flow chart for Mathematica code for $c \geq \frac{h}{2}(1+\gamma)$.

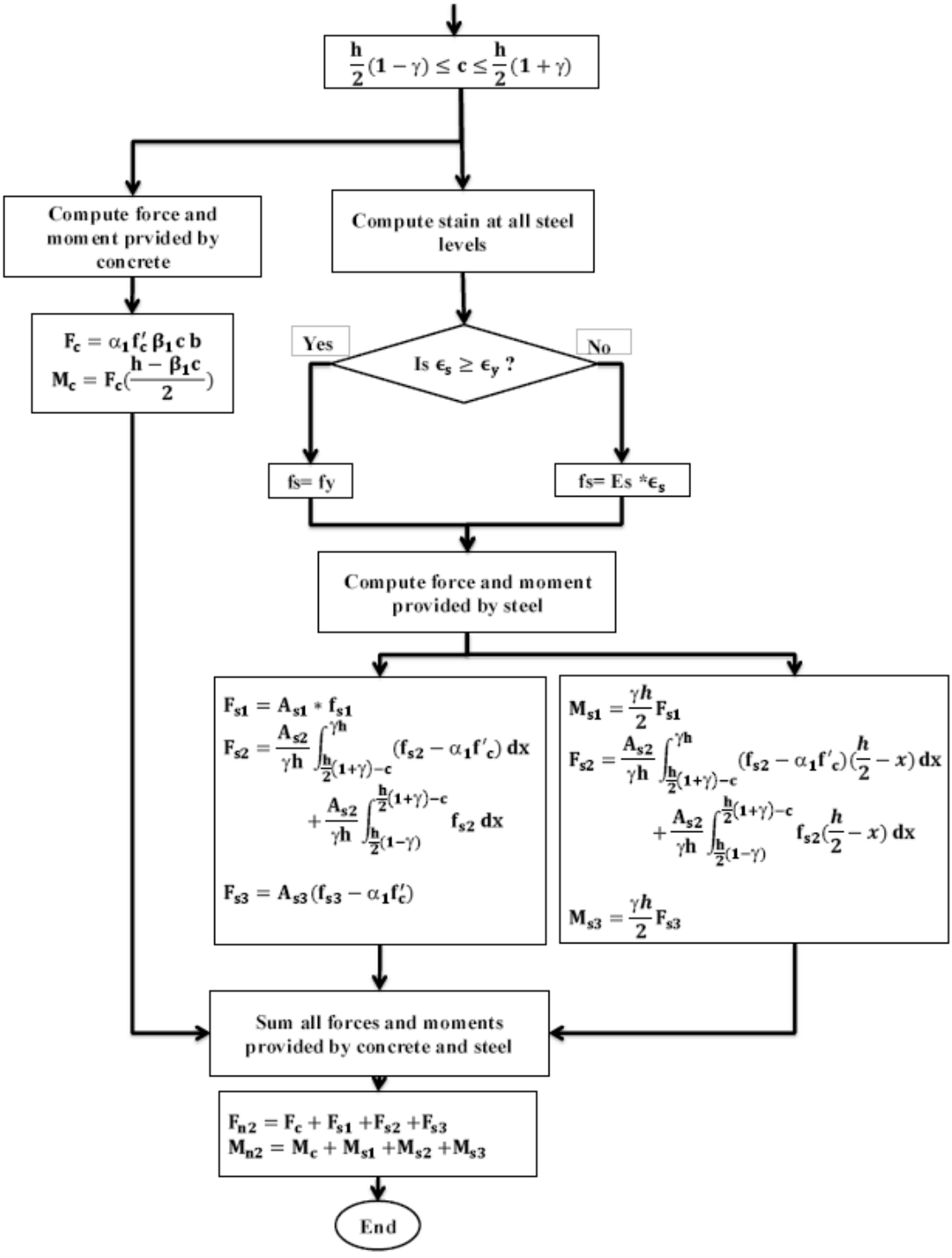

Figure 3.17-b: Flow chart for Mathematica code for $\frac{h}{2}(1-\gamma) \le c \le \frac{h}{2}(1+\gamma)$.

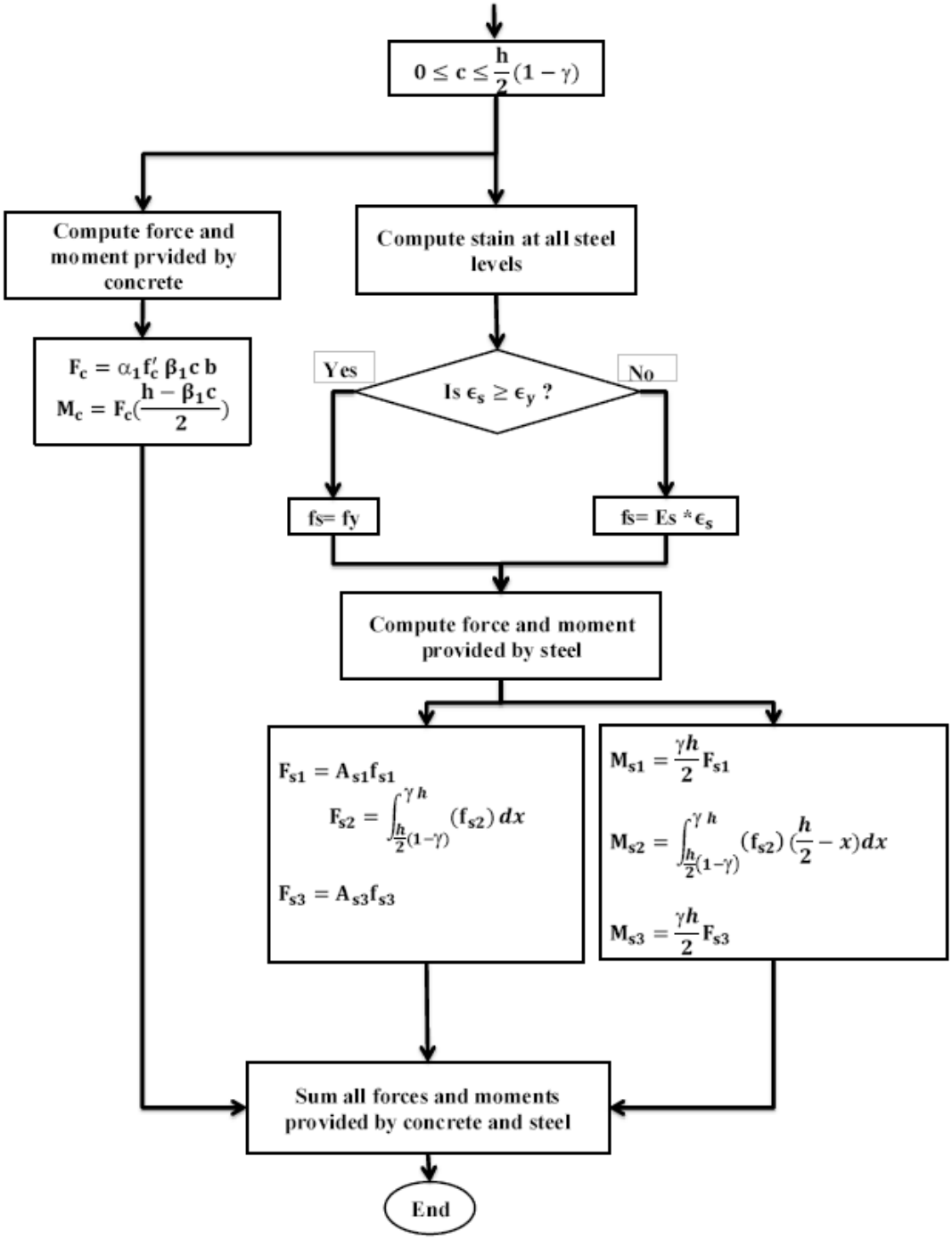

Figure 3.17-c: Flow chart for Mathematica code $0 \le c \le \frac{h}{2}(1-\gamma)$.

3.6 Validation using ACI-Interaction Diagrams

The developed code has been validated using ACI [31] Interaction diagrams and PCA software. ACI interaction diagrams were generated for concrete strength up to 12 ksi using the equivalent rectangular stress block as proposed by ACI318 code [1], while PCA software uses the equivalent rectangular stress block model for the concrete with arbitrary values of α_1 and β_1.

3.6.1 Comparison with ACI interaction curves

For the purpose of comparison, three different cross sections have been analyzed: circular, rectangular with steel distributed on two faces and rectangular with steel distributed on four faces. For all analyzed sections, the following material and geometric properties have been assumed:

$f_y = 60$ ksi

$f'_c = 4{,}6$ ksi

$\gamma = 0.7, 0.9$

$\rho = 1\%, 2\%, 3\%, 4\%, 5\%, 6\%, 7\%, 8\%$

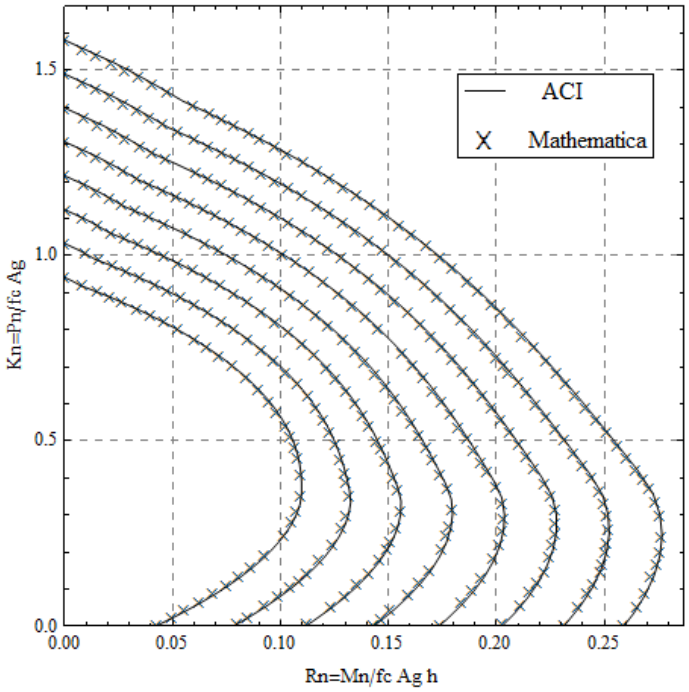

Figure 3.18: ACI [31] vs. Mathematica-developed interaction diagrams for circular column with γ=0.9, f'$_c$=6ksi and f$_y$=60ksi.

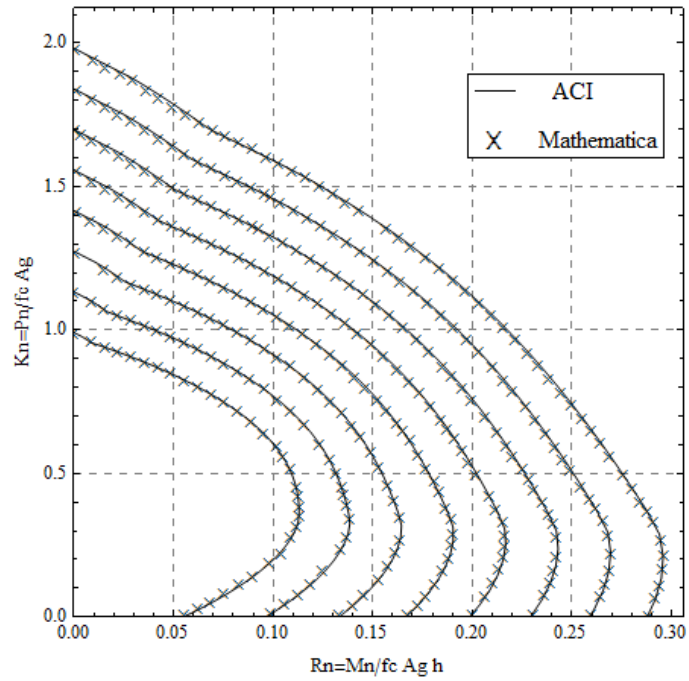

Figure 3.19: ACI [31] vs. Mathematica-developed interaction diagrams for circular column with γ=0.7, f'c=4ksi and f$_y$=60ksi.

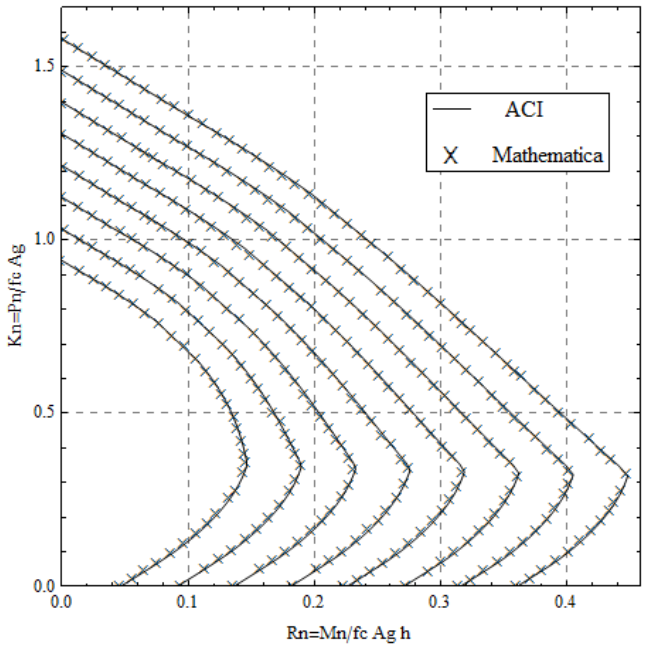

Figure 3.20: ACI [31] vs. Mathematica-developed interaction diagrams for rectangular column with steel on two faces only and γ=0.9, f'c=6ksi and f_y=60ksi.

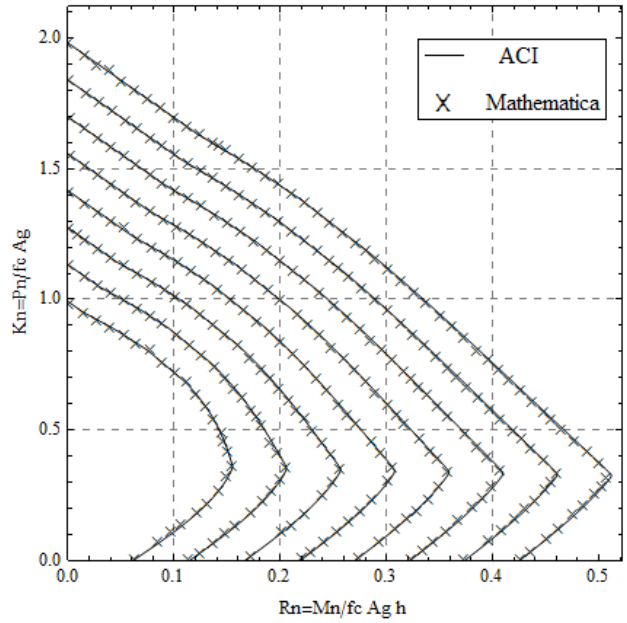

Figure 3.21: ACI [31] vs. Mathematica-developed interaction diagrams for rectangular column with steel on two faces only and γ=0.7, f'c=4ksi and f_y=60ksi.

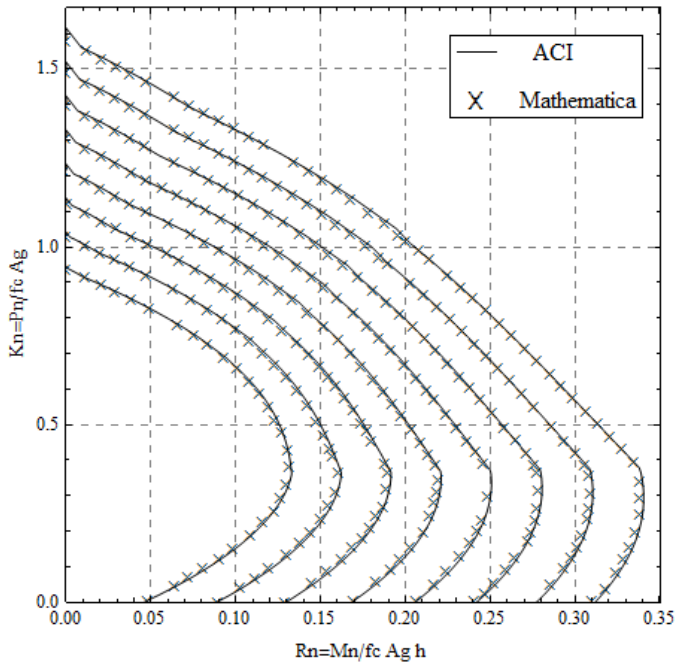

Figure 3.22: ACI [31] vs. Mathematica-developed interaction diagrams for Rectangular column with steel on four faces and γ=0.9, f'c=6ksi and f_y=60ksi.

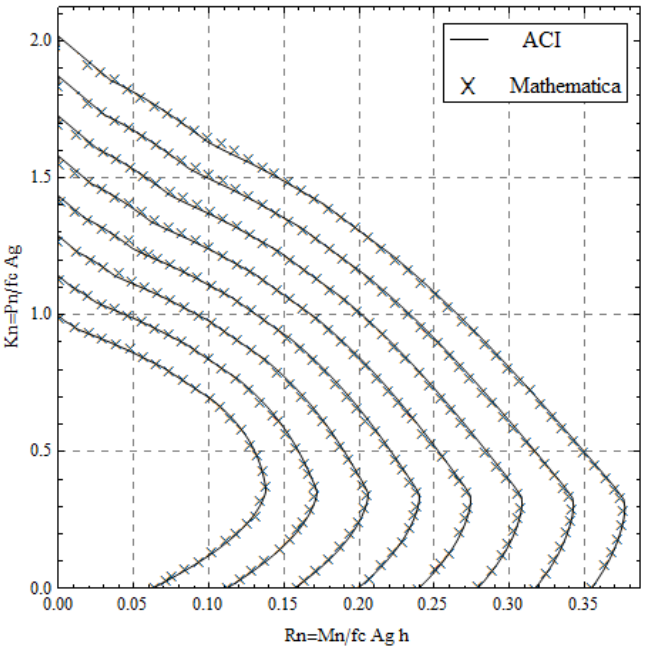

Figure 3.23: ACI [31] vs. Mathematica-developed interaction diagrams for Rectangular column with steel on four faces and γ=0.7, f'c=4ksi and f_y=60ksi.

Since both Mathematica code and ACI interaction curves are based on non-dimensional parameters and they are generated using the same assumptions and formulations, both curves are exactly coinciding, as expected.

3.6.2 Comparison with PCA software

Portland Cement Association (PCA) software was developed to design and investigate reinforced concrete columns. Columns can be any shape with or without openings. Slenderness effect of the columns can be considered in PCA. The stress-stain relationship of concrete under compression is represented in PCA by the equivalent rectangular stress block and the default stress block is that which was proposed by the ACI code. The main important thing is that stress block parameters can be changed to any arbitrary values.

Unlike ACI curves which are based on non-dimensional parameters, PCA generates a one dimensional interaction diagram corresponding to the assigned cross section. The comparison was carried out for the following cases:

Case 1: Rectangular cross section with steel distributed uniformly around the all faces.

The column has the following material and geometric properties:

$f_y = 75$ ksi

$f'_c = 4$ ksi

$\gamma = 0.75$

$\rho = 3.29\%$ & 1.32%

Figure 3.24 shows that both Mathematica-developed and PCA-generated interaction curves are exactly coinciding because the percentage of steel is high ($\rho = 3.29\%$) resulting in more uniformly distributed steel as assumed by Mathematica code. However, as the percentage of steel gets smaller($\rho = 1.32\%$), the steel distribution becomes more discrete and therefore the two curves deviate from each other as shown in Figure 3.25.

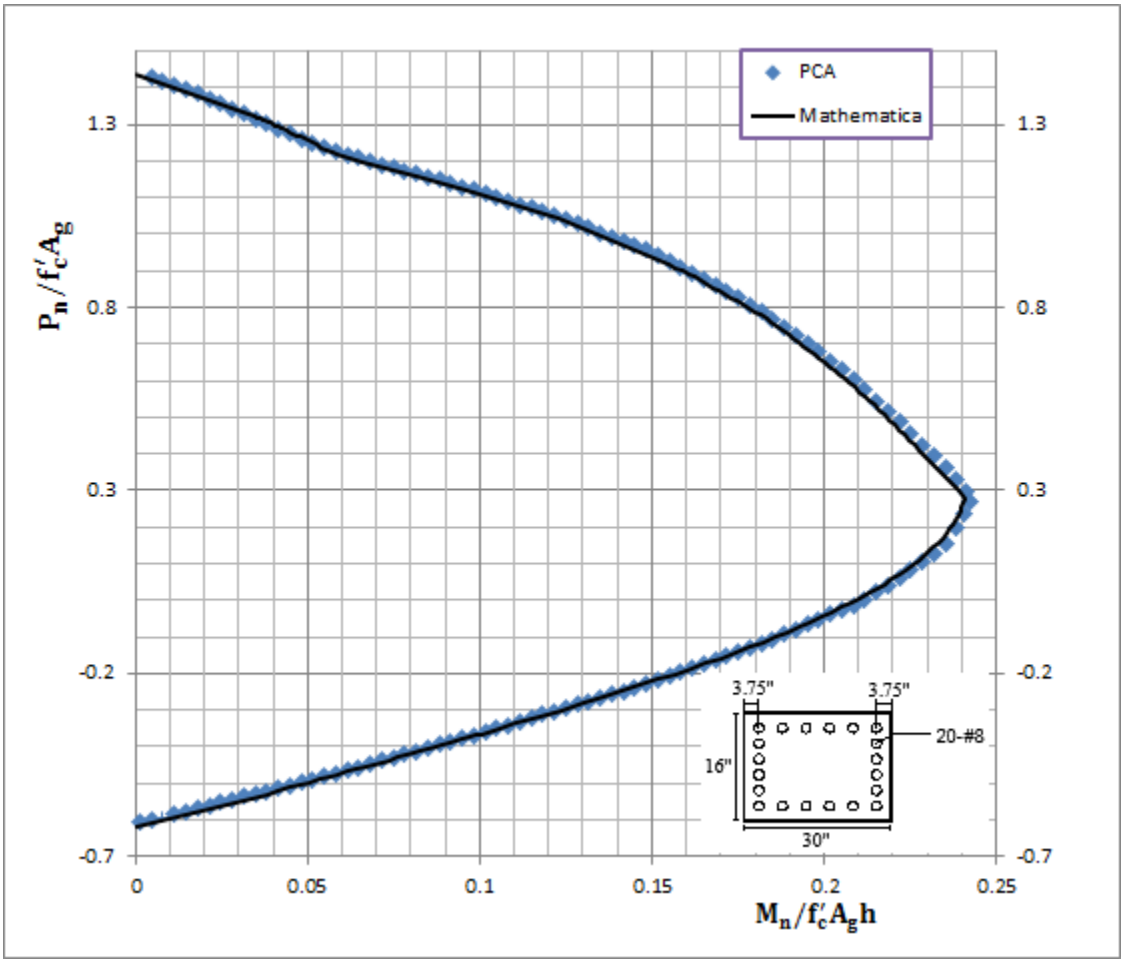

Figure 3.24: Mathematica vs. PCA interaction diagrams for case 1 with $\rho = 3.29\%, f_y = 75$ ksi, $f'_c = 4$ ksi and $\gamma = 0.75$.

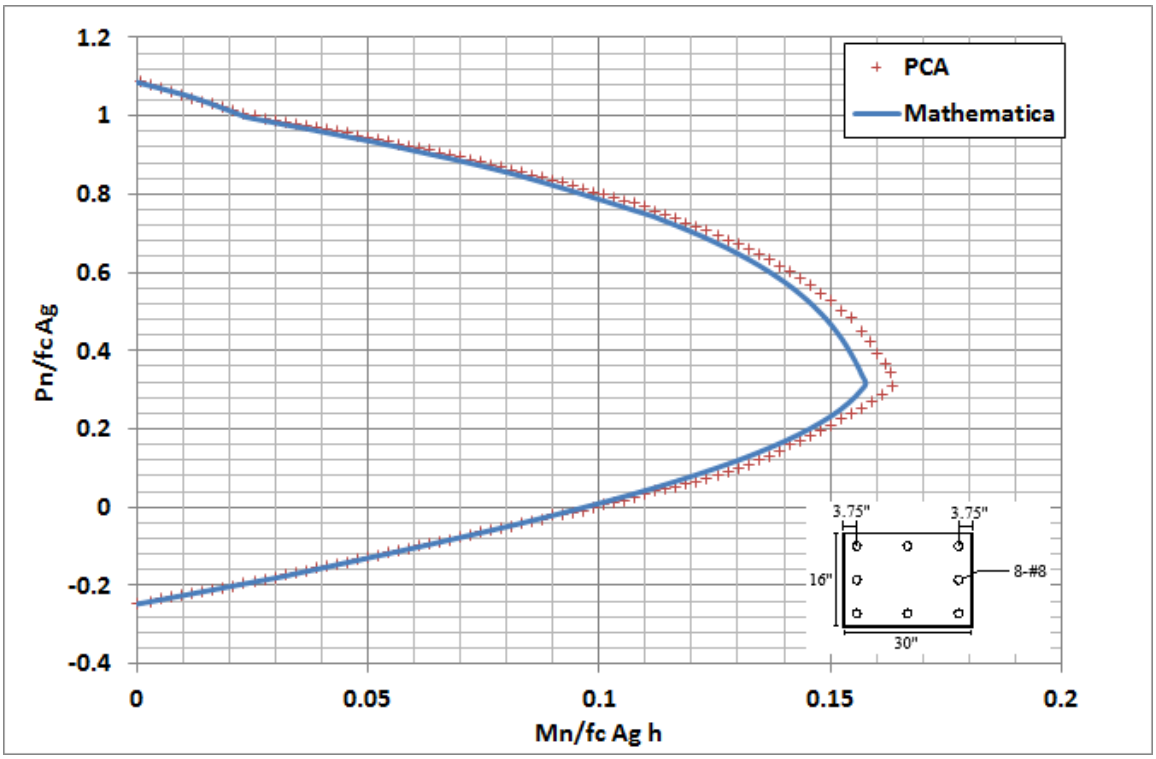

Figure 3.25: Mathematica vs. PCA interaction diagrams for case 1 with $\rho = 1.32\%, f_y = 75$ ksi, $f'_c = 4$ ksi and $\gamma = 0.75$

Case2: rectangular cross section with steel distributed on two faces only.

The column has the following material and geometric properties as below:

$f_y = 60$ ksi

$f'_c = 6$ ksi

$\gamma = 0.8$

$\rho = 2.74\%$ & 1.1%

Figure 3.26 and Figure 3.27 show that for two-side steel arrangement, there is no difference between Mathematica-developed and PCA-generated interaction curves irrespective of the steel ratio, since the column capacity does not depend on the distribution of the steel on the two sides but rather on the amount of steel.

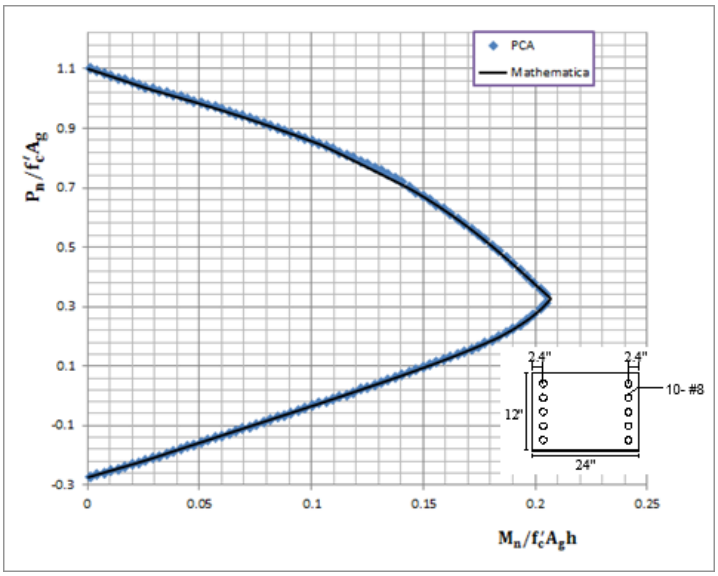

Figure 3.26: Mathematica vs. PCA interaction diagrams for case 2 with$\rho = 2.74\%, f_y = 60$ ksi, $f'_c = 6$ ksi and $\gamma = 0.8$.

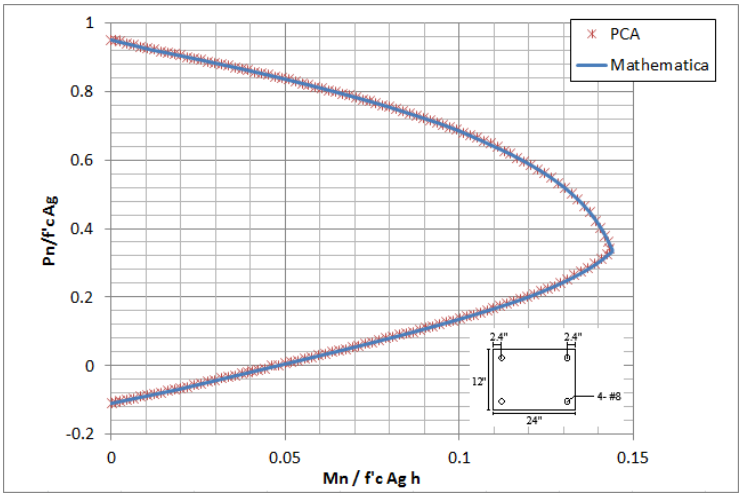

Figure 3.27: Mathematica vs. PCA interaction diagrams for case 2 with$\rho = 1.1\%, f_y = 60$ ksi, $f'_c = 6$ ksi and $\gamma = 0.8$.

Case3: circular cross section with steel distributed uniformly around the perimeter of the circle.

The column has the following material and geometric properties as below:

$f_y = 60$ ksi

$f'_c = 5$ ksi

$\gamma = 0.6$

$\rho = 4.18\%$ & 1.03%

As the percentage of steel increases, the two curves exactly coincide without noticeable difference because the steel is uniformly distributed and closes to the continuous distribution as shown in Figure 3.28. However, as the percentage of steel gets smaller, a small difference occurs because the steel in no longer continuously distributed as shown in Figure 3.29.

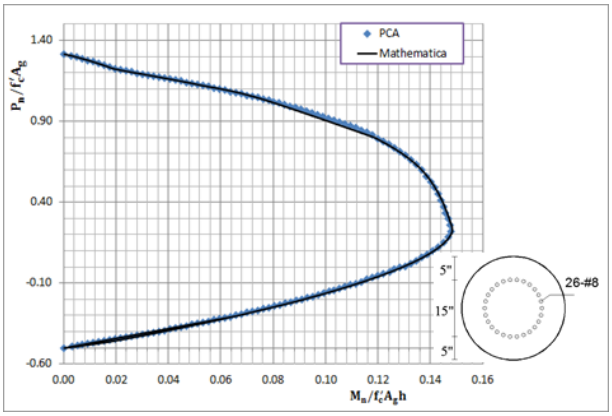

Figure 3.28: Mathematica vs. PCA interaction diagrams for case 3 with$\rho = 4.18\%, f_y = 60$ ksi, $f'_c = 5$ ksi and $\gamma = 0.6$.

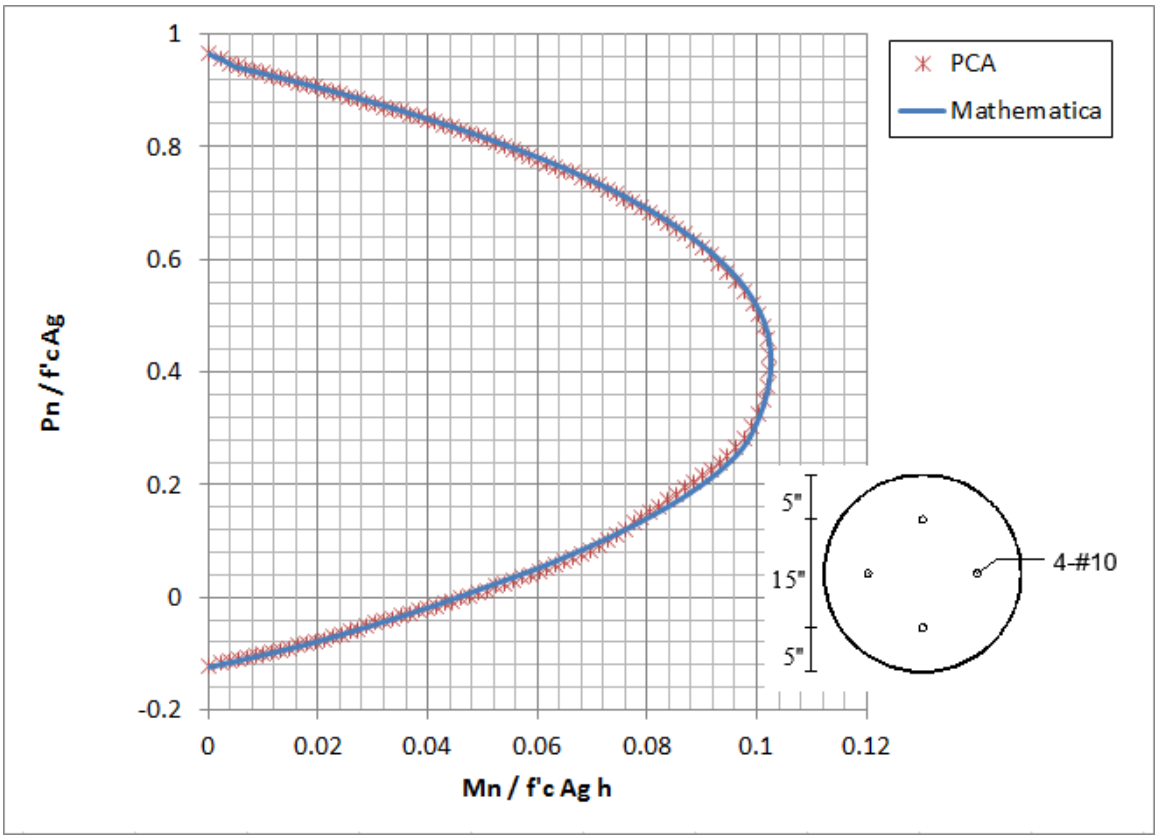

Figure 3.29: Mathematica vs. PCA interaction diagrams for case 3 with$\rho = 1.03\%, f_y = 60$ ksi, $f'_c = 5$ ksi and $\gamma = 0.6$.

CHAPTER FOUR

DEVELOPMENT OF INTERACTION CURVES FOR HSRC COLUMNS

4.1 Basic Assumptions

The formulation of the column capacity for the HSC case is based on the same assumptions used for NSC with the following changes:

- Force provided by concrete is found using the equivalent rectangular stress block with modified stress block parameters. The block parameters are based on the adopted stress-strain models discussed in section 4.2.
- Concrete strength is ranging from 12 ksi (82.5MPa) to 18 ksi (125MPa).

4.2 Effects of stress block parameters on the interaction diagrams

Using the proposed MATHEMATICA code for rectangular columns with steel on two faces only, a random case has been run four times with the random values for α_1(stress intensity factor) and β_1(Stress block depth factor) as shown in Figure 4.1 to Figure 4.3:

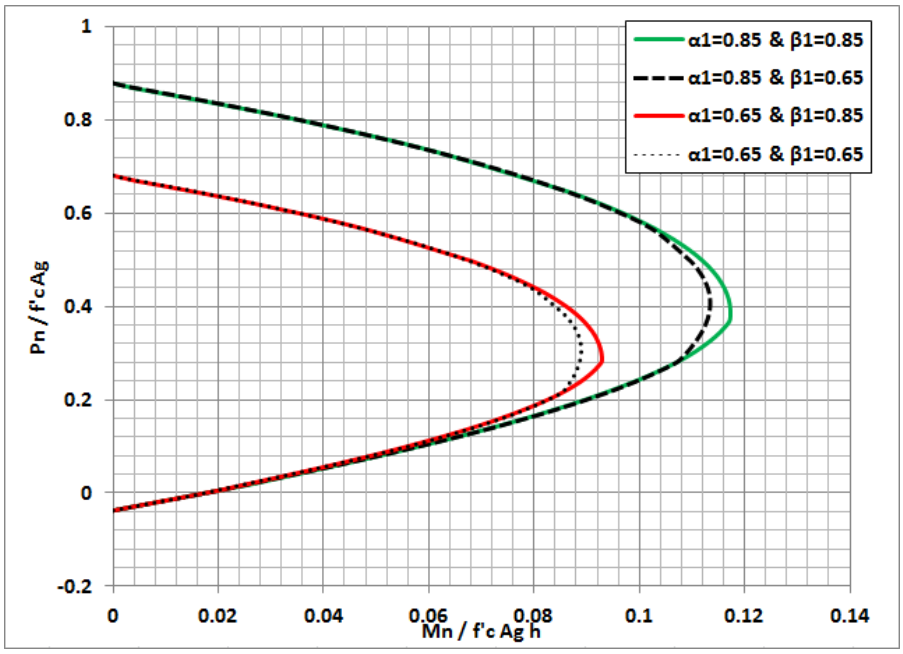

Figure 4.1: Effects of stress block parameters on the interaction diagrams for $\rho = 0.01, f_y = 60\ ksi, f'_c = 16\ ksi\ and\ \gamma = 0.75$.

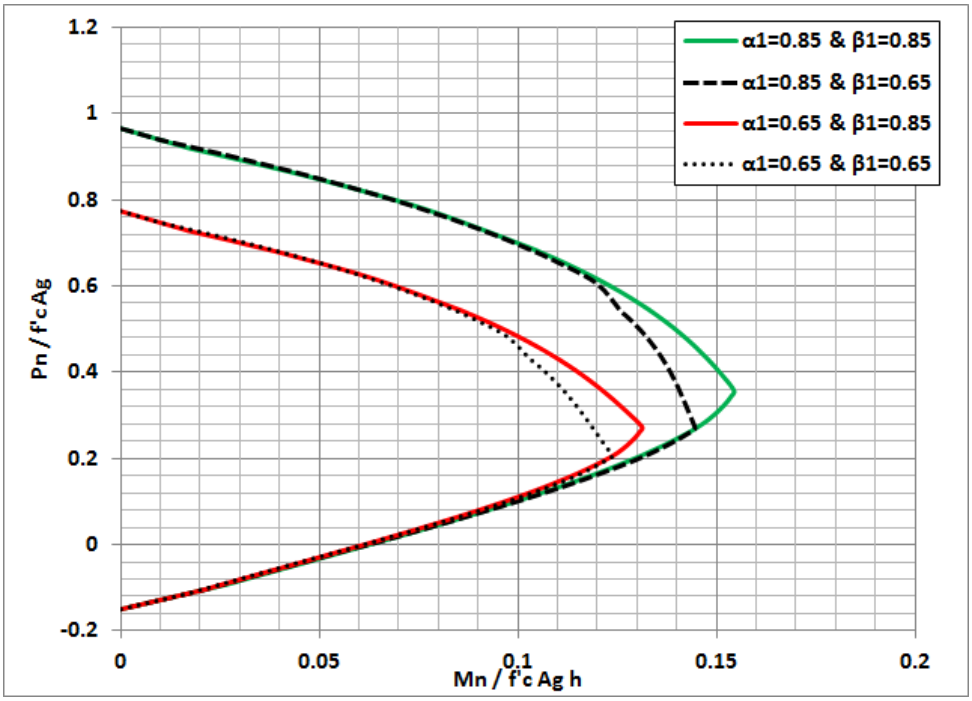

Figure 4.2: Effects of stress block parameters on the interaction diagrams for $\rho = 0.04, f_y = 60\ ksi, f'_c = 16\ ksi\ and\ \gamma = 0.75$.

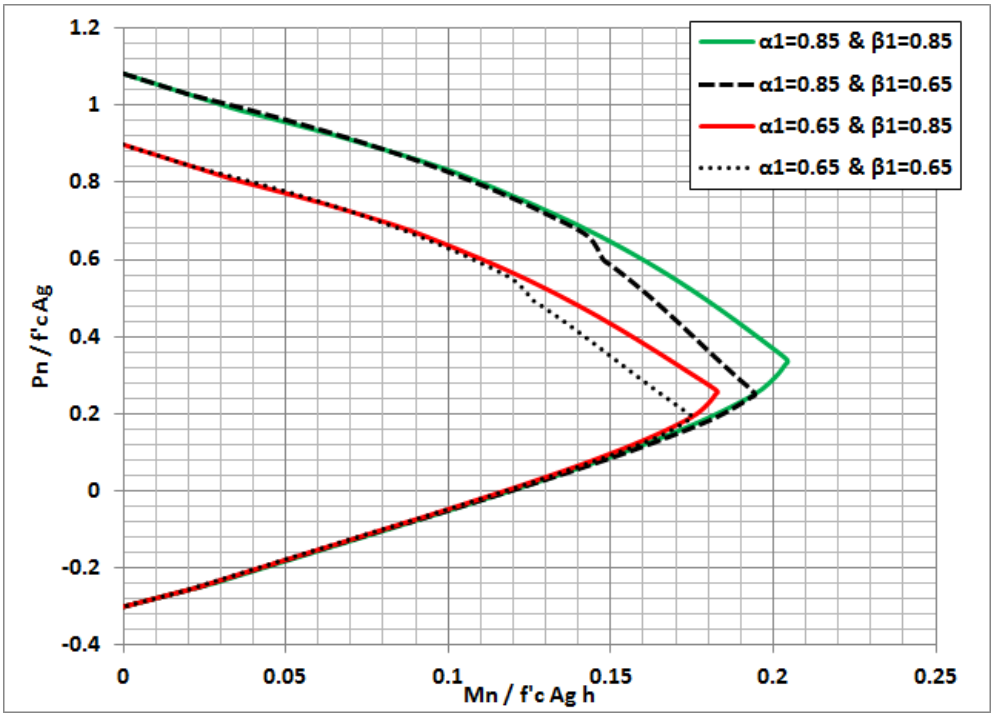

Figure 4.3: Effects of stress block parameters on the interaction diagrams for $\rho = 0.08, f_y = 60\ ksi, f'_c = 16\ ksi\ and\ \gamma = 0.75$.

As shown in Figure 4.1 and Figure 4.3 the major effect of the parameters on the interaction diagrams is in the compression zone and this is controlled mainly by α_1 parameters rather than β_1 parameter. However, β_1 parameter has small effect on the interaction diagrams near the balanced region.

Those parameters have no effects in the tension controlled region because the strength of the column is mainly controlled by the steel rather than concrete. Therefor all interaction diagrams in the figure above overlap each other. The next section 4.3 is required to study the actual parameters for stress block of HSC.

4.3 Adopted Stress-strain Models

Several stress-strain models have been proposed for HSC as shown earlier in the literature review, some of them are investigated here in order to find the best

representation of stress by the use of equivalent rectangular stress block for concrete under compression.

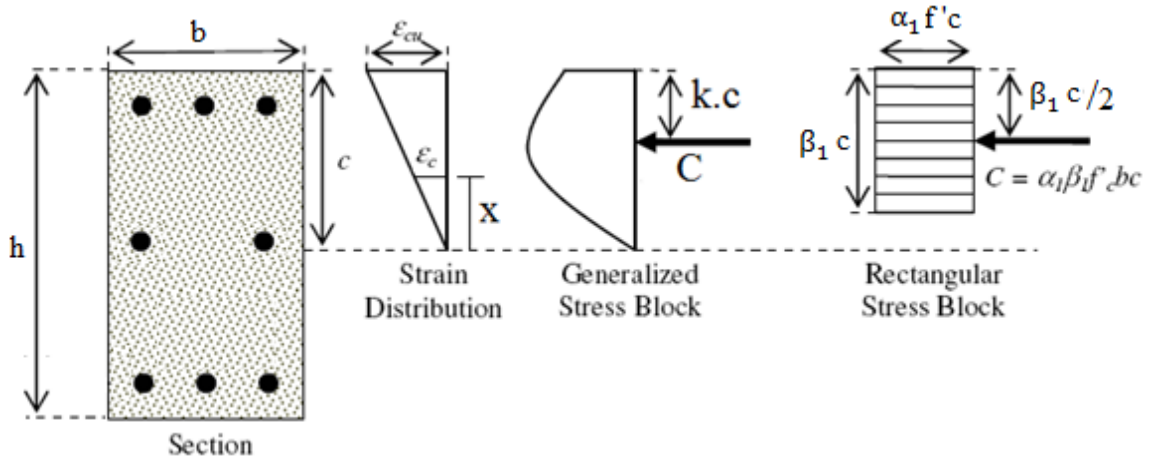

Figure 4.4: Equivalent rectangular stress block.

Oztekin et al., Model, 2003 [12]

Oztekin et al. used the stress-strain model which was proposed by Hognestad et al[3] to obtain a modified model for HSC. The following relation was proposed:

$$f_c = f'_c\left(k\frac{\epsilon_c}{\epsilon_{cu}} - (k-1)\left(\frac{\epsilon_c}{\epsilon_{cu}}\right)^2\right)$$

Where:

K: is a modification parameter as follow:

fc: stress in concrete as a function of concrete strain ϵ_c.

$$k = 2 - \frac{f'_c(MPa) - 40}{70}$$

$$\epsilon_{cu} = [2.2 + 0.015(f'_c(MPa) - 40)\,] \times 10^{-3}$$

Solving the following two equations for α_1 and β_1 with different f_c':

$$\int_0^{x_0} f_c \, d\epsilon_c = \alpha_1 \beta_1 f_c' \epsilon_{cu}$$

$$\int_0^{x_0} f_c \epsilon_c \, d\epsilon_c = \alpha_1 \beta_1 f_c' \epsilon_{cu} (1 - 0.5\beta_1) \epsilon_{cu}$$

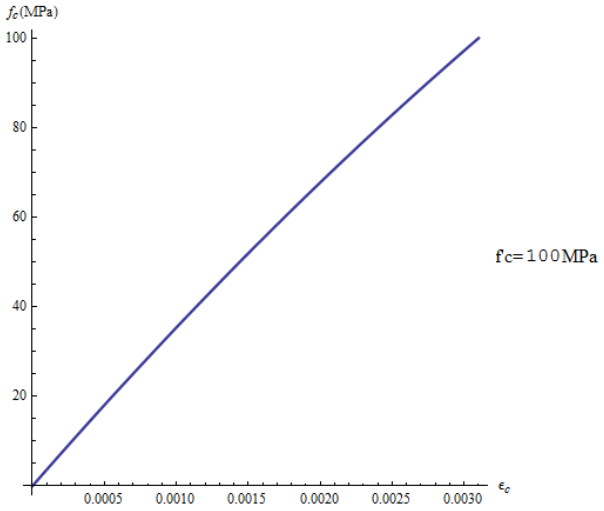

Figure 4.5: Stress-strain relationship for HSC based on Oztekin et al., Model. Carreira and Chu, 1985 [8]

They proposed the following stress-strain model for concrete under compression:

$$k = 32.4$$

$$\epsilon 0 = (0.71 f_c' + 168) * 10^{-5}$$

$$n = \left(\frac{f_c'}{k}\right)^3 + 1.55$$

$$f_c = \frac{\epsilon_c}{\epsilon_0} \frac{n f_c'}{(n-1) + (\frac{\epsilon_c}{\epsilon_0})^n}$$

Solving the following two equations for α_1 and β_1 with different f_c':

$$\int_0^{x_0} f_c \, d\epsilon_c = \alpha_1 \beta_1 f_c' \epsilon_{cu}$$

$$\int_0^{x_0} f_c \epsilon_c \, d\epsilon_c = \alpha_1 \beta_1 f_c' \epsilon_{cu} (1 - 0.5\beta_1) \epsilon_{cu}$$

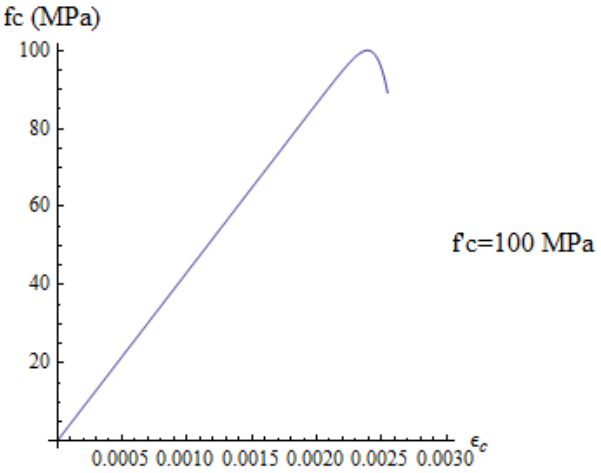

Figure 4.6: Stress-strain relationship for HSC based on Carreira and Chu Model.

Kumar, Collins et. al., 1993 [9]

$$E_{ci} = 3320\sqrt{f_c'} + 6900$$

$$n = 0.8 + \frac{f_c'}{17}$$

$$\epsilon_0 = \frac{n f_c'}{(n-1) E_{ci}}$$

$$k = \begin{bmatrix} k = 1 & \epsilon_c \le \epsilon_0 \\ k = 0.67 + \frac{f_c'}{62} & \epsilon_c > \epsilon_0 \end{bmatrix}$$

$$f_c = \frac{\epsilon_c}{\epsilon_0}(nf'_c)/((n-1)+(\frac{\epsilon_c}{\epsilon_0})^{nk})$$

Solving the following two equations for α_1 and β_1 with different f'_c:

$$\int_0^{x_0} f_c \, d\epsilon_c = \alpha_1 \beta_1 f'_c \epsilon_{cu}$$

$$\int_0^{x_0} f_c \epsilon_c \, d\epsilon_c = \alpha_1 \beta_1 f'_c \epsilon_{cu}(1 - 0.5\beta_1)\epsilon_{cu}$$

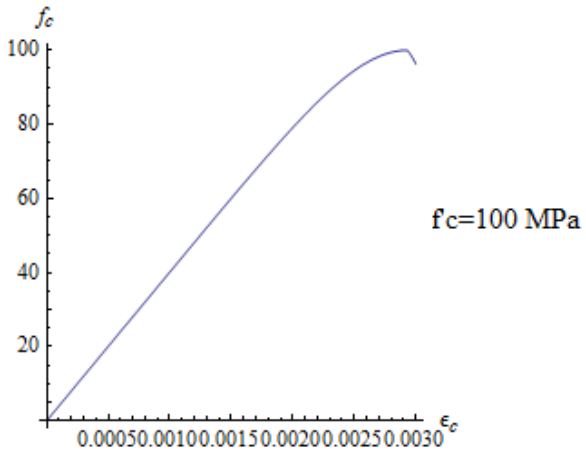

Figure 4.7: Stress-strain relationship for HSC based on Kumar, Collins Model.

Halit Cenan Mertol, 2006 [13]

He proposed the following stress-strain relationship for HSC:

$$n = 0.310 * 0.145fc + 0.78$$

$$k = 0.10 * 0.145fc + 1.2$$

$$\epsilon_{c0} = 0.0033 - 2 * 0.145f'_c * 10^{-5}$$

$$\epsilon_{cu} = 0.0038 - 4 * 0.145f'_c * 10^{-5}$$

$$f_c = \frac{\epsilon_c}{\epsilon_{c0}} \frac{nf'_c}{(n-1) + (\frac{\epsilon_c}{\epsilon_{c0}})^{n*k}}$$

Solving the following two equations for α_1 and β_1 with different f'_c:

$$\int_0^{x_0} f_c \, d\epsilon_c = \alpha_1 \beta_1 f'_c \epsilon_{cu}$$

$$\int_0^{x_0} f_c \epsilon_c \, d\epsilon_c = \alpha_1 \beta_1 f'_c \epsilon_{cu} (1 - 0.5\beta_1) \epsilon_{cu}$$

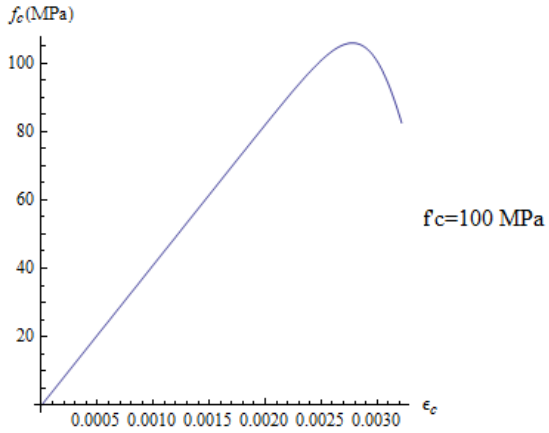

Figure 4.8: Stress-strain relationship for HSC based on Halit Cenan Mertol Model.

Table 4.1 summarizes the main results(α_1 and β_1) for the above four stress-strain models.

Table 4.1: Value of α_1 and β_1 with different f'_c for HSC.

f'_c(MPa)	Oztekin et al.		Halit Cenan Mertol		Kumar, Collins		Carreira and Chu	
	α_1	β_1	α_1	β_1	α_1	β_1	α_1	β_1
60	0.847	0.731	0.928	0.730	0.657	0.912	0.795	0.792
70	0.827	0.720	0.916	0.720	0.649	0.897	0.740	0.798
80	0.807	0.708	0.906	0.712	0.653	0.877	0.692	0.805
90	0.787	0.696	0.897	0.706	0.666	0.853	0.657	0.809
100	0.768	0.682	0.889	0.700	0.685	0.827	0.639	0.806
110	0.750	0.667	0.882	0.694	0.709	0.799	0.634	0.797

120	0.733	0.650	0.875	0.689	0.736	0.772	0.640	0.783
125	0.724	0.641	0.872	0.867	0.750	0.758	0.646	0.775

Table 4.1 is used to plot the Figure 4.1-8 below to show the linear variations of α_1 and β_1 with concrete strength.

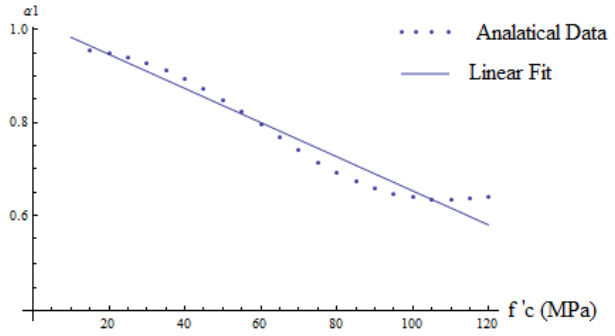

Figure 4.9: variation of α_1 with concrete strength f ’c based on Carreira and Chu [8] stress-strain model.

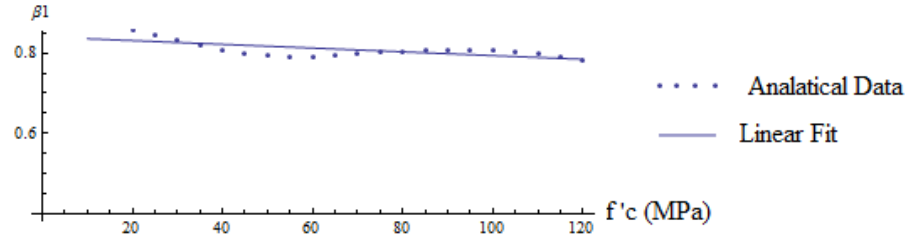

Figure 4.10: variation of β_1 with concrete strength f ’c based on Carreira and Chu [8] stress-strain model.

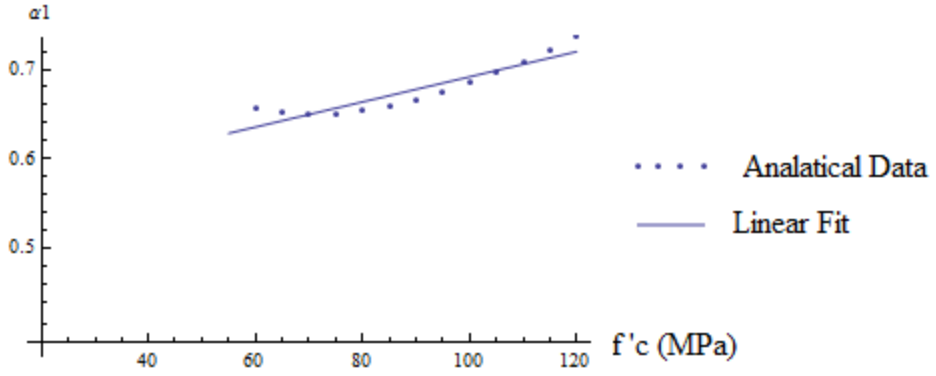

Figure 4.11: variation of α_1 with concrete strength f 'c based on Kumar, Collins et. al. [9] stress-strain model.

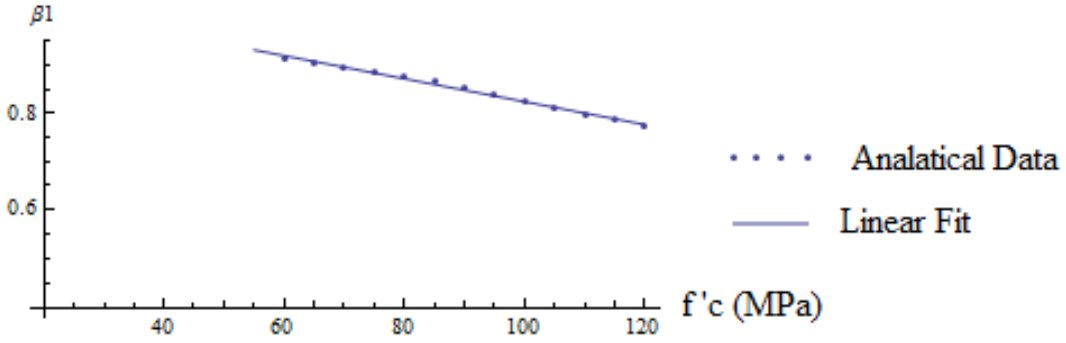

Figure 4.12: variation of β_1 with concrete strength f 'c based on Kumar, Collins et. al. [9] stress-strain model.

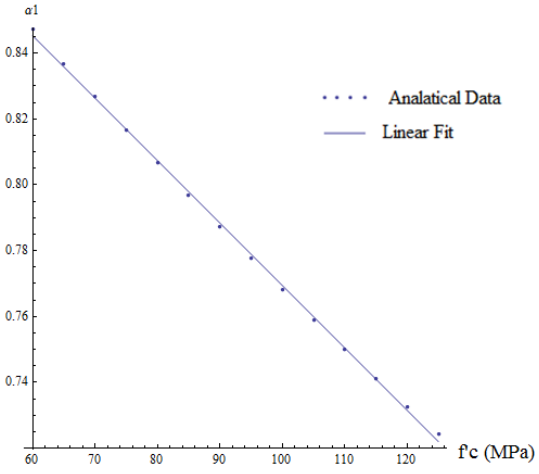

Figure 4.13: variation of α_1 with concrete strength f 'c based on Oztekin et al. [12] stress-strain model.

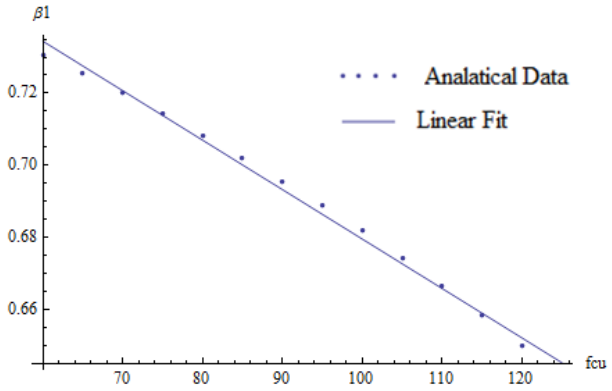

Figure 4.14: variation of β_1 with concrete strength f 'c based on Oztekin et al. [12] stress-strain model.

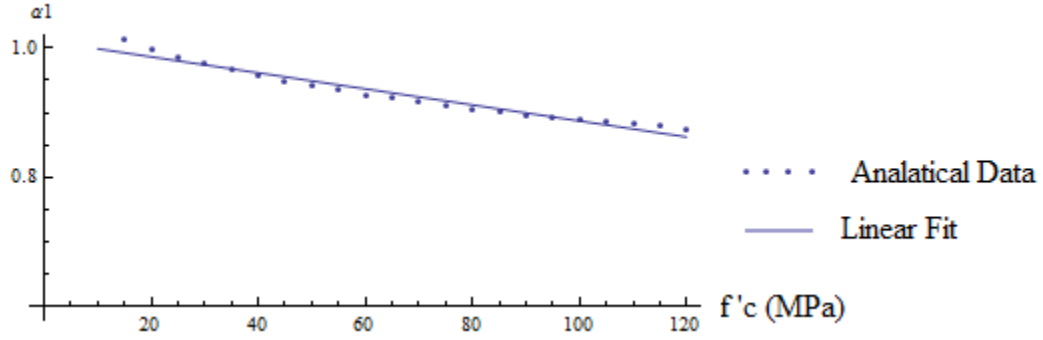

Figure 4.15: variation of α_1 with concrete strength f 'c based on Halit Cenan Mertol [13] stress-strain model.

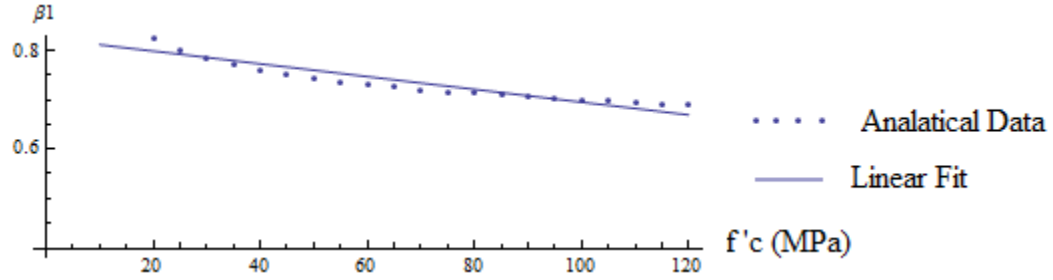

Figure 4.16: variation of β_1 with concrete strength f 'c based on Halit Cenan Mertol [13] stress-strain model.

Table 4.2 shows different relationships for α_1 and β_1 based on the data in Table 4.1 and linear fit function.

Table 4.2: α_1 and β_1 relationships based on different stress-strain model from literature.

Selected Model from Literature	α_1 and β_1 relationships
Oztekin et al. [12]	$\alpha_1 = 0.96588 - 0.0019858f'_c$
	$\beta_1 = 0.8033 - 0.001195f'_c$
Halit Cenan Mertol [13]	$\alpha_1 = 1.01133 - 0.00124f'_c$
	$\beta_1 = 0.8249 - 0.0013f'_c$
Kumar, Collins [9]	$\alpha_1 = 0.55088 + 0.0014077f'_c$
	$\beta_1 = 1.0643 - 0.002397f'_c$
Carreira and Chu [8]	$\alpha_1 = 1.0205 - 0.003677f'_c$
	$\beta_1 = 0.8409 - 0.0004669f'_c$

In order to assess the previously discussed stress-strain models and their corresponding stress block parameters in terms of closeness to practical cases, the following three cases are used. Each case represents a set of column capacity data (M_n, P_n) obtained experimentally by other researchers. The four assessed models are implemented in Mathematica code developed earlier to generate their interaction diagrams. The comparisons of the four models with the experimental results are given in Figure 4.17 to Figure 4.19.

Case 1: Tested by Lloyd, N. A., and Rangan, 1996 [55]

Case 2: Tested by Ibrahim H., and MacGregor, J. G., 1994 [26]

Case 3: Tested by Foster, S. J. and Attard, M. M., 1997 [48]

Table 4.3 contins material and cross section properties for each case, this is the input data which is implemented by Mathematica code. Table 4.4 contains the experimental data for each case which is used to validate the previous four models.

Table 4.3: Properties of the rectangular column section for the each case.

	Case 1	Case 2	Case 3
f'_c(Ksi)	14	18.27	13
f_y(Ksi)	58	58	58
b (mm)	175	200	175
h (mm)	175	300	150
γ	0.84	0.60	0.89
ρ	1.30	1.30%	1.3%

Table 4.4: Experimental data of the tested column for each case.

Case 1		Case 2		Case 3	
M_n (KN.m)	P_n (KN)	M_n (KN.m)	P_n (KN)	M_n (KN.m)	P_n (KN)
59.90	742.66	177.72	3746.06	20.53	1606.15
59.11	751.47	180.44	3949.79	20.21	1659.55
60.46	998.04	180.02	4204.89	23.01	1707.75
58.89	965.75	202.89	4406.33	36.50	1353.12
42.79	1969.67	226.41	4403.67	37.25	1374.52
39.69	1928.57			47.12	787.35
				48.70	822.15

Figure 4.17 to Figure 4.19 show the comparison of the results obtained from the developed Mathematica code using different stress block parameters from Table 4.2 against the experimental data from literature in Table 4.4.

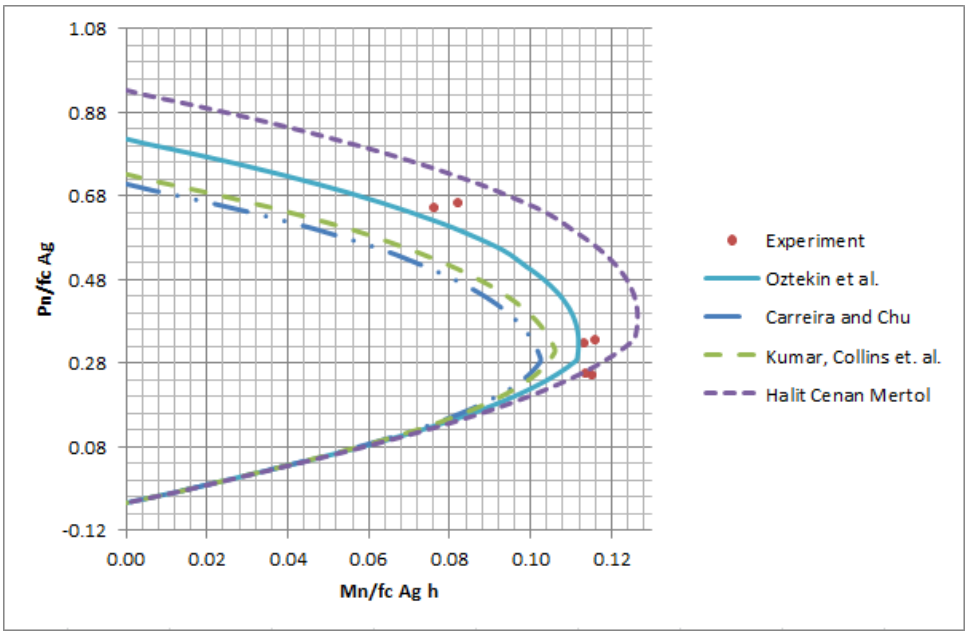

Figure 4.17: Interaction diagrams corresponding to case 1 based on different stress block parameters from Table 4.2.

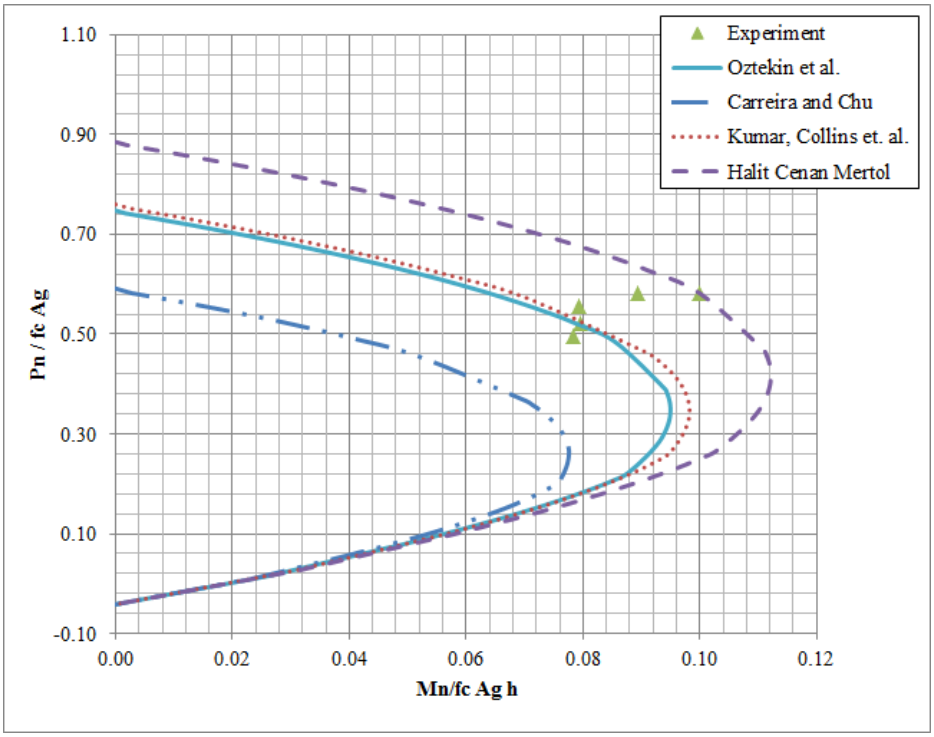

Figure 4.18: Interaction diagrams corresponding to case 2 based on different stress block parameters from Table 4.2.

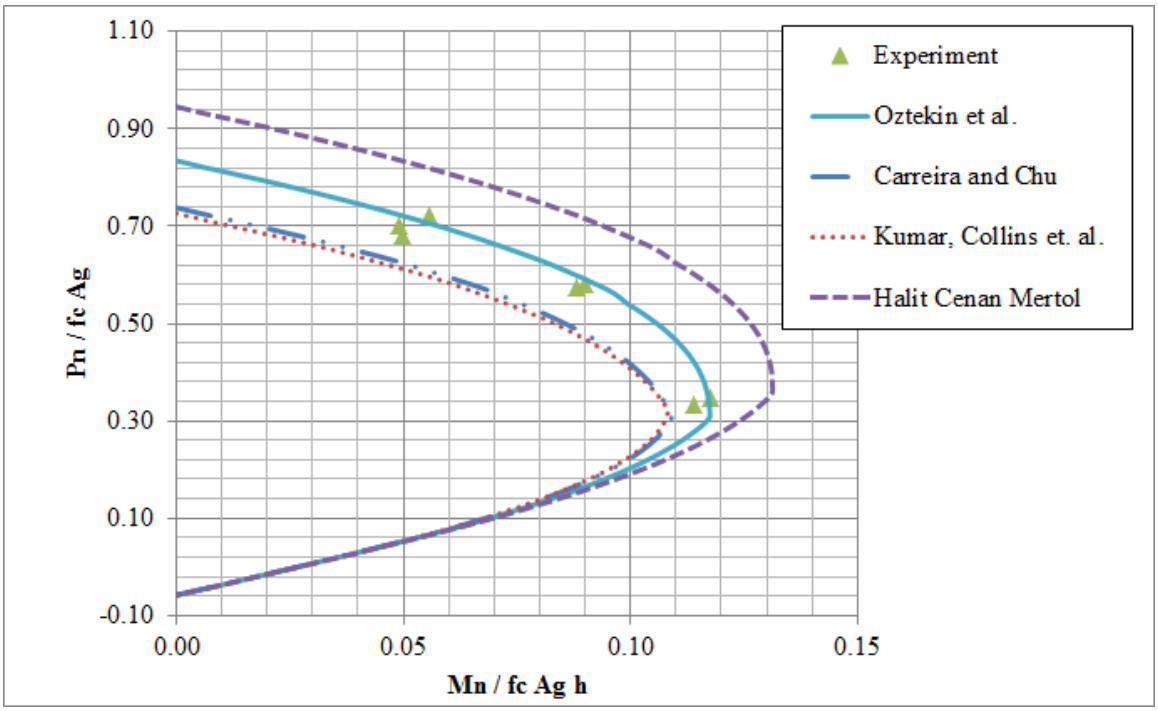

Figure 4.19: Interaction diagrams corresponding to case 3 based on different stress block parameters from Table 4.2.

As shown in Figure 4.17 to Figure 4.19, the best model against the experimental results is the stress-strain model proposed by Oztekin [12]. Based on this model the proposed stress block parameters are derived as follow:

$$\alpha_1 = 0.96588 - 0.0019858 f'_c (\text{MPa})$$

$$\beta_1 = 0.8033 - 0.001195 f'_c (\text{MPa})$$

4.4 Formulation of the Column Capacity

Formulation of the Column Capacity in the case of HSRC columns is similar to that for NSRC but the equivalent rectangular stress block parameters are modified to reflect the adopted stress-strain model.

4.5 MATHEMATICA Code

MATHEMATICA software has been used to generate the interaction diagrams for HSRC columns under uniaxial bending moment with compression. The code is given in Appendix A. The code is based on the same flow chart presented earlier for NSRC columns.

4.6 Validation using PCA Software

PCA program has been used to validate the results obtained for both NSRC and HSRC columns. This software has the ability to generate the interaction curves for arbitrary values of the stress block parametersα_1 and β_1. Using the proposed parameters, the following cases of different sections have been investigated using PCA software. The figures below compare the Mathematica-developed interaction curves with those generated using PCA software.

Case 1: rectangular cross section with steel distributed uniformly around the all faces.

A rectangular column section was investigated using PCA software; this column has the following material and geometric properties:

$f_y = 75$ ksi

$f'_c = 18$ ksi

$\gamma = 0.75$

$\rho = 3.29\%$

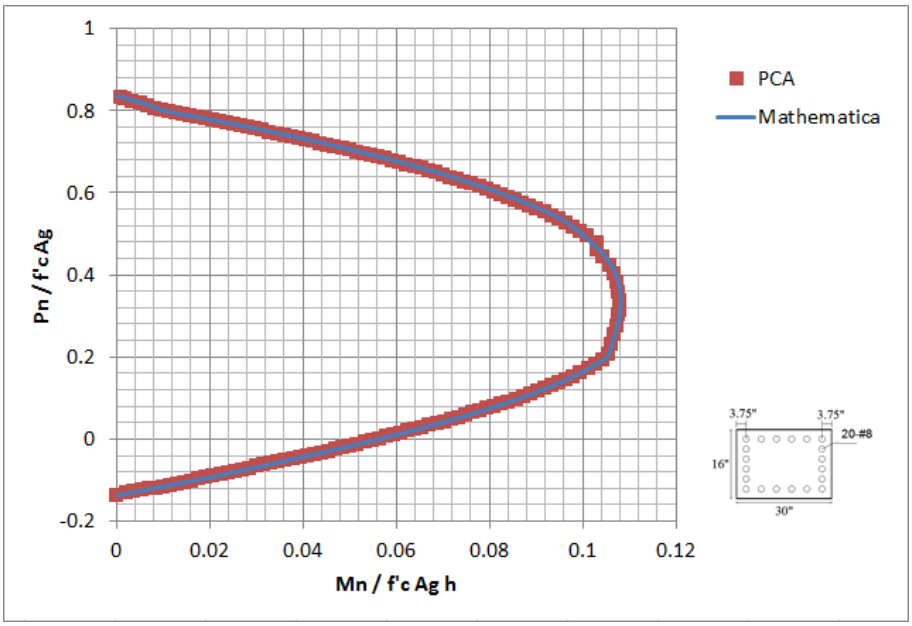

Figure 4.20: Mathematica vs. PCA interaction diagrams for $f'c = 18ksi, f_y = 75\ ksi, \gamma = 0.75$ and $\rho = 3.29\%$.

Case2: rectangular cross section with steel distributed on two faces only.

The column has the following material and geometric properties as below:

$f_y = 60$ ksi

$f'_c = 15$ ksi

$\gamma = 0.8$

$\rho = 2.74\%$

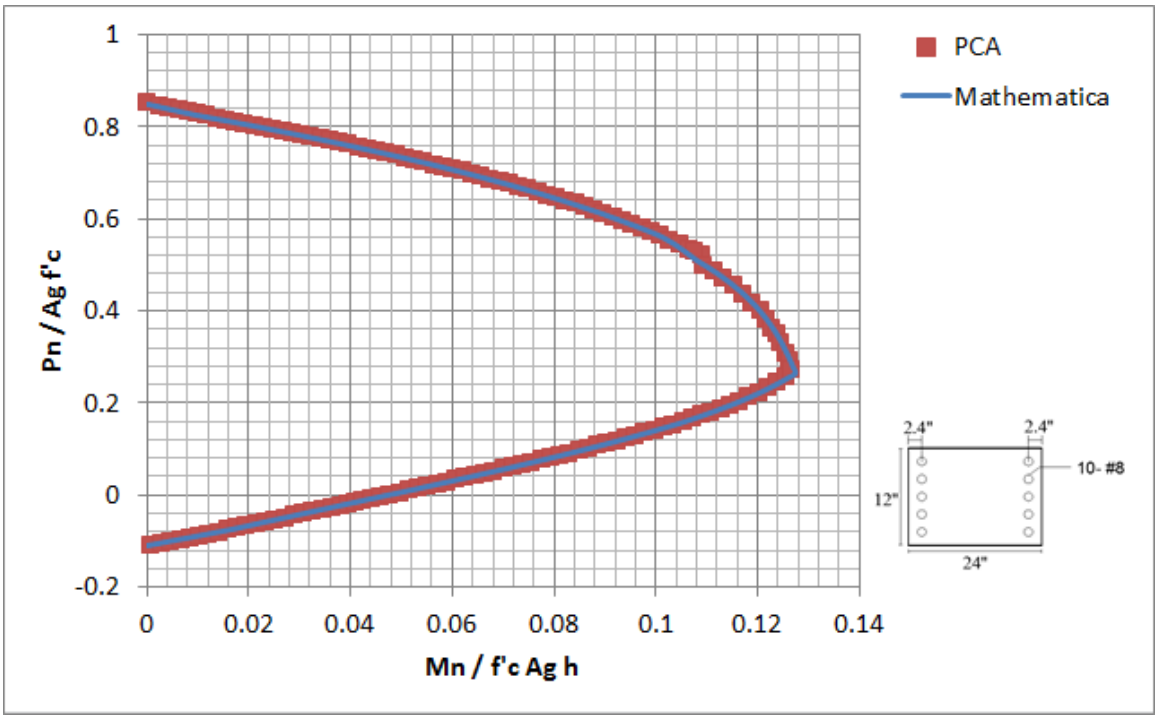

Figure 4.21: Mathematica vs. PCA interaction diagrams for $f'c = 15$ ksi, $f_y = 60$ ksi, $\gamma = 0.8$ and $\rho = 2.74\%$.

Case3: circular cross section with steel distributed uniformly around the perimeter of the circle.

The column has the following material and geometric properties as below:

$f_y = 75$ ksi

$f'_c = 18$ ksi

$\gamma = 0.6$

$\rho = 4.18\%$

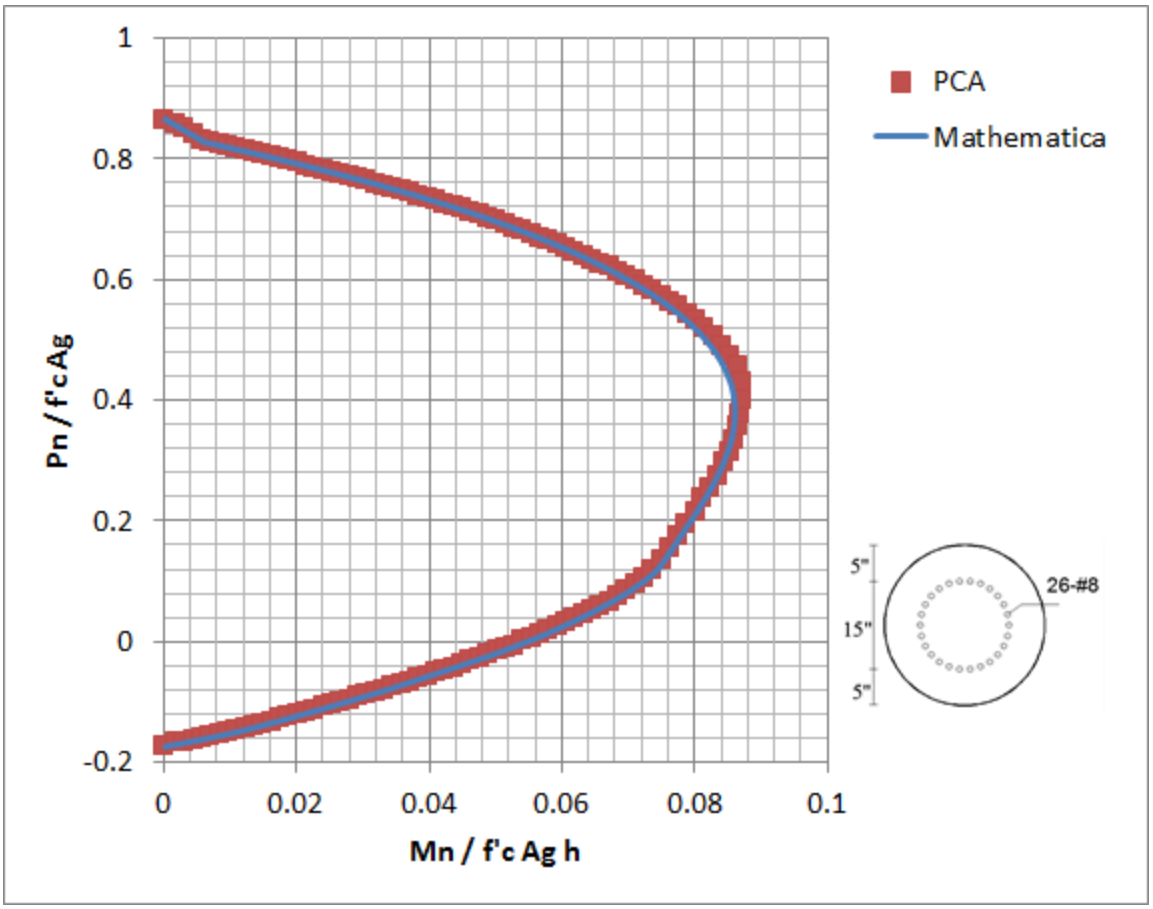

Figure 4.22: Mathematica vs. PCA interaction diagrams for f'c = 18ksi, f_y = 75 ksi, γ = 0.6 and ρ = 4.18%.

4.7 Comparison with Previous Experimental Work

Another validation of the developed Mathematica code is by comparison with existing experimental data from literature. Based on some selected references from literature of the experimental work, the experimental data has been plotted on the same interaction diagrams. The following figures show the interaction diagrams for different concrete strengths and section properties:

Case 1: Tested by Lloyd, N. A., and Rangan, 1996 [55]

Table 4.5: Properties of the rectangular column section for case 1.

b	175 mm
h	175 mm
f'_c	14 ksi
f_y	58 ksi
γ	0.84
ρ	1.30

Table 4.6: Experimental results of the tested column for case 1.

M_n (KN.m)	P_n (KN)
59.90	742.66
59.11	751.47
60.46	998.04
58.89	965.75
42.79	1969.67
39.69	1928.57

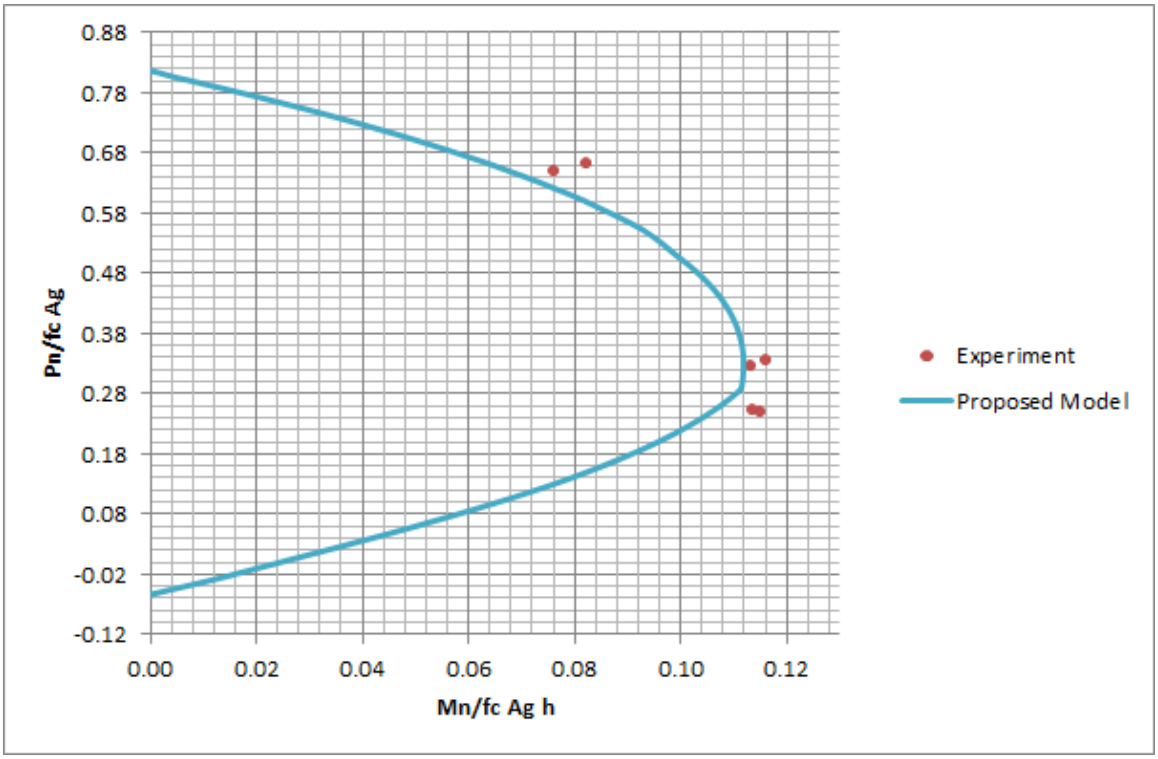

Figure 4.23: Interaction diagrams for case 1.

Case 2: Tested by Ibrahim H., and MacGregor, J. G., 1994 [26]

Table 4.7: Properties of the rectangular column section for case 2.

f'_c	18.27 ksi
f_y	58 ksi
b	200 mm
h	300 mm
γ	0.60
ρ	1.30%

Table 4.8: Experimental results of the tested column for case 2.

M_n (KN.m)	P_n (KN)
177.72	3746.06
180.44	3949.79
180.02	4204.89
202.89	4406.33
226.41	4403.67

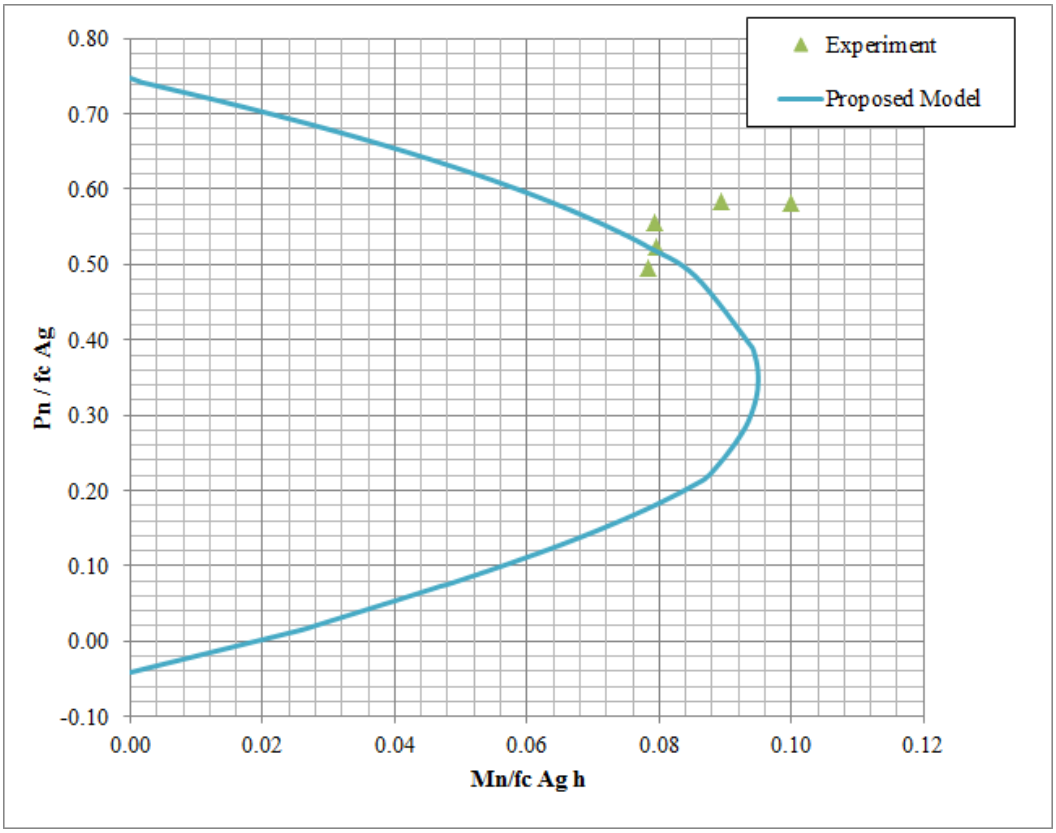

Figure 4.24: Interaction diagrams for case 2.

Case 3: Tested by Foster, S. J. and Attard, M. M., 1997 [48]

Table 4.9: Properties of the rectangular column section for case 3.

f'_c	13 ksi
f_y	58 ksi
b	175 mm
h	150 mm
γ	0.89
ρ	1.3%

Table 4.10: Experimental results of the tested column for case 3.

M_n (KN.m)	P_n (KN)
20.53	1606.15
20.21	1659.55
23.01	1707.75
36.50	1353.12
37.25	1374.52
47.12	787.35
48.70	822.15

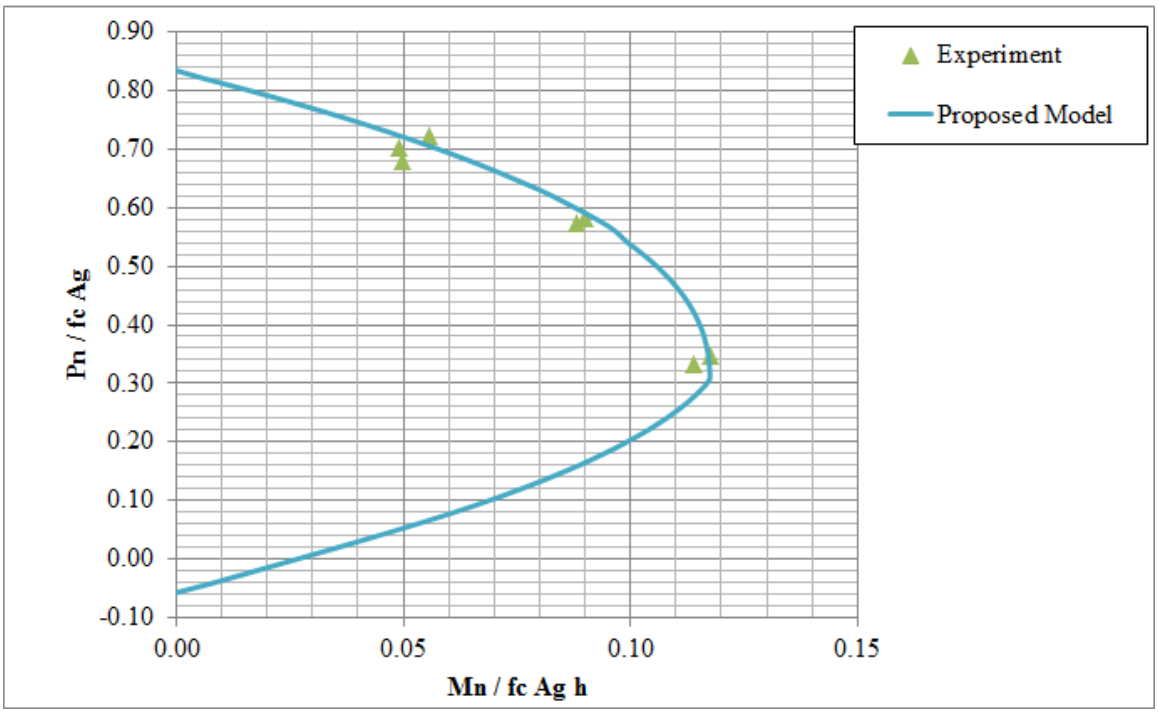

Figure 4.25: Interaction diagrams for case 3.

Based on the proposed stress block for concrete under compression, the above interaction diagrams are developed. Those diagrams are validated against the experimental data and they are close to each other.

4.8 Comparison between proposed and ACI stress block

ACI stress block is used to generate the interaction diagrams for the same three cases in section 4.7. The following figures show the developed interaction diagrams based on the proposed and ACI stress blocks against the experimental data:

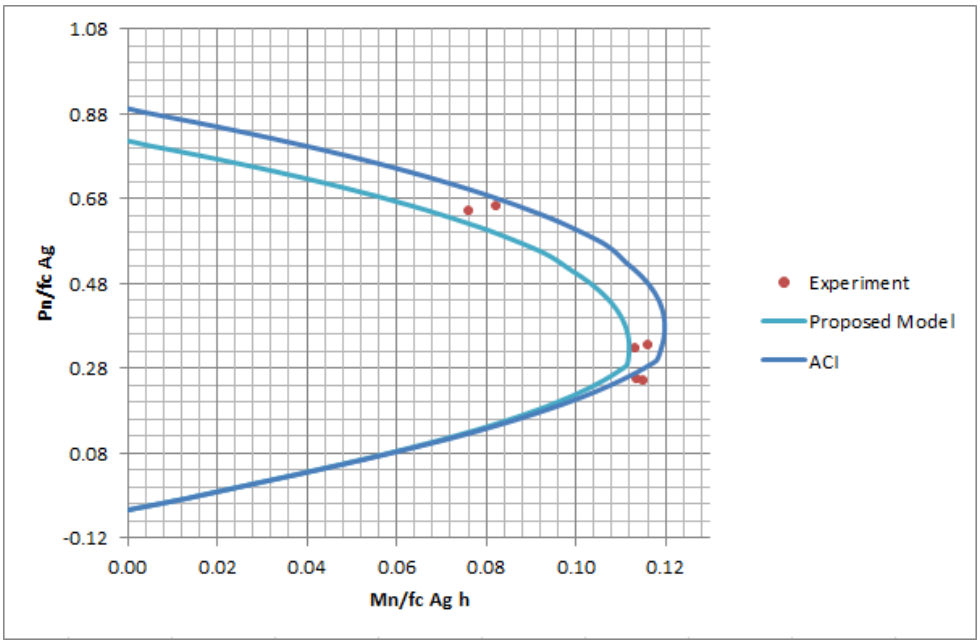

Figure 4.26: ACI and Proposed against the experimental data for case 1.

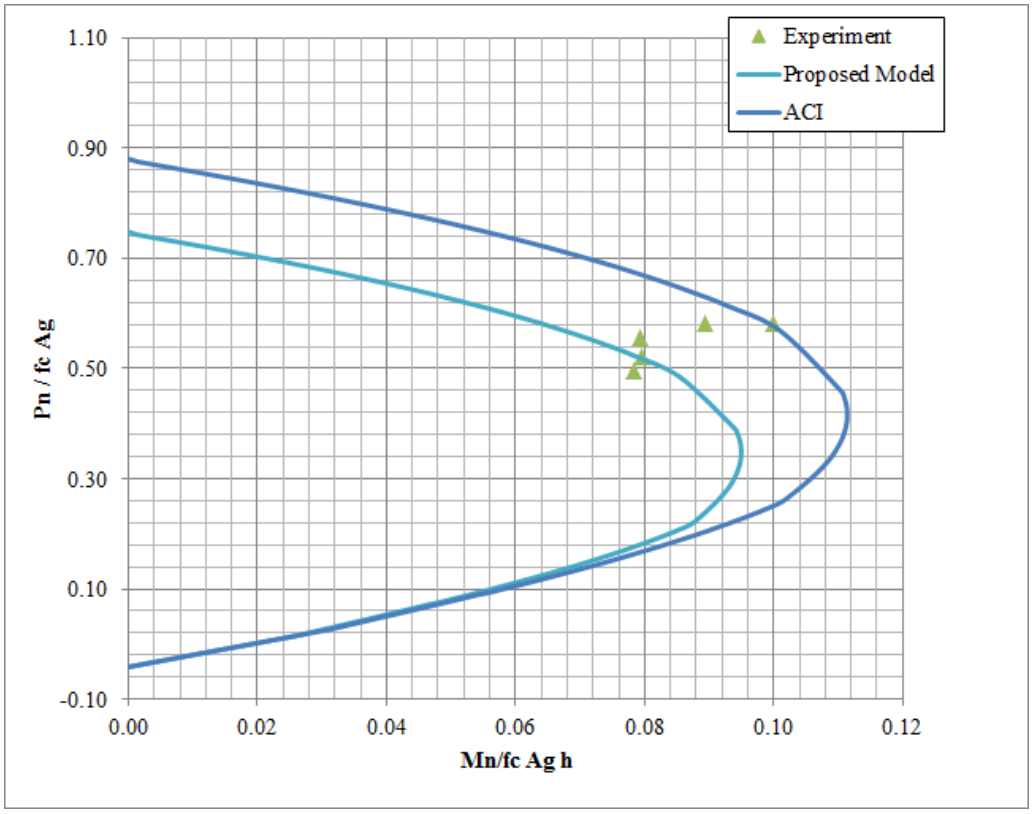

Figure 4.27: ACI and Proposed against the experimental data for case 2.

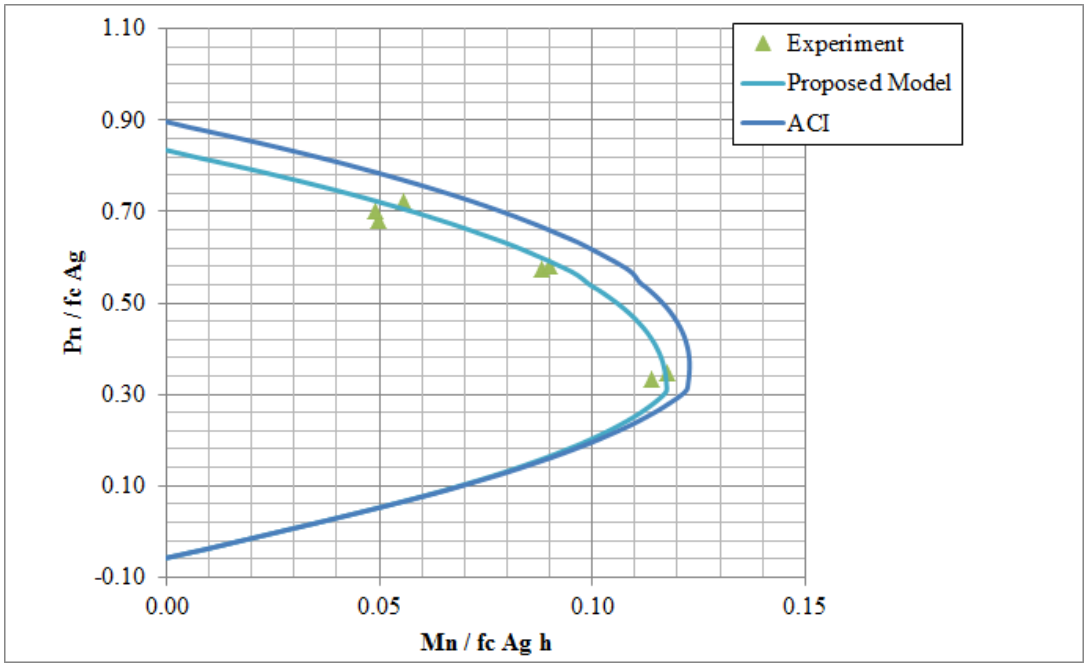

Figure 4.28: ACI and Proposed against the experimental data for case 3.

Figure 4.26 to Figure 4.28 show that the two interaction diagrams are coinciding in the tension control region. However, reasonable differences are obtained in the compression-controlled region and overestimation in the column capacity is noticed when ACI stress block is used.

CHAPTER FIVE

INTERACTION EQUATION FOR COLUMNS SUBJECTED TO COMPRESSION AND BIAXIAL BENDING

5.1 Basic approach

It involves the extension of the uniaxial formulation for columns and codes to the general case of compression and biaxial bending. This is achieved through the use of the concept of load contour method which was proposed by Bresler and Hsu. Bresler and Hsu proposed the following contour equations:

1. Bresler load contour method [34]:

This method represents the relationship between the moments about the principal axes of the rectangular section at certain constant axial force:

$$\left(\frac{M_x}{M_{xo}}\right)^{\alpha} + \left(\frac{M_y}{M_{yo}}\right)^{\alpha} = 1.0$$

Where:

$\alpha = 1.5$

M_x=moment component in direction of major axis.

M_y=moment component in direction of minor axis.

M_{xo}=moment capacity when the load acts along the major axis.

M_{yo}=moment capacity when the load acts along the minor axis.

2. Hsu load contour method [39]:

This method represents the relationship between the moments about the principal axes of the rectangular section and the axial force corresponding to those moments:

$$\frac{P_n - P_{nb}}{P_o - P_{nb}} + \left(\frac{M_{nx}}{M_{nbx}}\right)^{1.5} + \left(\frac{M_{ny}}{M_{nby}}\right)^{1.5} = 1.0$$

Where:

P_n = nominal axial compression or tension.

M_{nx}, M_{ny} = nominal bending moments about x and y axis.

P_o = maximum nominal axial compression or tension.

P_{nb} = nominal axial compression at balanced condition.

M_{nbx}, M_{nby} = nominal bending moments about x and y axis at balanced strain condition.

5.2 Experimental validation for NSC

Both Bresler [34] and Hus [39] equations are validated against experimental data from literature to find accurate representation for the contour lines. Some experimental cases from literature [56] are used for this purpose as follow:

Table 5.1: Experimental data for concrete columns under compression and biaxial bending.

Case No.	b(mm)×h(mm)	ρ%	f'c (MPa)	fy (MPa)	P (KN)	Mx (KN.mm)	My (KN.mm)
1	125×125	1.29	73.42	550	249	11205	11205
2	125×125	1.29	53.82	550	211	8440	8440
3	125×125	1.29	58.46	550	194	8730	8730

4	125×125	1.29	69.28	550	159	7950	7950

These experimental data in Table 5.1 are plotted against the theoretical contour lines which were proposed by Bresler and Hus as in Figure 5.1 to Figure 5.4:

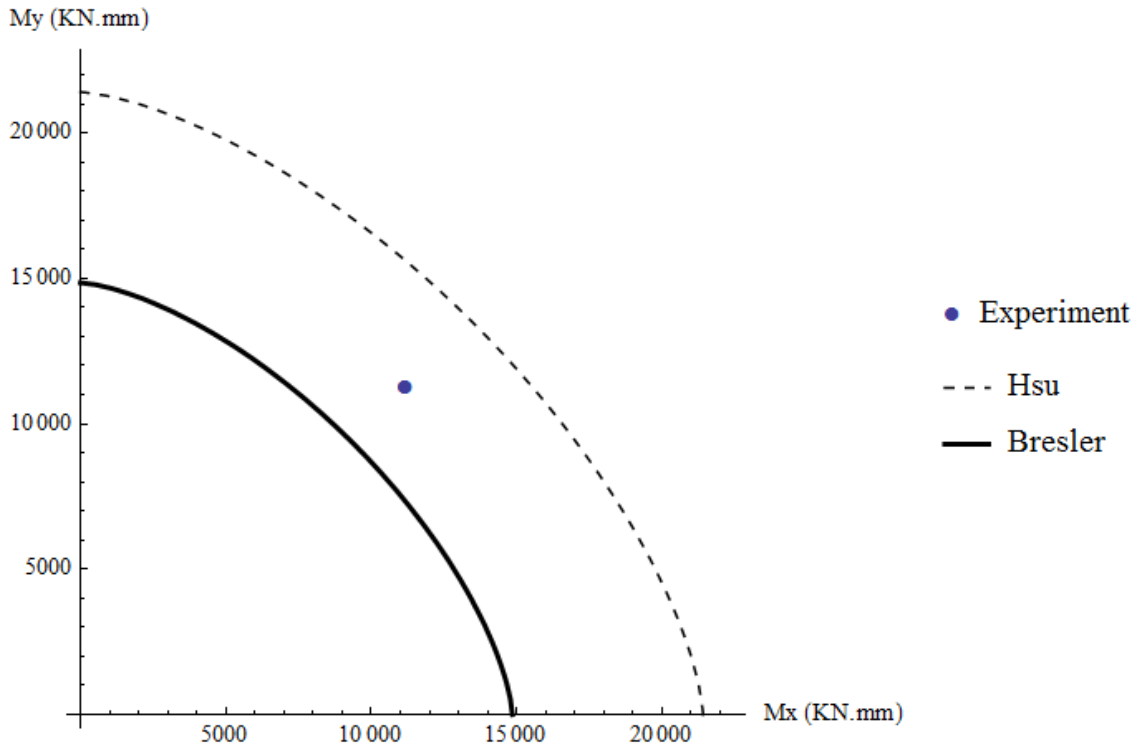

Figure 5.1: interaction diagram for case 1.

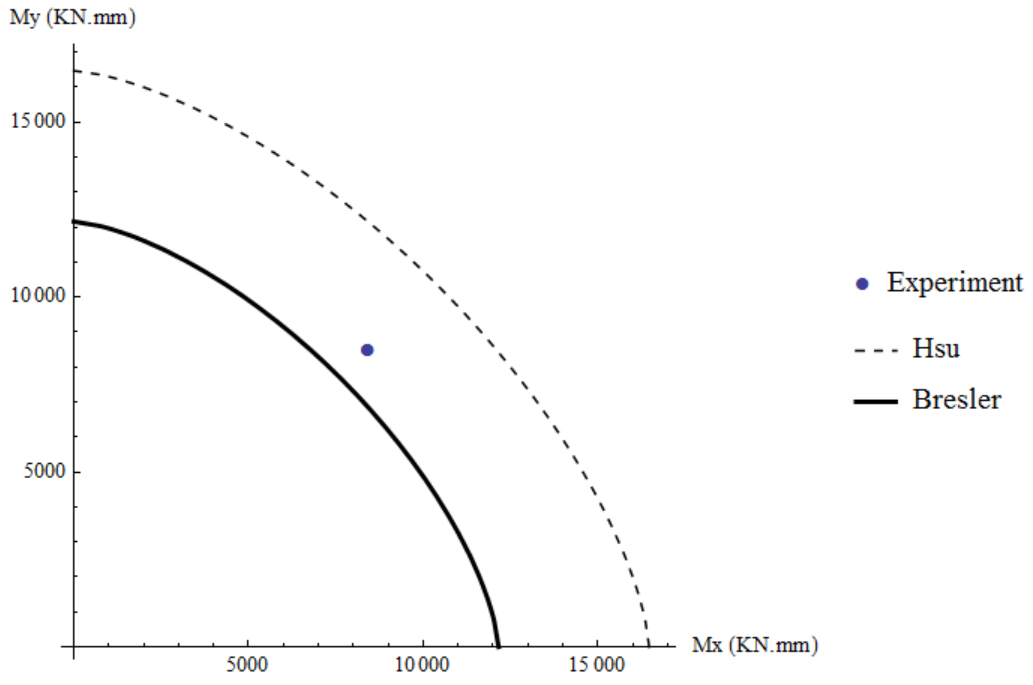

Figure 5.2: interaction diagram for case 2.

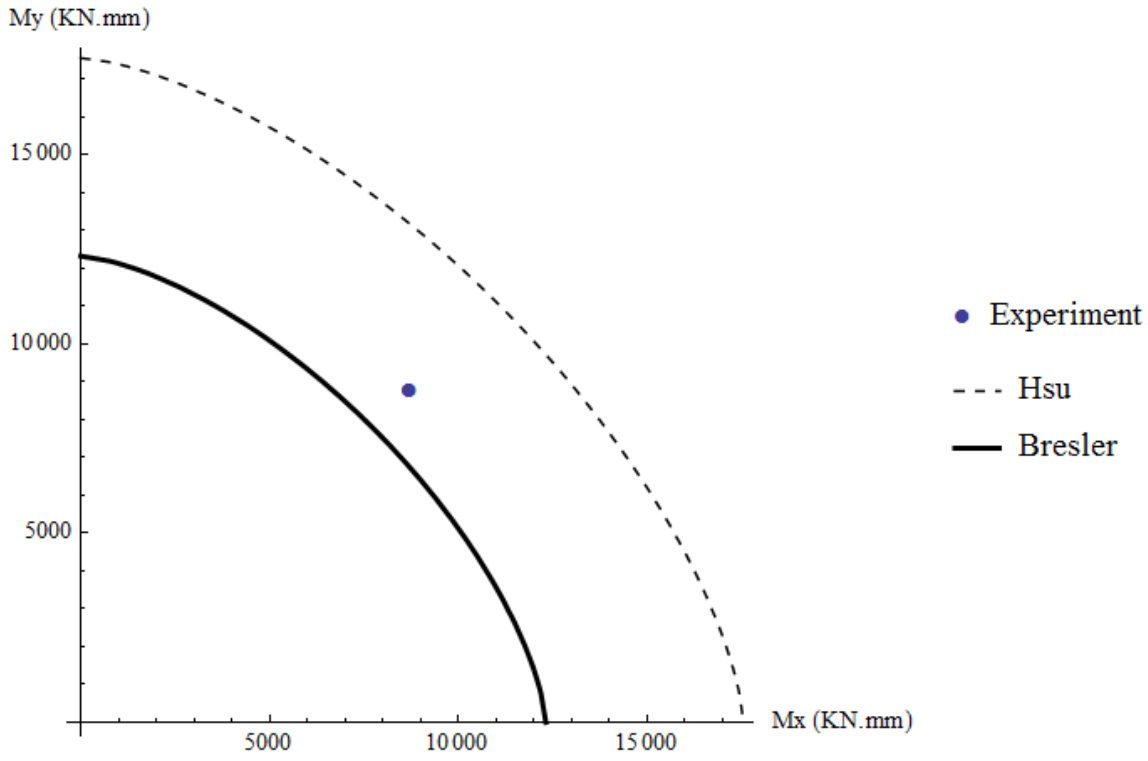

Figure 5.3: interaction diagram for case 3.

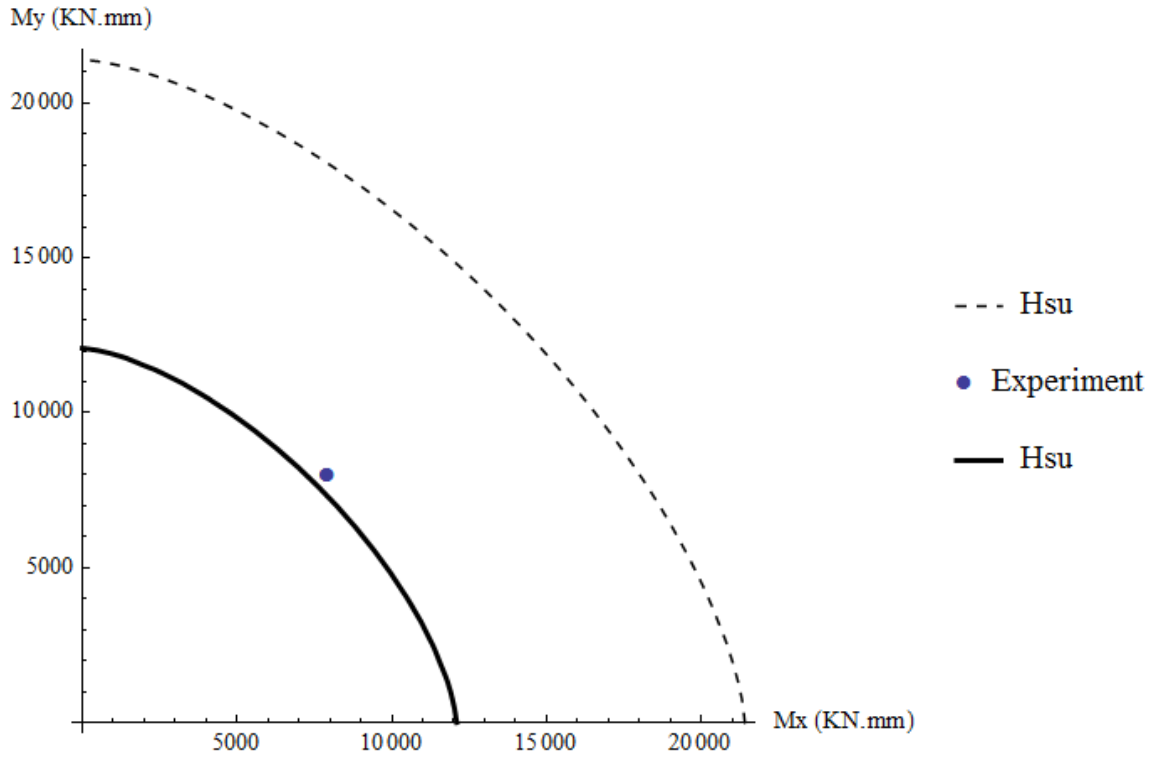

Figure 5.4: interaction diagram for case 4.

Figure 5.1 to Figure 5.4 show that Bresler contour equation is more conservative and closer to the experimental data than that by Hsu's equation. This implies that Bresler contour method is recommended for the design of concrete columns under compression and biaxial bending.

5.3 Experimental validation for HSC

Both Bresler [34] and Hus [39] equations are validated against experimental data from literature for HSRC columns. Some experimental cases from literature [54] are used for this purpose as follow:

Table 5.2: Experimental data for HSRC columns under compression and biaxial bending.

Case No.	b(mm)×h(mm)	ρ%	f'c (MPa)	fy (MP)	P (KN)	Mx (KN.mm)	My (KN.mm)
1	100×200	1.54	100	558	175.2	6266.9	25072.9
2	100×200	1.54	101	558	166.1	9396.3	21010
3	100×200	1.54	100	558	142.0	10160.1	10160.1

These experimental data in Table 5.2 are plotted against the theoretical contour lines which were proposed by Bresler and Hus as in Figure 5.5 to Figure 5.7:

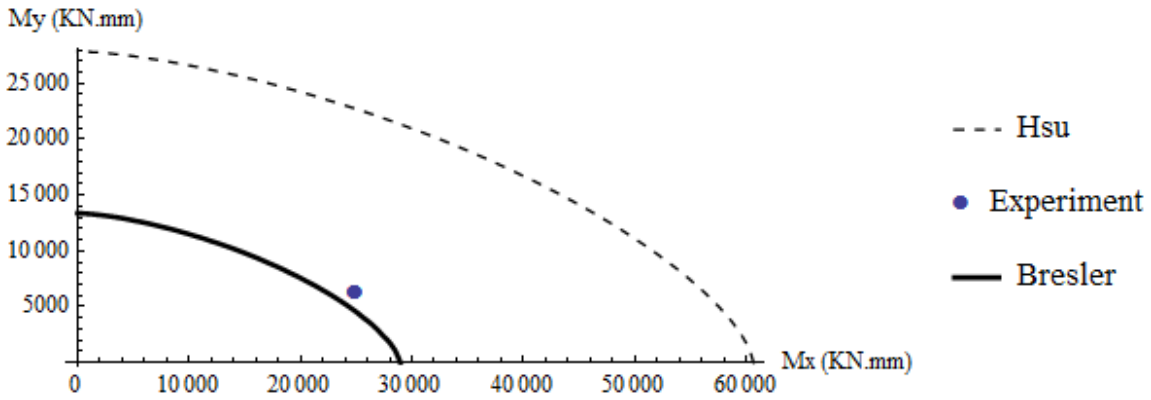

Figure 5.5: interaction diagram for case 1.

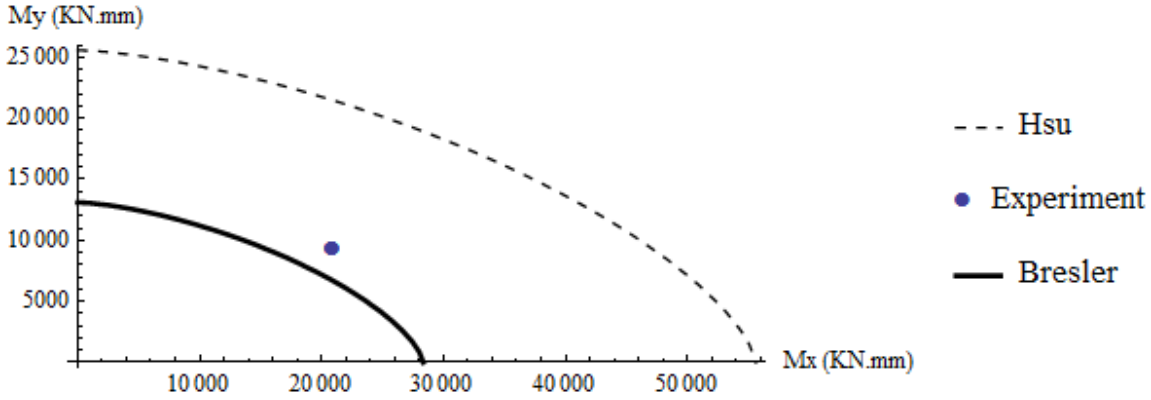

Figure 5.6: interaction diagram for case 2.

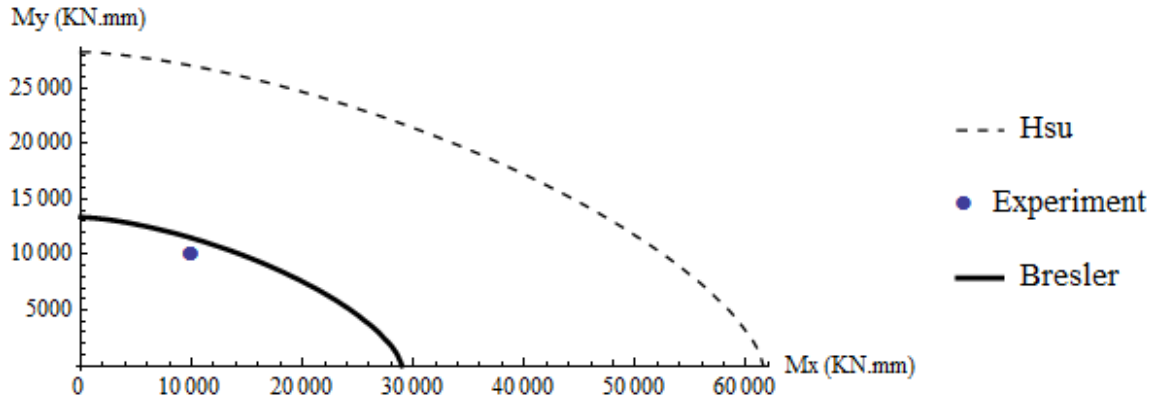

Figure 5.7: interaction diagram for case 3.

Bresler is more conservative than Hus for both NSC and HSC as shown in Figure 5.1 to Figure 5.7. Therefore, it is recommended to use Bresler load contour method for design of any reinforced concrete columns subjected to compression and biaxial bending. It does not matter whether columns are made from NSC or HSC to use load contour method because the concrete strength effects have been already taken into account in the analysis of uniaxial bending case.

5.4 Mathematica Code

Load contour method has been programed in the same Mathematica code for the uniaxial bending case. Contour equation is plotted based on the values of the principal moments at a certain constant axial load. The values of principal moments are used without normalizing.

5.5 Contour Generation

As recommended in section 5.2, Bresler contour method is used to generate contours for reinforced concrete columns under compression and biaxial bending. The following is a case study on applying Bresler contour method:

Table 5.3: Case study data on Bresler load contour method.

Case No.	b×h in^2	ρ%	f'c (Ksi)	fy	γ
1	12×24	2.19(8_#8)	12 ksi	60 ksi	0.75

Figure 5.8 shows the interaction diagrams for the case study based on the Bresler load contour method. Seven interaction diagrams are drawn, each is corresponing to certain constant axial load.

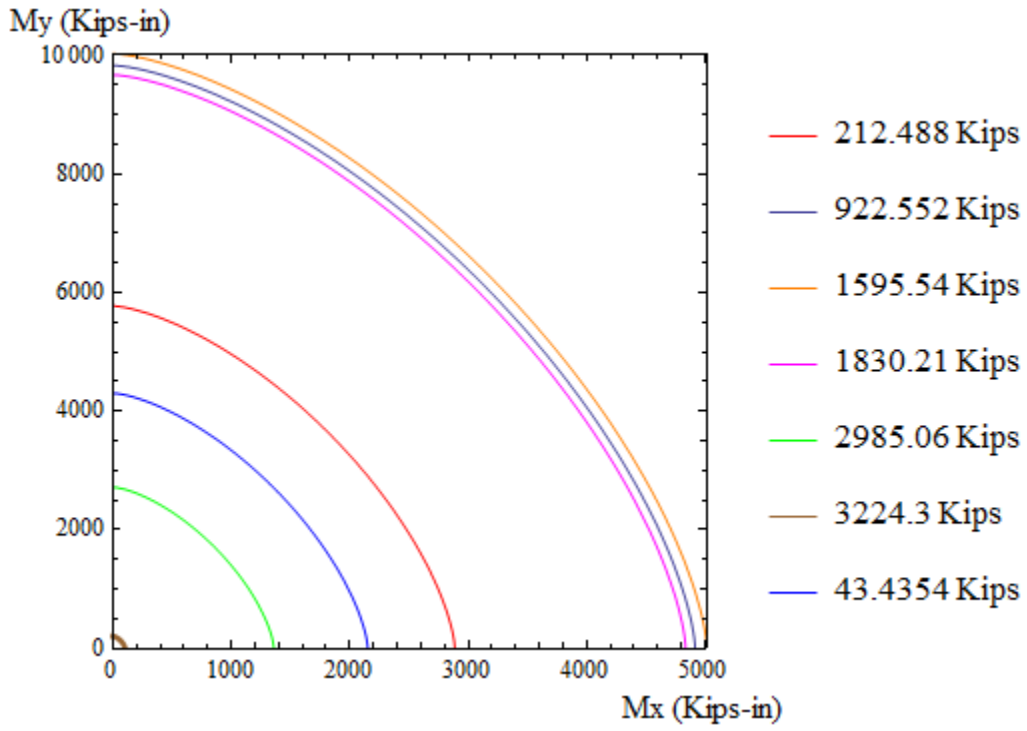

Figure 5.8: Contour lines for the case study using Bresler load contour method.

Load contour method is the easiest and simplest method for finding the column capacity under the biaxial bending with compression. This contour equation is plotted at constant axial force and it represents a simple relationship between the two bending moments about the two principal axes of the cross section.

CHAPTER SIX

NUMERICAL EXAMPLES

Design of columns can be performed using the interaction diagrams that have been developed in the previous chapters. Those diagrams are simple used to design reinforced concrete columns subjected to compression force and bending moment without much calculation. This chapter concludes design examples as an application on the analysis of reinforced concrete columns.

Example #1:

Design a reinforced concrete column, with steel distributed on four faces, subjected to compression force and uniaxial bending under the following requirements of loading, dimensions and material properties:

Required nominal load:

$M_n = 5600 \text{ kip.in}$

$P_n = 800 \text{ kip}$

Cross section:

$b \times h = 16 \text{ in} \times 20 \text{ in}$

$\gamma = 0.75$

Materials' strength:

$f'_c = 4$ ksi

$f_y = 60$ ksi

Solution:

$$K_n = \frac{P_n}{f'_c A_g} = \frac{800}{4 \times 16 \times 20} = 0.625$$

$$R_n = \frac{M_n}{f'_c A_g h} = \frac{5600}{4 \times 16 \times 20 \times 20} = 0.21875$$

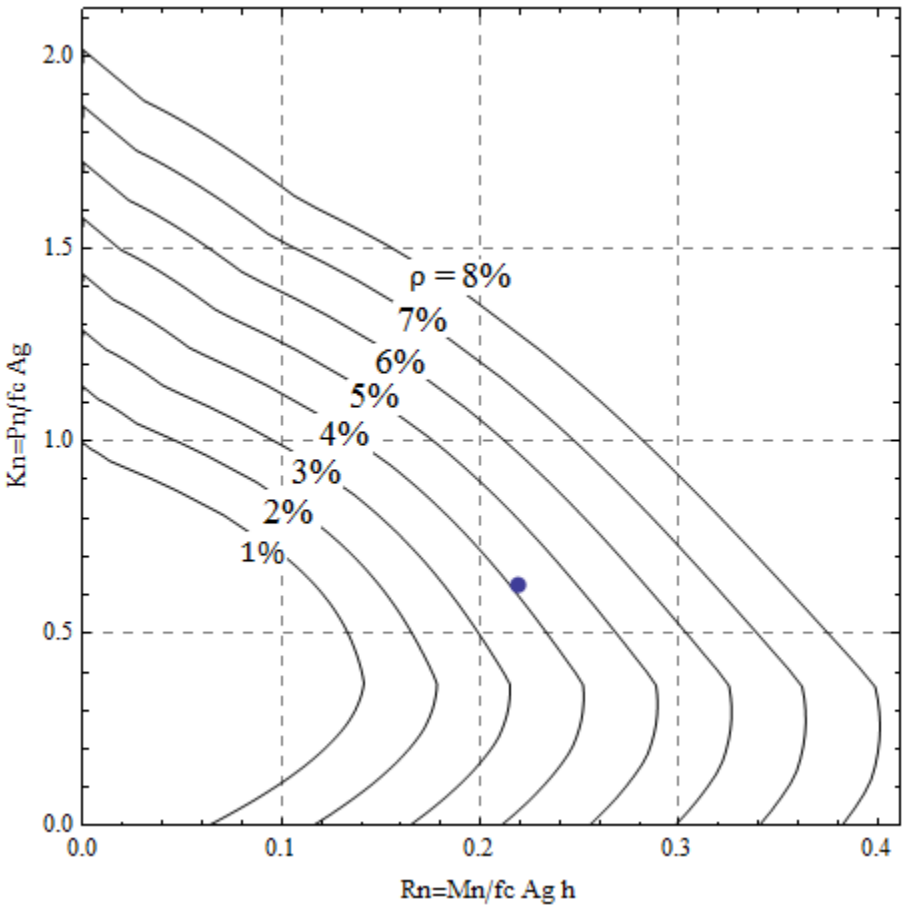

Figure 6.1: Design output for example 1 from Mathematica code.

As shown in Figure 6.1 the required percentage of rebar is 4.1%, which means that the area of required steel is $\frac{4.1}{100} * 16 * 20 = 13.12 \text{ in}^2$

Example #2:

Design a reinforced concrete column, with steel distributed on two faces only, subjected to compression force and uniaxial bending under the following requirements of loading, dimensions and material properties:

Required nominal load:

$M_n = 3986 \text{ kip. in}$

$P_n = 943 \text{ kip}$

Cross section:

$b \times h = 14 \text{ in} \times 20 \text{ in}$

$\gamma = 0.8$

Materials' strength:

$f'_c = 9 \text{ ksi}$

$f_y = 60 \text{ ksi}$

Solution:

$$K_n = \frac{P_n}{f'_c A_g} = \frac{943}{9 \times 14 \times 18} = 0.416$$

$$R_n = \frac{M_n}{f'_c A_g h} = \frac{3986}{9 \times 14 \times 18 \times 18} = 0.0976$$

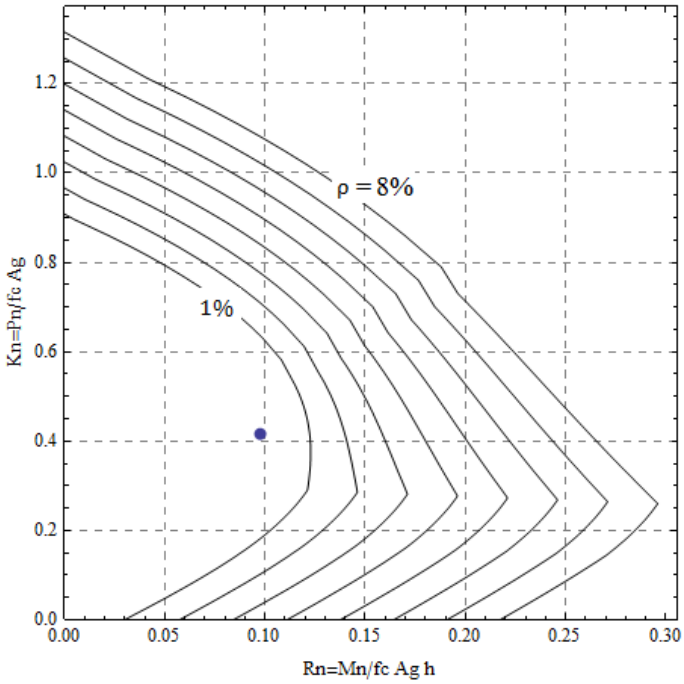

Figure 6.2: Design output for example 2 from Mathematica code.

As shown in Figure 6.2 the required percentage of rebar is 1%, which means that the area of required steel is $0.01 * 14 * 20 = 2.80\ \text{in}^2$

Example #3:

Design a circular reinforced concrete column subjected to compression force and uniaxial bending under the following requirements of loading, dimensions and material properties:

Required nominal load:

$M_n = 686\ \text{kip.in}$

$P_n = 1343\ \text{kip}$

Cross section:

$\text{Diameter} = 15 \text{ in}$

$\gamma = 0.70$

Materials' strength:

$f_c' = 6 \text{ ksi}$

$f_y = 60 \text{ ksi}$

Solution:

$$K_n = \frac{P_n}{f_c' A_g} = \frac{1343}{6 \times \frac{\pi}{4} \times 15^2} = 1.267$$

$$R_n = \frac{M_n}{f_c' A_g h} = \frac{686}{6 \times \frac{\pi}{4} \times 15^2 \times 15} = 0.0431$$

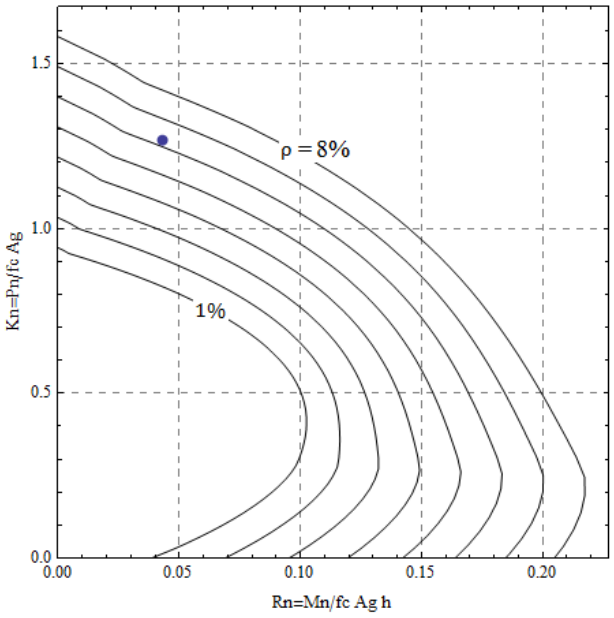

Figure 6.3: Design output for example 3 from Mathematica code.

As shown in Figure 6.3 the required percentage of rebar is 6.30%, which means that the area of required steel is $0.01 * 6.30 * \frac{\pi}{4} \times 15^2 = 11.13 \text{ in}^2$

Example #4:

Comparison between ACI stress block and the proposed stress block in chapter 4 for HSC case and measuring the difference in the required steel bars percentage. The column is subjected to compression force and uniaxial bending under the following requirements of loading and dimensions:

Required nominal load:

$M_n = 5500 \text{ kip. in}$

$P_n = 1150 \text{ kip}$

Cross section:

$b \times h = 12 \text{ in} \times 16 \text{ in}$

$\gamma = 0.85$

Materials' strength:

$f'_c = 16 \text{ ksi}$

$f_y = 60 \text{ ksi}$

Solution:

$$K_n = \frac{P_n}{f'_c A_g} = \frac{1150}{16 \times 12 \times 16} = 0.3743$$

$$R_n = \frac{M_n}{f'_c A_g h} = \frac{5500}{16 \times 12 \times 16 \times 16} = 0.1119$$

The column is design as a rectangular column with steel distributed on two faces only using the stress block as proposed in chapter 4 and ACI code as follow:

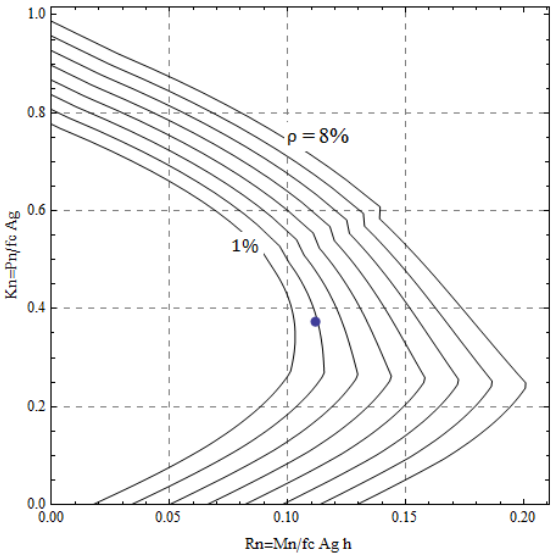

Figure 6.4: Design output for example 4 from Mathematica code using stress block as proposed in chapter 4.

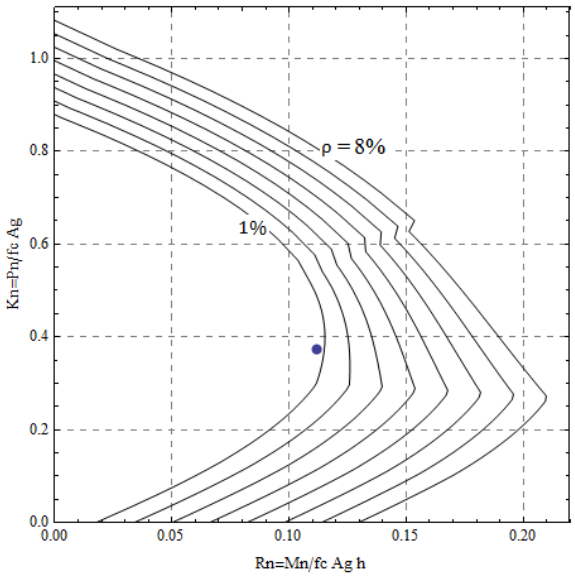

Figure 6.5: Design output for example 4 from Mathematica code using stress block as proposed ACI code for NSC.

As shown in Figure 6.4 and Figure 6.5 the required percentage of rebar is 2% and 1%, respectively. This confirms that the ACI stress block overestimates the column capacity for HSC case. A reduction in steel area by 1% because of the use of ACI stress-block for HSC column, this results into unsafe design and may imply failure of such columns under the required resistance load. Therefore, the required area of steel is $0.02 * 12 * 16 = 3.84\ \text{in}^2$.

Example #5:

Check the adequacy of a reinforced concrete column subjected to compression and biaxial bending with the following loading, material and geometrical requirements:

Required nominal load:

$\mathrm{P_n} = 265\ \text{kip}$

$\mathrm{M_{nx}} = 1325\ \text{kip.in}$

$\mathrm{M_{ny}} = 927\ \text{kip.in}$

Cross section:

$\mathrm{b} \times \mathrm{h} = 12\ \text{in} \times 14\ \text{in}$

$\gamma = 0.70$

$\rho = 0.03 \rightarrow A_s = 0.03 \times 12 \times 14 = 5.04\ \text{in}^2$ This steel is distributed on two faces only.

Materials' strength:

$\mathrm{f_c'} = 16\ \text{ksi}$

$f_y = 60$ ksi

Solution:

$$K_n = \frac{P_n}{f'_c A_g} = \frac{265}{16 \times 12 \times 14} = 0.09859$$

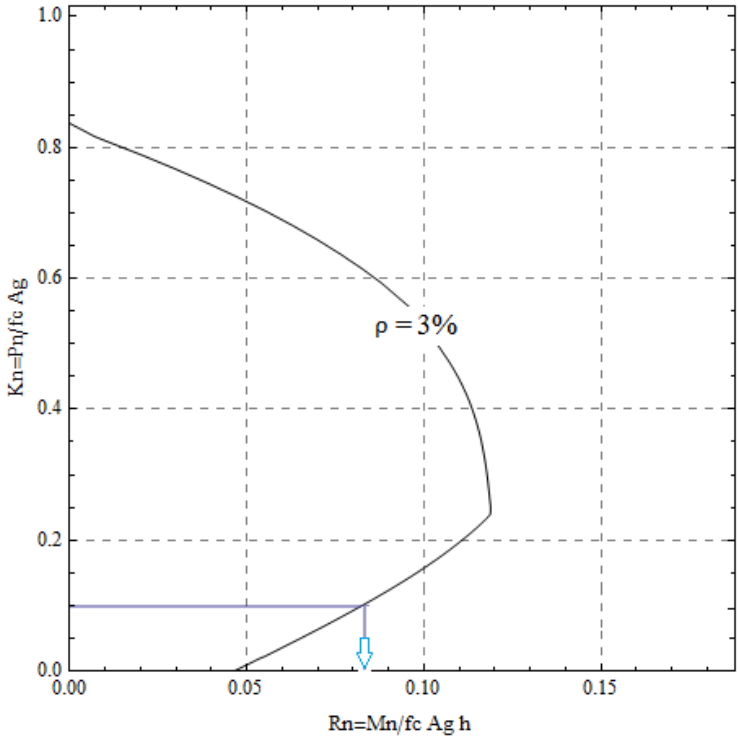

Figure 6.6: Mathematica-developed interaction diagram at steel percentage 3% for the column data as given in this example.

From Figure 6.6 $R_{nx}$and R_{ny} can be found by measuring the coordinate from the horizontal axis which are as follow:

$$\frac{M_{nxo}}{f'_c A_g h} = 0.0833 \rightarrow M_{nxo} = 0.0833 \times 16 \times 12 \times 14 \times 14 = 3134.74 \text{ kip. in}$$

$$\frac{M_{nyo}}{f'_c A_g b} = 0.0833 \rightarrow M_{nyo} = 0.0833 \times 16 \times 12 \times 14 \times 12 = 2686.92 \text{ kip. in}$$

Using Bresler load contour equation to check the adequacy of the column as follow:

$$\left(\frac{M_{nx}}{M_{nox}}\right)^{1.5} + \left(\frac{M_{ny}}{M_{noy}}\right)^{1.5} = 1$$

$$\left(\frac{1325}{3134.74}\right)^{1.5} + \left(\frac{927}{2686.92}\right)^{1.5} = 0.48 < 1 \rightarrow \text{This column is adequate.}$$

Example #6:

Design a rectangular-tied concrete column subjected to compression and biaxial bending with the following loading, material and geometrical requirements:

Required ultimate load:

$P_u = 650$ kip

$M_{ux} = 110$ kip. ft

$M_{uy} = 180$ kip. ft

Materials' strength:

$f'_c = 14$ ksi

$f_y = 60$ ksi

Solution:

❖ Preliminary sizing of the column cross section:

Assume $\rho_g = 0.015$

$$A_g \geq \frac{P_u}{0.40\left(f_c' + f_y\,\rho_g\right)} = \frac{650}{0.40(14 + 0.015 \times 60)} = 109.06\ in.^2\ \ or\ 10.4\ in.square$$

This column is also subjected to biaxial bending. So, try 14-in.-square column with 8 bars number 7.

❖ Calculate $\gamma,\ \rho_g$:

Assume 1.5 in. concrete cover.

$$\gamma = \frac{14 - 2 \times 1.5}{14} = 0.79$$

$$\rho_g = \frac{8 \times 0.6}{14 \times 14} = 0.0245$$

❖ Calculate P_{nx} , $P_{no}\ and\ P_{ny}$:

$$\rho_g = 0.0245$$

$$\frac{e_x}{b} = \frac{M_{uy}}{b\,P_u} = \frac{180 \times 12}{14 \times 650} = 0.237$$

$$\frac{e_y}{h} = \frac{M_{ux}}{h\,P_u} = \frac{110 \times 12}{14 \times 650} = 0.145$$

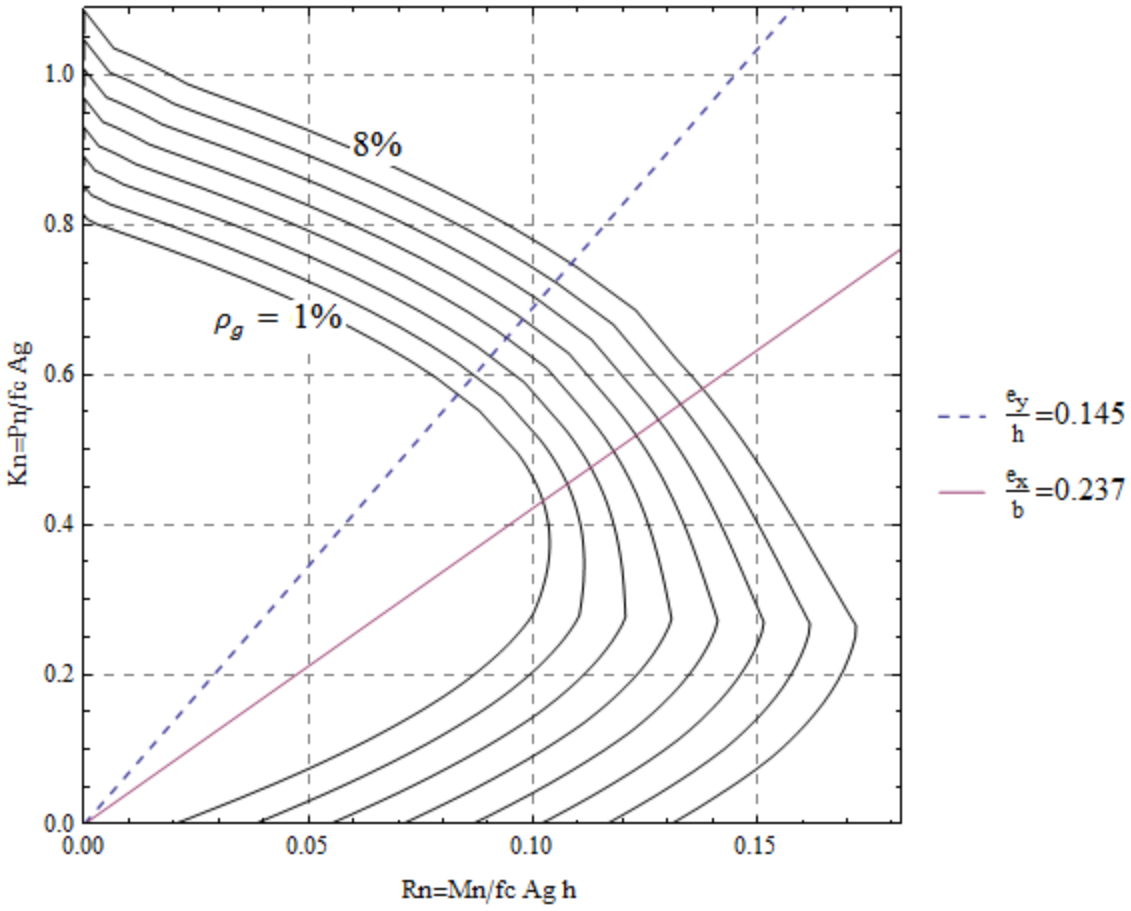

Figure 6.7: Mathematica-developed interaction diagrams.

$$\frac{P_{nx}}{\mathrm{f_c'\,A_g}} = 0.64 = \frac{P_{nx}}{14 \times 14 \times 14} \rightarrow P_{nx} = 1756.16\ kips$$

$$\frac{P_{ny}}{\mathrm{f_c'\,A_g}} = 0.475 = \frac{P_{ny}}{14 \times 14 \times 14} \rightarrow\ P_{ny} = 1303.4\ kips$$

$$P_{no} = 0.774 \times 14 \times 14 \times 14 + 0.0245 \times 14 \times 14 \times (60 - 0.774 \times 14)$$

$$= 2359.94 \text{ kips}$$

❖ Using Bresler method to calculate ϕP_n :

$$\frac{1}{P_n} = \frac{1}{P_{nx}} + \frac{1}{P_{ny}} - \frac{1}{P_{no}} = \frac{1}{1756.16} + \frac{1}{1303.4} - \frac{1}{2359.94} = 9.129 \times 10^{-4} \rightarrow P_n$$

$$= 1095.4\ kips$$

$$\phi P_n = 0.65(1095.4) = 712\ kips \geq P_u = 650\ kips$$

Therefore, 14×14 in. square cross section and 2.45% steel percentage are adequate.

Finally, interaction diagrams are developed for both NSC and HSC reinforced columns. Those diagrams are used for either design or investigation for any rectangular and circular columns concrete columns. The above six examples summarize the basics and fundamentals for analysis and design of reinforced concrete columns.

CHAPTER SEVEN

CONCLUSIONS AND RECOMMENDATIONS

7.1 Conclusions

An effort has been made in this work to develop interaction curves and contours to be used for the analysis and design of HSRC columns. Based on the results of this work, the following conclusions can be drawn:

1. The use of equivalent rectangular stress block for concrete under compression is equivalent to the exact stress-strain relationships.
2. Concrete stress-strain relationship can be idealized by the equivalent rectangular stress block for both NSC and HSC. A new rectangular stress block has been proposed for HSC, because NSC stress block (assumed in ACI curves) overestimates the column capacity for the case of HSC.
3. Mathematica is capable of developing short and efficient codes for generating interaction diagrams for any circular and rectangular NSRC or HSRC columns
4. Mathematica-generated interaction curves for NSRC columns have been successfully validated using ACI curves, PCA software and the available data from the literature.
5. Mathematica-generated interaction curves for HSRC columns have been successfully validated using PCA software and the available data from the literature.
6. Both ACI and Mathematica-developed interaction curves are more conservative than PCA software for NSRC columns

7. The deviations between ACI/Mathematica-developed and PCA interaction curves occur in the compression-controlled part of the curves.
8. Oztekin's model is the best among all investigated modes for representing the tress-strain relationship of HSC. The stress block parameters, computed based on this model, have yielded results that are closer to the literature experimental data.
9. Bresler load contour method is proposed for biaxial bending columns, and it is found conservative for such cases based on the experimental validation.

7.2 Recommendations

Finally, as is the case with any other computational-based research, there is a scope for further enhancement of the study. Below are some of the recommendations that can be made:

1. The developed interaction curves are based on concrete stress-strain relationships for unconfined concrete (neglecting the effect of the column tie bars). Although this yields conservative design column capacity, it does not accurately resemble the real case and therefore, more realistic results may be obtained if the concrete confinement is accounted for.
2. The current literature survey shows that there is a lack of experimental data for HSRC columns with higher steel ratios ($\rho > 1.3\%$). More comprehensive literature search should be performed to get the ones corresponding to medium to high values of ρ. Otherwise; new experiments have to be conducted to generate the missing data.

REFERENCES

[1] ACI Committee 318, “Building Code Requirement for Reinforced Concrete (ACI318-08) and Commentary (318R-08),” American Concrete Institute, Farmington Hills, MI (2008) 443 pp.

[2] WANG, W. & HONG, H. 2002. Appraisal of Reciprocal Load Method for Reinforced Concrete Columns of Normal and High Strength Concrete. Journal of Structural Engineering, 128, 1480-1486.

[3] Eivind Hognestad, a Study of Combined Bending and Axial Load in Reinforced Concrete Members, Bulletin 399, University of Illinois Engineering Experiment Station, Urbana, III. November 1951, 128 pp.

[4] Claudio E. Todeschini, Albert C. Bianchini, and Clyde E. Kesler, “Behavior of concrete columns reinforced with high strength steels, “ ACI Journal, Proceedings, Vol. 61, June 1964, pp. 701-716.

[5] P., Desayie, and S., Krishnan, “Equation for the Stress-Strain behavior of Concrete”, ACI Journal Proc., Vol. 61, No. 3, March, 1964.

[6] S., Popovics, “A Numerical Approach to the Complete Stress-Strain Curve of Concrete”, Cement and Concrete Research, Vol. 3, No. 5, Sept. 1973.

[7] Thorefeldt, E., Tomaszewicz, A. And Jensen, J. J., “Mechanical Properties of High Strength Concrete and Application to Design, “Proceedings of the Symposium: Utilization of High-Strength Concrete,” Stavanger, Norway, June 1987, Tapir, Trondheim, pp. 149-159.

[8] D. J., Carreira, and K. H., Chu, “Stress-Strain Relationship for Plain Concrete in Compression”, ACI Journal Proc., Vol. 82, No. 6, Nov-Dec. 1985.

[9] P., Kumar, “Effect of Strain Ratio on Equivalent Stress Block Parameters for Normal Weight high Strength Concrete”, Structural Eng. Division, India, Accepted Jan. 2006.

[10] Wee, T. H., Chin, M. S., and Mansur, M. A., “Stress-Strain Relationship of High-Strength Concrete in Compression,” ASCE Journal of Materials in Civil Engineering, Vol. 8, No. 2, May 1996, pp. 70-76.

[11] Van Gysel, A. and Taerwe, L., “Analytical Formulation of the Complete Stress-Strain Curve for High Strength Concrete,” Materials and Structures, Vol. 29, November 1996, pp. 529-533.

[12] Oztekin, E., Pul, S., and Husem, M., “Determination of Rectangular Stress Block Parameters for High Strength Concrete,” Engineering Structures, Vol. 25, No. 3, February 2003, pp. 371-376.

[13] MERTOL, HALIT CENAN, “ Behavior of High-Strength Concrete Members Subjected to Combined Flexure and Axial Compression Loadings”, North Carolina State University, December 2006.

[14] WHITNEY, C. S. Design of reinforced concrete members under flexure or combined flexure and direct compression. ACI Journal Proceedings, 1937. ACI.

[15] Togay Ozbakkaloglu and Murat Saatcioglu (2004).Rectangular Stress Block for High-Strength Concrete.ACI Structural Journal, V. 101, No. 4, July-August 2004.

[16] Rizkalla et al., “Final Report for NCHRP Project 12-64,” TRB Publication, 2007 S. Kim, H. C. Mertol, S. Rizkalla, P. Zia(2006).Behavior of High-Strength Concrete Rectangular Columns.

[17] PENG, J., HO, J. C. M. & PAM, H. J. 2011. Modification on Equivalent Stress Block of Normal-Strength Concrete by Incorporating Strain Gradient Effects. Procedia Engineering, 14, 2246-2253.

[18] American Association of State Highway and Transportation Officials, “AASHTO LRFD Bridge Design Specifications - Third Edition including 2005 and 2006 Interim Revisions.” Washington, DC (2004).

[19] NZS 3101-1995, “The Design of Concrete Structures,” Standards New Zealand, Wellington, New Zealand (1995) 520 pp.

[20] Li, B., Park, R., and Tanaka, H., “Strength and Ductility of Reinforced Concrete Members and Frames Constructed Using High-Strength Concrete,” Research Report No. 94-5, Department of Civil Engineering, University of Canterbury, Christchurch, New Zealand (1994) 373 pp.

[21] CSA, “Design of Concrete Structures for Buildings (CAN3-A23.2-94),” Canadian Standards Association, Rexdale, Ontario (1994) 199 pp.

[22] CEB-FIP Model Code 1990, Comite Euro-International du Beton, Thomas Telford (1990) 437 pp. A Najmi,”interaction diagrams of short columns under biaxial bending”, Accepted publication 1997. ACI 544.4R-88,”Design Considerations for Steel Fiber Reinforced Concrete”, Reapproved 1999.

[23] Rizkalla et al., "Final Report for NCHRP Project 12-64," TRB Publication, 2007 S. Kim, H. C. Mertol, S. Rizkalla, P. Zia(2006).Behavior of High-Strength Concrete Rectangular Columns.

[24] ACI-ASCE Committee 441, (1997), "High-strength concrete columns: state-of the art," ACI Structural Journal, V.94, No. 3, May-June, pp. 323-335

[25] Azizinamini, A., Kuska, S. S. B., Brungardt, P. and Hatfield, E., "Seismic Behavior of Square High-Strength Concrete Columns," ACI Structural Journal, Vol. 91, No. 3, 1994, pp. 336-345.

[26] Ibrahim, H. H. H. and MacGregor, G., "Modification of the ACI Rectangular Stress Block for High-Strength Concrete," ACI Structural Journal, Vol. 94, No. 1, 1997, pp. 40-48.

[27] Pendyala, R. and Mendis, P. A., "A Rectangular Stress Block for High Strength Concrete," Structural Engineering Journal, Institution of Engineers, Australia, Vol. CE39, No. 4, 1998, pp.135-144.

[28] Attard, M. M. and Stewart, M. G., "A Two Parameter Stress Block for High Strength Concrete," ACI Structural Journal, Vol. 95, No. 3, 1998, pp. 305-317.

[29] Bae, S. and Bayrak, O., "Stress Block Parameters for High-Strength Concrete Members," ACI Structural Journal, Vol. 100, No. 5, 2003, pp. 626-636.

[30] Asst. Lect. Ali Abdul Hussein Jawad Al-Ghalib."Toward an Appeal for Revision on ACI Stress Block Parameters for High Strength Concrete, "Journal of Engineering and Development, Vol. 11, No. 2, September (2007)

[31] Building Code Requirements for Structural Concrete-AC1 318, Chapters 9 and 10, and"Ultimate Strength Design of Reinforced Concrete Columns", AC1 Special Publication SP-7,by Everard and Cohen, 1964, pp. 152-182 (with corrections).

[32] Noel J. Everard. 1997, "Axial Load-Moment Interaction for Cross Section-Sections Having Longitudinal Reinforcement Arranged in A Circle", ACI Structural Journal, V.94, No.6, Novemeber-December 1997.

[33] Ramon V. Jarquio,"Analytical Prediction of Ultimate Strength in Reinforced Concrete Columns",ASCE 2004.

[34] Bresler, B. 1960. ''Design, Criteria for Reinforced Columns under Axial Load Bi-Axial Bending.'' Proceeuings V. 57. No. 11. Nov., 1960, pp. 481-490

[35] Weber, Donald C., "Ultimate strength design charts for columns with biaxial sending.", ACI Journal proceedings, Vol. 63, Nov. 1966, pp. 1205-1231.

[36] Warner, R. F., "Biaxial moment thrust curveture relations", Journal of Structural Division. ASCE proceeding ST5, May. 1969, pp.923-940.

[37] Furlong, Richard W., "Concrete columns under biaxially eccentric thrust." , ACI Journal, Vol. 76 No. 10 Oct.1979, pp. 1093-1118.

[38] YEN, J. R. 1991. Quasi-Newton method for reinforced-concrete column analysis and design. Journal of Structural Engineering, 117, 657-666.

[39] Hsu, L. S., and Hsu, C. T. T. 1994. "Complete Stress-Strain Behavior of High-Strength Concrete under Compression." Magazine of Concrete Research 46 (169): 301–312.

[40] M.Y. Rafiq, C. Southcombe,"Genetic algorithms in optimal design and detailing of reinforced concrete biaxial columns supported by a declarative approach for capacity checking",Computers and Structures 69 (1998) 443-457.

[41] FAFITIS, A. 2001. Interaction surfaces of reinforced-concrete sections in biaxial bending. Journal of Structural Engineering, 127, 840-846. [43] L. Cedolin, G. Cusatis, S. Eccheli, M. Roveda,"Biaxial Bending of Concrete Columns:An Analytical Solution",STUDIES AND RESEARCHES - V.26, 2006.

[42] BONET, J., MIGUEL, P., FERNANDEZ, M. & ROMERO, M. 2004. Analytical approach to failure surfaces in reinforced concrete sections subjected to axial loads and biaxial bending. Journal of Structural Engineering, 130, 2006-2015.

[43] L. Cedolin, G. Cusatis, S. Eccheli, M. Roveda, "Biaxial bending of concrete columns: an analyical solution:, STUDIES AND RESEARCHES – V. 26, 2006.

[44] L. Pallarés, Pedro F. Miguel, Miguel A. Fernández-Prada,"A numerical method to design reinforced concrete sections subjected to axial forces and biaxial bending based on ultimate strain limits",Engineering Structures 31 (2009) 3065-3071.

[45] Marinella Fossetti a, Maurizio Papia,"Dimensionless analysis of RC rectangular sections under axial load and biaxial bending", Engineering Structures 44 (2012) 34-45.

[46] Ibrahim, H. H. H. and MacGregor, J. G. "Flexural Behavior of Laterally Reinforced High-Strength Concrete Sections," ACI Structural Journal, Vol. 93, No. 6 (Nov. 1996) pp.674-684

[47] Ibrahim, H. H. H. and MacGregor, J. G. “Tests of Eccentrically Loaded High-Strength Concrete Columns,” ACI Structural Journal, Vol. 93, No. 5 (Sep. 1996) pp. 585-594

[48] Foster, S. J. and Attard, M. M., “Experimental Tests on Eccentrically Loaded High-Strength Concrete Columns,” ACI Structural Journal, Vol. 94, No. 3 (May 1997), pp. 295-303

[49] Lee, J., and Son, H. “Failure and Strength of High-Strength Concrete Columns Subjected to Eccentric Loads,” ACI Structural Journal, Vol. 97, No. 1 (Jan. 2000) pp. 75-85

[50] Tan, T. H. and Nguyen, N., “Flexural Behavior of Confined High-Strength Concrete Columns,” ACI Structural Journal, Vol. 102, No. 2 (Mar. 2005) pp. 198-205.

[51] Hany A. Kottb, Nasser F. El-Shafey, Akram A. Torkey,”Behavior of high strength concrete columns under eccentric loads”,HBRC Journal (2014).

[52] J.L. Bonet, P.F. Miguel, M.A. Fernandez, M.L. Romero,”Biaxial bending moment magnifier method”,Engineering Structures 26 (2004) 2007–2019.

[53] Amarjit Singh Bajaj and P. Mendis,”New Method to Evaluate the Biaxial Interaction Exponent for RC Columns”,J. Struct. Eng. 2005.131:1926-1930.

[54] PALLARÉS, L., BONET, J., MIGUEL, P. & FERNÁNDEZ PRADA, M. 2008. Experimental research on high strength concrete slender columns subjected to compression and biaxial bending forces. Engineering Structures, 30, 1879-1894.

[55] Lloyd, N. A., and Rangan, B. V., “Studies on High-Strength Concrete Columns under Eccentric Compression,” ACI Structural Journal, V. 93, No. 6, Nov.-Dec. 1996, pp. 631-638.

[56] Serkan Tokgoz, Cengiz Dundar, A. Kamil Tanrikulu, “Experimental behaviour of steel fiber high strength reinforced concrete and composite columns”, Journal of Constructional Steel Research 74 (2012) 98–107.

APPENDIX

This code was prepared to draw interaction diagrams for circular reinforced concrete columns with steel distributed on circular perimeter of the column cross section.

Input Material and Geometric Properties of the column cross section here

```
ClearAll["Global`*"]
γ = 0.7;
fy = 60;(*ksi*)
fc = 6;(*ksi*)
n1 = 50;
n2 = 30;
n3 = 30;
ρ =.; h = 1; α1 =.; β1 =.;
ϵcu = 3/1000;  Es = 29000; ϵy = fy/Es;
If[fc ≤ 12, α1 = 85/100]
If[12 < fc ≤ 23, α1 = 0.96588 - 0.0019858 fc * 1000/145]
If[fc > 23, α1 = 65/100]
If[fc ≤ 4, β1 = 85/100]
If[4 < fc ≤ 8, β1 = 85/100 - 5/100 (fc - 4)]
If[8 < fc ≤ 12, β1 = 65/100]
If[12 < fc < 18.6, β1 = 0.8033 - 0.001195 fc * 1000/145]
If[fc ≥ 18.6, β1 = 0.65]

Ag = π/4 h^2;
As = ρ Ag;
```

$\frac{17}{20}$

$\frac{3}{4}$

Region 1 on the interaction diagram where $c \geq \frac{h}{2}(1+\gamma)$

```
c =.; θ =.; θ1 =.; θ2 =.; θ3 =.; θ4 =.; θ5 =.; fs =.; P =.; M =.;
Ff =.; Mf =.; Fc =.; Mc =.; Fs =.; i =.; M1 =.; P1 =.; ρ =.;
ϵs1 =.; ϵs3 =.; Fsc =.; Fst =.; Msc =.; Mst =.; x =.; θθ3 =.;
```

```
Do[c[i] = (0.02 i + 1) h/2 (1 + γ), {i, 1, n1}]

Do[{εs1[i] = εcu/c[i] (c[i] - h/2 (1 + γ)), εs3[i] = εcu/c[i] (c[i] - h/2 (1 - γ))}, {i, 1, n1}]

Do[{θ1[i] = N[ArcCos[1/γ (1 - 2 c[i]/h)]], θ2[i] = N[ArcCos[1 - 2 β1 c[i]/h]],
  θ3[i] = N[ArcCos[1/γ (1 - 2 c[i]/h (1 - εy/εcu))]], θ5[i] = N[ArcCos[1/γ - 2 β1 c[i]/(γ h)]]}, {i, 1, n1}]

Do[If[β1 c[i] > h, Fc[i] = α1 fc Ag,
  Fc[i] = FullSimplify[-α1 fc/2 h^2 NIntegrate[(Sin[θ])^2, {θ, θ2[i], 0}]]], {i, 1, n1}]

Do[If[β1 c[i] > h, Mc[i] = 0,
  Mc[i] = FullSimplify[-α1 fc/4 h^3 NIntegrate[(Cos[θ]) (Sin[θ])^2, {θ, θ2[i], 0}]]], {i, 1, n1}]

Do[If[β1 c[i] ≥ h/2 (1 + γ), Ff[i] = -α1 fc ρ Ag, Ff[i] = (-α1 fc ρ Ag)/π θ5[i]], {i, 1, n1}]

Do[If[β1 c[i] ≥ h/2 (1 + γ), Mf[i] = 0, Mf[i] = -((α1 fc ρ Ag γ h Sin[θ5[i]])/(2 π))], {i, 1, n1}]

Do[fs[i] = N[Es εcu/c[i] (c[i] - h/2 (1 - γ Cos[θ]))], {i, 1, n1}]

Do[x[i] = ((εcu - εy)/εcu) c[i], {i, 1, n1}]

Do[If[x[i] > h/2 (1 - γ) && x[i] < h/2 (1 + γ), θθ3[i] = ArcCos[1/γ - 2 c[i]/(γ h) (1 - εy/εcu)]], {i, 1, n1}]

Do[If[x[i] ≤ h/2 (1 - γ), Fsc[i] = As/(2 π) (NIntegrate[fs[i], {θ, 0, π}])], {i, 1, n1}]

Do[If[x[i] > h/2 (1 - γ) && x[i] < h/2 (1 + γ), Fsc[i] =
    As/(2 π) (NIntegrate[fy, {θ, 0, θθ3[i]}] + NIntegrate[fs[i], {θ, θθ3[i], π}])], {i, 1, n1}]

Do[If[x[i] > h/2 (1 + γ), Fsc[i] = As/(2 π) (NIntegrate[fy, {θ, 0, π}])], {i, 1, n1}]

Do[If[x[i] ≤ h/2 (1 - γ), Msc[i] = γ h As/(2 π) (NIntegrate[(Cos[θ]) fs[i], {θ, 0, π}])], {i, 1, n1}]

Do[If[x[i] > h/2 (1 - γ) && x[i] < h/2 (1 + γ),
  Msc[i] = γ h As/(2 π) (NIntegrate[(Cos[θ]) fy, {θ, 0, θθ3[i]}] +
      NIntegrate[(Cos[θ]) fs[i], {θ, θθ3[i], π}])], {i, 1, n1}]

Do[If[x[i] > h/2 (1 + γ), Msc[i] = 0], {i, 1, n1}]
Do[{Mst[i] = 0, Fst[i] = 0}, {i, 1, n1}]
Do[{P[i] = 2 (Fsc[i] + Fst[i]) + Fc[i] + Ff[i],
  M[i] = (Mst[i] + Msc[i]) + Mc[i] + Mf[i]}, {i, 1, n1}]
```

```
Do[{P1[i] = FullSimplify[P[i]/(fc Ag)], M1[i] = FullSimplify[M[i]/(fc Ag h)]}, {i, 1, n1}]
Do[data1[ii] = Reverse[Table[{M1[i], P1[i]} /. ρ → 0.01 ii, {i, 1, n1}]], {ii, 1, 8}]
```

Region 2 on the interaction diagram where $\frac{h}{2}(1-\gamma) < c < \frac{h}{2}(1+\gamma)$

```
c = .; θ1 = .; θ2 = .; θ3 = .; θ4 = .; θ5 = .; fs = .; P = .; M = .; P2 = .; M2 = .; Ff = .; Mf = .; Fc = .;
Mc = .; Fs = .; ϵs1 = .; i = .; M = .; ρ = .; ϵs1 = .; ϵs3 = .; Fsc = .; Fst = .; Msc = .; Mst = .;
Do[c[i] = h/2 (1 + γ) - 0.9 i/n2 (γ h), {i, 1, n2}]
Do[{ϵs1[i] = ϵcu/c[i] (h/2 (1 + γ) - c[i]), ϵs3[i] = ϵcu/c[i] (c[i] - h/2 (1 - γ))}, {i, 1, n2}]
Do[{θ1[i] = N[ArcCos[1/γ (1 - 2 c[i]/h)]],
  θ2[i] = N[ArcCos[1 - 2 β1 c[i]/h]], θ3[i] = N[ArcCos[1/γ (1 - 2 c[i]/h (1 - ϵy/ϵcu))]],
  θ4[i] = N[ArcCos[1/γ (1 - 2 c[i]/h (1 + ϵy/ϵcu))]], θ5[i] = N[ArcCos[1/γ - 2 β1 c[i]/(γ h)]]}, {i, 1, n2}]
Do[If[β1 c[i] > h/2 (1 - γ), Ff[i] = -(α1 fc ρ Ag/π) θ5[i], Ff[i] = 0], {i, 1, n2}]
Do[If[β1 c[i] > h/2 (1 - γ), Mf[i] = -(1/(2 π)) α1 fc ρ Ag γ h Sin[θ5[i]], Mf[i] = 0], {i, 1, n2}]
Do[{fs[i] = N[fy γ/(2 (c[i]/h) (ϵy/ϵcu)) (Cos[θ] - Cos[θ1[i]])],
  Fc[i] = FullSimplify[-α1 fc/2 h^2 NIntegrate[(Sin[θ])^2, {θ, θ2[i], 0}]],
  Mc[i] = FullSimplify[-α1 fc/4 h^3 NIntegrate[(Cos[θ]) (Sin[θ])^2, {θ, θ2[i], 0}]]}, {i, 1, n2}]
Do[If[ϵs1[i] > ϵy, Fst[i] =
   As/(2 π) (NIntegrate[fs[i], {θ, θ1[i], θ4[i]}] + NIntegrate[-fy, {θ, θ4[i], π}]),
  Fst[i] = As/(2 π) (NIntegrate[fs[i], {θ, θ1[i], π}])], {i, 1, n2}]
Do[If[ϵs3[i] > ϵy, Fsc[i] = As/(2 π) (NIntegrate[fs[i], {θ, θ3[i], θ1[i]}] + fy θ3[i]),
  Fsc[i] = As/(2 π) (NIntegrate[fs[i], {θ, 0, θ1[i]}])], {i, 1, n2}]
Do[If[ϵs1[i] > ϵy, Mst[i] = γ h As/(2 π) (NIntegrate[(Cos[θ]) fs[i], {θ, θ1[i], θ4[i]}] +
     NIntegrate[-fy (Cos[θ]), {θ, θ4[i], π}]),
  Mst[i] = γ h As/(2 π) (NIntegrate[(Cos[θ]) fs[i], {θ, θ1[i], π}])], {i, 1, n2}]
Do[If[ϵs3[i] > ϵy, Msc[i] = γ h As/(2 π)
```

```
      (NIntegrate[(Cos[θ]) fs[i], {θ, θ3[i], θ1[i]}] + NIntegrate[(Cos[θ]) fy, {θ, 0, θ3[i]}]),
   Msc[i] = γ h As / (2 π) (NIntegrate[(Cos[θ]) fs[i], {θ, 0, θ1[i]}])], {i, 1, n2}]
Do[{P[i] = 2 (Fsc[i] + Fst[i]) + Fc[i] + Ff[i], M[i] = (Mst[i] + Msc[i]) + Mc[i] + Mf[i]},
 {i, 1, n2}]
Do[{P2[i] = FullSimplify[P[i] / (fc Ag)], M2[i] = FullSimplify[M[i] / (fc Ag h)]}, {i, 1, n2}]
Do[data2[ii] = Table[{M2[i], P2[i]} /. ρ → 0.01 ii, {i, 1, n2}], {ii, 1, 8}]
```

Region 3 on the interaction diagram where $0 < c \leq \frac{h}{2} (1 - \gamma)$

```
c = .; θ = .; θ1 = .; θ2 = .; θ3 = .; θ4 = .; θ5 = .; fs = .; P = .; M = .;
Ff = .; Mf = .; Fc = .; Mc = .; Fs = .; i = .; M3 = .; P3 = .; ρ = .;
ϵs1 = .; ϵs3 = .; Fsc = .; Fst = .; Msc = .; Mst = .; x = .; θθ4 = .;
Do[c[i] = (i/n3) h/2 (1 - γ), {i, 1, n3}]
Do[{ϵs1[i] = ϵcu/c[i] (c[i] - h/2 (1 + γ)), ϵs3[i] = ϵcu/c[i] (c[i] - h/2 (1 - γ))}, {i, 1, n3}]
Do[{θ1[i] = N[ArcCos[1/γ (1 - 2 c[i]/h)]], θ2[i] = N[ArcCos[1 - 2 β1 c[i]/h]],
  θ3[i] = N[ArcCos[1/γ (1 - 2 c[i]/h (1 - ϵy/ϵcu))]], θ5[i] = N[ArcCos[1/γ - 2 β1 c[i]/(γ h)]]}, {i, 1, n3}]
Do[Fc[i] = FullSimplify[-α1 fc/2 h^2 NIntegrate[(Sin[θ])^2, {θ, θ2[i], 0}]], {i, 1, n3}]
Do[Mc[i] = FullSimplify[-α1 fc/4 h^3 NIntegrate[(Cos[θ]) (Sin[θ])^2, {θ, θ2[i], 0}]], {i, 1, n3}]
Do[{Mf[i] = 0, Ff[i] = 0}, {i, 1, n3}]
Do[fs[i] = N[Es ϵcu/c[i] (-c[i] + h/2 (1 - γ Cos[θ]))], {i, 1, n3}]
Do[x[i] = ((ϵcu + ϵy)/ϵcu) c[i], {i, 1, n3}]
Do[If[x[i] > h/2 (1 - γ) && x[i] < h/2 (1 + γ), θθ4[i] = ArcCos[1/γ - 2 c[i]/(γ h) (1 + ϵy/ϵcu)]], {i, 1, n3}]
Do[If[x[i] ≤ h/2 (1 - γ), Fst[i] = As/(2 π) (NIntegrate[-fy, {θ, 0, π}])], {i, 1, n3}]
Do[If[x[i] > h/2 (1 - γ) && x[i] < h/2 (1 + γ), Fst[i] =
  As/(2 π) (NIntegrate[-fs[i], {θ, 0, θθ4[i]}] + NIntegrate[-fy, {θ, θθ4[i], π}])], {i, 1, n3}]
Do[If[x[i] > h/2 (1 + γ), Fst[i] = As/(2 π) (NIntegrate[-fs[i], {θ, 0, π}])], {i, 1, n3}]
Do[If[x[i] ≤ h/2 (1 - γ), Mst[i] = 0], {i, 1, n3}]
Do[If[x[i] > h/2 (1 - γ) && x[i] < h/2 (1 + γ),
  Mst[i] = γ h As/(2 π) (NIntegrate[-(Cos[θ]) fs[i], {θ, 0, θθ4[i]}] +
    NIntegrate[-(Cos[θ]) fy, {θ, θθ4[i], π}])], {i, 1, n3}]
Do[If[x[i] > h/2 (1 + γ), Mst[i] = γ h As/(2 π) (NIntegrate[-(Cos[θ]) fs[i], {θ, 0, π}])], {i, 1, n3}]
Do[{Msc[i] = 0, Fsc[i] = 0}, {i, 1, n3}]
Do[{P[i] = 2 (Fsc[i] + Fst[i]) + Fc[i] + Ff[i],
  M[i] = (Mst[i] + Msc[i]) + Mc[i] + Mf[i]}, {i, 1, n3}]
Do[{P3[i] = FullSimplify[P[i]/(fc Ag)], M3[i] = FullSimplify[M[i]/(fc Ag h)]}, {i, 1, n3}]
Do[data3[ii] = Reverse[Table[{M3[i], P3[i]} /. ρ → 0.01 ii, {i, 1, n3}]], {ii, 1, 8}]
```

Drawing of the Interaction Diagrams

```
P0 = .; t = .; d = .; Mr = .;
Mr = Max[Table[N[M2[i]] /. ρ → 0.08, {i, 1, n2}]];
P0 = ((Ag - ρ Ag) α1 fc + ρ Ag fy) / (fc Ag);
t = -(ρ Ag fy) / (fc Ag);
Do[d[i] =
  ListPlot[Join[{{0, P0}} /. ρ → 0.01 i, data1[i], data2[i], data3[i], {{0, t}} /. ρ → 0.01 i],
   PlotStyle → {Thickness[0.003], Black}, Joined → True], {i, 1, 8}]
Show[{d[1], d[2], d[3], d[4], d[5], d[6], d[7], d[8]}, AspectRatio → 1,
 GridLines → Automatic, GridLinesStyle → Directive[Gray, Dashed], Frame → True,
 PlotRangePadding → 0, PlotRange → {{Mr + 0.01, 0}, {t - 0.05 /. ρ → 0.08, P0 /. ρ → 0.08 + .01}},
 FrameLabel → {"Rn=Mn/fc Ag h", "Kn=Pn/fc Ag"}]
Show[{d[1], d[2], d[3], d[4], d[5], d[6], d[7], d[8]}, AspectRatio → 1,
 GridLines → Automatic, GridLinesStyle → Directive[Gray, Dashed], Frame → True,
 PlotRangePadding → 0, PlotRange → {{Mr + 0.01, 0}, {0, P0 /. ρ → 0.08 + .01}},
 FrameLabel → {"Rn=Mn/fc Ag h", "Kn=Pn/fc Ag"}]
```

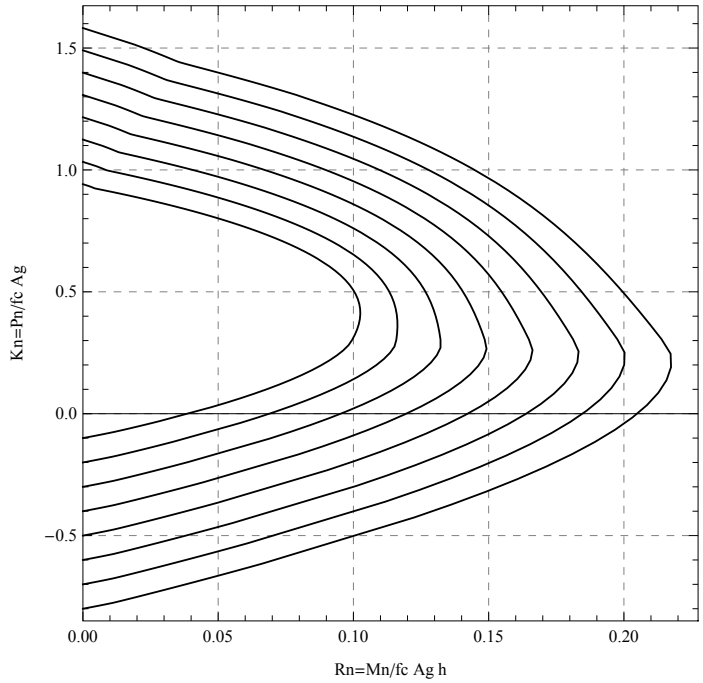

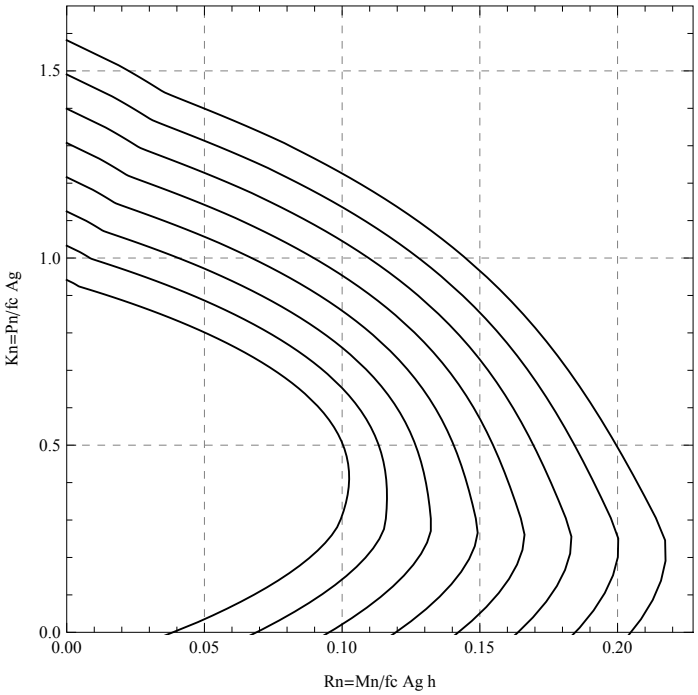
1.5
1.0
0.5
0.0
Kn=Pn/fc Ag
0.00
0.05
0.10
0.15
0.20
Rn=Mn/fc Ag h

This code was prepared to draw interaction diagrams for uniaxial rectangular reinforced concrete columns with steel distributed on two faces only of the column cross section.

Input Material and Geometric Properties of the column cross section here

In[1]:=
```
ClearAll["Global`*"]
```

$\gamma = 0.75;$

$fy = 60;(*ksi*)$

$fc = 16;(*ksi*)$

$n1 = 50;$

$n2 = 50;$

$n3 = 20;$

$\rho = .;\ b = 1;\ h = 1;$

$\alpha 1 = .;\ \beta 1 = .;\ \epsilon cu = \frac{3}{1000};\ \ Es = 29\,000;\ \epsilon y = \frac{fy}{Es};$

$If\left[fc \leq 12,\ \alpha 1 = \frac{85}{100}\right]$

$If\left[12 < fc \leq 23,\ \alpha 1 = 0.96588 - 0.0019858\, fc * \frac{1000}{145}\right]$

$If\left[fc > 23,\ \alpha 1 = \frac{65}{100}\right]$

$If\left[fc \leq 4,\ \beta 1 = \frac{85}{100}\right]$

$If\left[4 < fc \leq 8,\ \beta 1 = \frac{85}{100} - \frac{5}{100}\,(fc - 4)\right]$

$If\left[8 < fc \leq 12,\ \beta 1 = \frac{65}{100}\right]$

$If\left[12 < fc < 18.6,\ \beta 1 = 0.8033 - 0.001195\, fc * \frac{1000}{145}\right]$

$If[fc \geq 18.6,\ \beta 1 = 0.65]$

$As1 = As3 = \frac{\rho\, b\, h}{2};$

Out[11]= 0.746757

Out[16]= 0.671438

Region 1 on the interaction diagram where $c \geq \frac{h}{2}(1+\gamma)$

In[19]:=
```
c = .; ϵs1 = .; ϵs3 = .; Fs1 = .; Fs2 = .; Fs3 = .; Fc = .; fs1 = .;
fs3 = .; y1 = .; ϵ = .; P2 = .; M2 = .; P = .; M = .; ρ = .; i = .; Mc = .;
mc2 = .; mt2 = .; Fsc2 = .; Fst2 = .; Fs = .;
Do[c[i] = h, {i, 1, 1}]
Do[c[i] = (0.04 i + 1) h, {i, 2, n1}]
Do[{ϵs1[i] = ϵcu/c[i] (c[i] - h/2 (1 + γ)), ϵs3[i] = ϵcu/c[i] (c[i] - h/2 (1 - γ))}, {i, 1, n1}]
Do[If[β1 c[i] > h, Fc[i] = α1 fc b h, Fc[i] = α1 fc b β1 c[i]], {i, 1, n1}]
Do[If[β1 c[i] > h, Mc[i] = 0, Mc[i] = α1 fc b β1 c[i] ((h - β1 c[i])/2)], {i, 1, n1}]
Do[If[ϵs1[i] ≥ ϵy, fs1[i] = fy, fs1[i] = ϵs1[i] Es], {i, 1, n1}]
Do[If[ϵs3[i] ≥ ϵy, fs3[i] = fy, fs3[i] = ϵs3[i] Es], {i, 1, n1}]
Do[Fs1[i] = As1 (fs1[i] - α1 fc), {i, 1, n1}]
Do[Fs3[i] = As3 (fs3[i] - α1 fc), {i, 1, n1}]
Do[{Fs[i] = Fs3[i] + Fs1[i], P[i] = Fc[i] + Fs[i]}, {i, 1, n1}]
Do[M[i] = (-Fs1[i] + Fs3[i]) (γ h/2) + Mc[i], {i, 1, n1}]
Do[P1[i] = FullSimplify[P[i]/(fc b h)], {i, 1, n1}]
Do[M1[i] = FullSimplify[M[i]/(fc b h^2)], {i, 1, n1}]
Do[data1[ii] = Reverse[Table[{N[M1[i]], N[P1[i]]} /. ρ → 0.01 ii, {i, 1, n1}]], {ii, 1, 8}]
```

Region 2 on the interaction diagram where $\frac{h}{2}(1-\gamma) < c < \frac{h}{2}(1+\gamma)$

In[35]:=
```
c =.; εs1 =.; εs3 =.; Fs1 =.; Fs2 =.; Fs3 =.; Fc =.; fs1 =.;
fs3 =.; y1 =.; ε =.; P2 =.; M2 =.; P =.; M =.; ρ =.; i =.;
mc2 =.; mt2 =.; Fsc2 =.; Fst2 =.; Fs =.;
Do[c[i] = h/2 (1 + γ) - (i - 1)/n2 γ h, {i, 1, n2}]
Do[{εs1[i] = εcu/c[i] (h/2 (1 + γ) - c[i]), εs3[i] = εcu/c[i] (c[i] - h/2 (1 - γ))}, {i, 1, n2}]
Do[Fc[i] = α1 fc b β1 c[i], {i, 1, n2}]
Do[If[εs1[i] ≥ εy, fs1[i] = fy, fs1[i] = εs1[i] Es], {i, 1, n2}]
Do[If[εs3[i] ≥ εy, fs3[i] = fy, fs3[i] = εs3[i] Es], {i, 1, n2}]
Do[Fs1[i] = As1 (fs1[i]), {i, 1, n2}]
Do[Fs3[i] = As3 (fs3[i] - α1 fc), {i, 1, n2}]
Do[{Fs[i] = Fs3[i] - Fs1[i], P[i] = Fc[i] + Fs[i]}, {i, 1, n2}]
Do[M[i] = (Fs1[i] + Fs3[i]) (γ h/2) + Fc[i] ((h - β1 c[i])/2), {i, 1, n2}]
Do[P2[i] = FullSimplify[P[i]/(fc b h)], {i, 1, n2}]
Do[M2[i] = FullSimplify[M[i]/(fc b h^2)], {i, 1, n2}]
Do[data2[ii] = Table[{N[M2[i]], N[P2[i]]} /. ρ → 0.01 ii, {i, 1, n2}], {ii, 1, 8}]
```

Region 3 on the interaction diagram where $0 < c \le \frac{h}{2}(1-\gamma)$

In[49]:=
```
c =.; εs1 =.; εs3 =.; Fs1 =.; Fs2 =.; Fs3 =.; Fc =.; fs1 =.;
fs3 =.; y1 =.; ε =.; P3 =.; M3 =.; P =.; M =.; ρ =.; i =.;
mc2 =.; mt2 =.; Fsc2 =.; Fst2 =.; Fs =.;
Do[c[i] = h/2 (1 - γ) - (i - 1)/n3 * 5/12 * (h/2 (1 - γ)), {i, 1, n3}]
Do[{εs1[i] = εcu/c[i] (h/2 (1 + γ) - c[i]), εs3[i] = εcu/c[i] (h/2 (1 - γ) - c[i])}, {i, 1, n3}]
Do[Fc[i] = α1 fc b β1 c[i], {i, 1, n3}]
Do[If[εs1[i] ≥ εy, fs1[i] = fy, fs1[i] = εs1[i] Es], {i, 1, n3}]
Do[If[εs3[i] ≥ εy, fs3[i] = fy, fs3[i] = εs3[i] Es], {i, 1, n3}]
Do[Fs1[i] = As1 (fs1[i]), {i, 1, n3}]
Do[Fs3[i] = As3 (fs3[i]), {i, 1, n3}]
Do[{Fs[i] = -Fs3[i] - Fs1[i], P[i] = Fc[i] + Fs[i]}, {i, 1, n2}]
Do[M[i] = (Fs1[i] - Fs3[i]) (γ h/2) + Fc[i] ((h - β1 c[i])/2), {i, 1, n3}]
Do[P3[i] = FullSimplify[P[i]/(fc b h)], {i, 1, n3}]
Do[M3[i] = FullSimplify[M[i]/(fc b h^2)], {i, 1, n3}]
Do[data3[ii] = Table[{N[M3[i]], N[P3[i]]} /. ρ → 0.01 ii, {i, 1, n3}], {ii, 1, 8}]
```

Drawing of the Interaction Diagrams

In[63]:=
```
P0 = .; t = .; d = .; Mr = .;
Mr = Max[Table[N[M2[i]] /. ρ → 0.08, {i, 1, n2}]];
P0 = ((Ag - ρ Ag) α1 fc + ρ Ag fy) / (fc Ag);
t = -(ρ Ag fy) / (fc Ag);
Do[d[i] =
  ListPlot[Join[{{0, P0}} /. ρ → 0.01 i, data1[i], data2[i], data3[i], {{0, t}} /. ρ → 0.01 i],
   PlotStyle → {Thickness[0.003], Black}, Joined → True], {i, 1, 8}]
Show[{d[1], d[2], d[3], d[4], d[5], d[6], d[7], d[8]}, AspectRatio → 1,
 GridLines → Automatic, GridLinesStyle → Directive[Gray, Dashed], Frame → True,
 PlotRangePadding → 0, PlotRange → {{Mr + 0.01, 0}, {t - 0.05 /. ρ → 0.08, P0 /. ρ → 0.08 + .01}},
 FrameLabel → {"Rn=Mn/fc Ag h", "Kn=Pn/fc Ag"}]
Show[{d[1], d[2], d[3], d[4], d[5], d[6], d[7], d[8]}, AspectRatio → 1,
 GridLines → Automatic, GridLinesStyle → Directive[Gray, Dashed], Frame → True,
 PlotRangePadding → 0, PlotRange → {{Mr + 0.01, 0}, {0, P0 /. ρ → 0.08 + .01}},
 FrameLabel → {"Rn=Mn/fc Ag h", "Kn=Pn/fc Ag"}]
```

Out[68]=

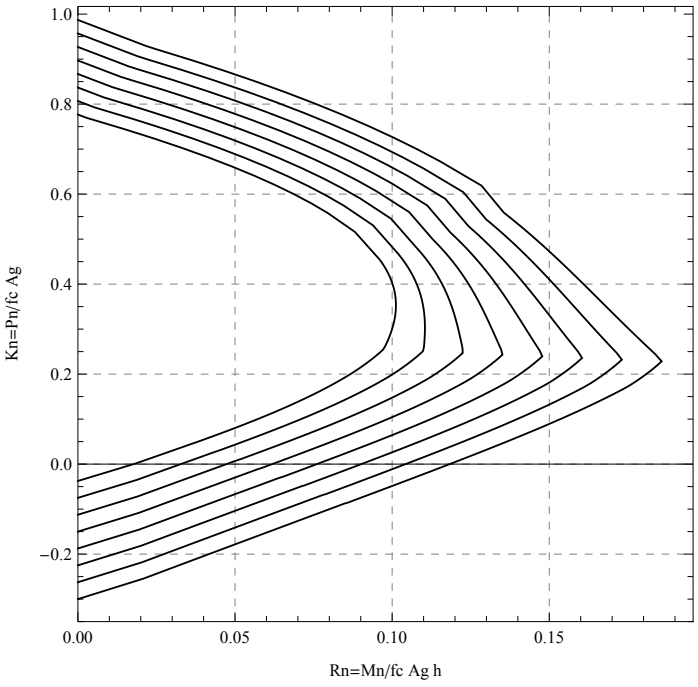

Out[69]=

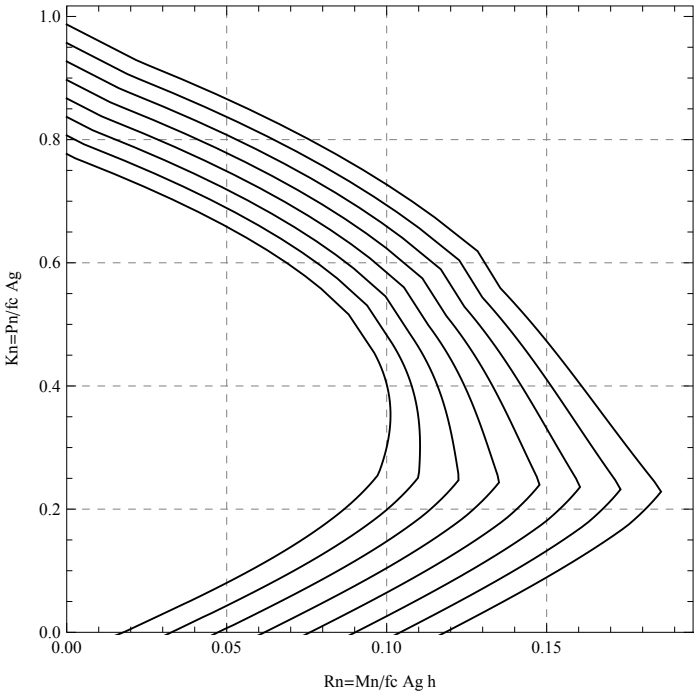

This code was prepared to draw interaction diagrams for uniaxial rectangular reinforced concrete columns with steel distributed uniformly and continuously on the four faces of the column cross section.

Input Material and Geometric Properties of the column cross section here

In[1]:=
```
ClearAll["Global`*"]
γ = 0.79;
fy = 60;(*ksi*)
fc = 14;(*ksi*)
n1 = 50;
n2 = 50;
n3 = 20;
ρ =.; b = 1; h = 1; α1 =.; β1 =.;
εcu = 3/1000;  Es = 29000; εy = fy/Es;
If[fc ≤ 12, α1 = 85/100]
If[12 < fc ≤ 23, α1 = 0.96588 - 0.0019858 fc * 1000/145]
If[fc > 23, α1 = 65/100]
If[fc ≤ 4, β1 = 85/100]
If[4 < fc ≤ 8, β1 = 85/100 - 5/100 (fc - 4)]
If[8 < fc ≤ 12, β1 = 65/100]
If[12 < fc < 18.6, β1 = 0.8033 - 0.001195 fc * 1000/145]
If[fc ≥ 18.6, β1 = 0.65]
As1 = As3 = ρ b h/4;
As2 = ρ b h/2;
```

Out[4]= $Null^2$

Out[10]= 0.774148

Out[15]= 0.687921

Region 1 on the interaction diagram where $c \geq \frac{h}{2}(1+\gamma)$

In[19]:=
```
c = .; εs1 = .; εs3 = .; Fs1 = .; Fs2 = .; Fs3 = .; Fc = .; fs3 = .;
y1 = .; ε = .; P2 = .; M2 = .; P = .; M = .; ρ = .; i = .; Mc = .;
mc2 = .; mt2 = .; Fsc2 = .; Fst2 = .; Fs = .;
Do[c[i] = h, {i, 1, 1}]
Do[c[i] = (0.04 i + 1) h, {i, 2, n1}]
Do[{εs1[i] = εcu/c[i] (c[i] - h/2 (1 + γ)), εs3[i] = εcu/c[i] (c[i] - h/2 (1 - γ))}, {i, 1, n1}]
Do[ε[i] = εcu/c[i] (c[i] - x), {i, 1, n1}]
Do[If[β1 c[i] > h, Fc[i] = α1 fc b h, Fc[i] = α1 fc b β1 c[i]], {i, 1, n1}]
Do[If[β1 c[i] > h, Mc[i] = 0, Mc[i] = α1 fc b β1 c[i] ((h - β1 c[i])/2)], {i, 1, n1}]
Do[If[εs1[i] ≥ εy, fs1[i] = fy, fs1[i] = εs1[i] Es], {i, 1, n1}]
Do[If[εs3[i] ≥ εy, fs3[i] = fy, fs3[i] = εs3[i] Es], {i, 1, n1}]
Do[Fs1[i] = As1 (fs1[i] - α1 fc), {i, 1, n1}]
Do[Fs3[i] = As3 (fs3[i] - α1 fc), {i, 1, n1}]
Do[{sol = Solve[ε[i] == εy, x], x1[i] = x /. sol[[1]]}, {i, 1, n1}]
Do[If[x1[i] ≤ h/2 (1 - γ),
  Fsc2[i] = As2/(γ h) (NIntegrate[(ε[i] Es - α1 fc), {x, h/2 (1 - γ), γ h}])], {i, 1, n1}]
Do[If[x1[i] > h/2 (1 - γ) && x1[i] ≤ h/2 (1 + γ),
  Fsc2[i] = As2/(γ h) (NIntegrate[(εy Es - α1 fc), {x, h/2 (1 - γ), x1[i]}] +
      NIntegrate[(ε[i] Es - α1 fc), {x, x1[i], γ h}])], {i, 1, n1}]
Do[If[x1[i] > h/2 (1 + γ), Fsc2[i] = As2 fy], {i, 1, n1}]
Do[If[x1[i] ≤ h/2 (1 - γ),
  mc2[i] = As2/(γ h) (NIntegrate[(ε[i] Es - α1 fc) (h/2 - x), {x, h/2 (1 - γ), γ h}])], {i, 1, n1}]
Do[If[x1[i] > h/2 (1 - γ) && x1[i] ≤ h/2 (1 + γ),
  mc2[i] = As2/(γ h) (NIntegrate[(εy Es - α1 fc) (h/2 - x), {x, h/2 (1 - γ), x1[i]}] +
      NIntegrate[(ε[i] Es - α1 fc) (h/2 - x), {x, x1[i], γ h}])], {i, 1, n1}]
Do[If[x1[i] > h/2 (1 + γ), mc2[i] = 0], {i, 1, n1}]
Do[{mt2[i] = 0, Fst2[i] = 0}, {i, 1, n1}]

Do[{Fs2[i] = Fst2[i] + Fsc2[i],
  Fs[i] = Fs3[i] + Fs2[i] + Fs1[i], P[i] = Fc[i] + Fs[i]}, {i, 1, n1}]
```

```
Do[M[i] = (-Fs1[i] + Fs3[i]) (γ h / 2) + Mc[i] + mc2[i] + mt2[i], {i, 1, n1}]
Do[P1[i] = FullSimplify[P[i] / (fc b h)], {i, 1, n1}]
Do[M1[i] = FullSimplify[M[i] / (fc b h^2)], {i, 1, n1}]
Do[data1[ii] = Reverse[Table[{N[M1[i]], N[P1[i]]} /. ρ → 0.01 ii, {i, 1, n1}]], {ii, 1, 8}]
```

Region 2 on the interaction diagram where $\frac{h}{2}(1-\gamma) < c < \frac{h}{2}(1+\gamma)$

In[44]:=

```
c = .; ϵs1 = .; ϵs3 = .; Fs1 = .; Fs2 = .; Fs3 = .; Fc = .;
fs3 = .; y1 = .; ϵ = .; P2 = .; M2 = .; P = .; M = .; ρ = .; i = .;
mc2 = .; mt2 = .; Fsc2 = .; Fst2 = .; Fs = .;
Do[c[i] = h/2 (1 + γ) - (i - 1)/n2 γ h, {i, 1, n2}]
Do[ϵ[i] = ϵcu (x - h/2 (1 + γ)) / c[i] + ϵcu, {i, 1, n2}]
Do[{ϵs1[i] = ϵcu/c[i] (h/2 (1 + γ) - c[i]), ϵs3[i] = ϵcu/c[i] (c[i] - h/2 (1 - γ))}, {i, 1, n2}]
Do[Fc[i] = α1 fc b β1 c[i], {i, 1, n2}]
Do[If[ϵs1[i] ≥ ϵy, fs1[i] = fy, fs1[i] = ϵs1[i] Es], {i, 1, n2}]
Do[If[ϵs3[i] ≥ ϵy, fs3[i] = fy, fs3[i] = ϵs3[i] Es], {i, 1, n2}]
Do[Fs1[i] = As1 (fs1[i]), {i, 1, n2}]
Do[Fs3[i] = As3 (fs3[i] - α1 fc), {i, 1, n2}]
Do[{sol = Solve[ϵ[i] == ϵy, x], x1[i] = x /. sol[[1]]}, {i, 1, n2}]
Do[{sol = Solve[ϵ[i] == -ϵy, x], x2[i] = x /. sol[[1]]}, {i, 1, n2}]
Do[If[ϵs3[i] > ϵy, Fsc2[i] = As2/(γ h) (NIntegrate[(ϵy Es - α1 fc), {x, x1[i], γ h}] +
      NIntegrate[(ϵ[i] Es - α1 fc), {x, h/2 (1 + γ) - c[i], x1[i]}]),
   Fsc2[i] = As2/(γ h) NIntegrate[(ϵ[i] Es - α1 fc), {x, h/2 (1 + γ) - c[i], γ h}]], {i, 1, n2}]
Do[If[ϵs1[i] > ϵy, Fst2[i] = As2/(γ h) (NIntegrate[(-ϵy Es), {x, 0, x2[i]}] +
      NIntegrate[(ϵ[i] Es), {x, x2[i], h/2 (1 + γ) - c[i]}]),
   Fst2[i] = As2/(γ h) (NIntegrate[(ϵ[i] Es), {x, 0, h/2 (1 + γ) - c[i]}])], {i, 1, n2}]
Do[{Fs2[i] = Fst2[i] + Fsc2[i], Fs[i] = Fs3[i] + Fs2[i] - Fs1[i], P[i] = Fc[i] + Fs[i]},
 {i, 1, n2}]

Do[If[ϵs3[i] > ϵy, mc2[i] = As2/(γ h) (NIntegrate[(ϵy Es - α1 fc) (x - γ h/2), {x, x1[i], γ h}] +
      NIntegrate[(ϵ[i] Es - α1 fc) (x - γ h/2), {x, h/2 (1 + γ) - c[i], x1[i]}]),
```

```
mc2[i] = As2/(γ h) NIntegrate[(ϵ[i] Es - α1 fc) (x - γ h/2), {x, h/2 (1 + γ) - c[i], γ h}]], {i, 1, n2}]

Do[If[ϵs1[i] > ϵy, mt2[i] = As2/(γ h) (NIntegrate[(-ϵy Es) (x - γ h/2), {x, 0, x2[i]}] +
      NIntegrate[(ϵ[i] Es) (x - γ h/2), {x, x2[i], h/2 (1 + γ) - c[i]}]),
   mt2[i] = As2/(γ h) (NIntegrate[(ϵ[i] Es) (x - γ h/2), {x, 0, h/2 (1 + γ) - c[i]}])], {i, 1, n2}]

Do[M[i] = (Fs1[i] + Fs3[i]) (γ h/2) + Fc[i] ((h - β1 c[i])/2) + mc2[i] + mt2[i], {i, 1, n2}]

Do[P2[i] = FullSimplify[P[i]/(fc b h)], {i, 1, n2}]

Do[M2[i] = FullSimplify[M[i]/(fc b h^2)], {i, 1, n2}]

Do[data2[ii] = Table[{N[M2[i]], N[P2[i]]} /. ρ → 0.01 ii, {i, 1, n2}], {ii, 1, 8}]
```

Region 3 on the interaction diagram where $0 < c \le \frac{h}{2}(1-\gamma)$

In[65]:=
```
c = .; ϵs1 = .; ϵs3 = .; Fs1 = .; Fs2 = .; Fs3 = .; Fc = .;
fs3 = .; y1 = .; ϵ = .; P3 = .; M3 = .; P = .; M = .; ρ = .; i = .;
mc2 = .; mt2 = .; Fsc2 = .; Fst2 = .; Fs = .;
Do[c[i] = h/2 (1 - γ) - (i - 1)/n3 * 5/12 * (h/2 (1 - γ)), {i, 1, n3}]
Do[{ϵs1[i] = ϵcu/c[i] (h/2 (1 + γ) - c[i]), ϵs3[i] = ϵcu/c[i] (h/2 (1 - γ) - c[i])}, {i, 1, n3}]
Do[ϵ[i] = ϵcu (h/2 (1 + γ) - x - c[i])/c[i], {i, 1, n3}]
Do[Fc[i] = α1 fc b β1 c[i], {i, 1, n3}]
Do[If[ϵs1[i] ≥ ϵy, fs1[i] = fy, fs1[i] = ϵs1[i] Es], {i, 1, n3}]
Do[If[ϵs3[i] ≥ ϵy, fs3[i] = fy, fs3[i] = ϵs3[i] Es], {i, 1, n3}]
Do[Fs1[i] = As1 (fs1[i]), {i, 1, n3}]
Do[Fs3[i] = As3 (fs3[i]), {i, 1, n3}]
Do[{sol = Solve[ϵ[i] == ϵy, x], x2[i] = x /. sol[[1]]}, {i, 1, n3}]
Do[Fsc2[i] = 0, {i, 1, n3}]
Do[If[x2[i] < γ h,
  Fst2[i] = As2/(γ h) (NIntegrate[(ϵy Es), {x, 0, x2[i]}] + NIntegrate[(ϵ[i] Es), {x, x2[i], γ h}]),
  Fst2[i] = As2/(γ h) (NIntegrate[(ϵ[i] Es), {x, 0, γ h}])], {i, 1, n3}]
Do[{Fs2[i] = -Fst2[i] + Fsc2[i], Fs[i] = -Fs3[i] + Fs2[i] - Fs1[i], P[i] = Fc[i] + Fs[i]},
 {i, 1, n3}]
Do[mc2[i] = 0, {i, 1, n3}]
Do[If[x2[i] < γ h, mt2[i] = As2/(γ h) (NIntegrate[(-ϵy Es) (x - γ h/2), {x, 0, x2[i]}] +
      NIntegrate[-(ϵ[i] Es) (x - γ h/2), {x, x2[i], γ h}]),
  mt2[i] = As2/(γ h) (NIntegrate[-(ϵ[i] Es) (x - γ h/2), {x, 0, γ h}])], {i, 1, n3}]
Do[M[i] = (Fs1[i] - Fs3[i]) (γ h/2) + Fc[i] ((h - β1 c[i])/2) + mc2[i] + mt2[i], {i, 1, n3}]
Do[P3[i] = FullSimplify[P[i]/(fc b h)], {i, 1, n3}]
Do[M3[i] = FullSimplify[M[i]/(fc b h^2)], {i, 1, n3}]
Do[data3[ii] = Table[{N[M3[i]], N[P3[i]]} /. ρ → 0.01 ii, {i, 1, n3}], {ii, 1, 8}]
```

Drawing of the Interaction Diagrams

In[93]:=
```
P0 = .; t = .; d = .; Mr = .;
Mr = Max[Table[N[M2[i]] /. ρ → 0.08, {i, 1, n2}]];
P0 = ((Ag - ρ Ag) α1 fc + ρ Ag fy) / (fc Ag);
t = -(ρ Ag fy) / (fc Ag);
Do[d[i] =
  ListPlot[Join[{{0, P0}} /. ρ → 0.01 i, data1[i], data2[i], data3[i], {{0, t}} /. ρ → 0.01 i],
   Joined → True, PlotStyle → {Thickness[0.003], Black}], {i, 1, 8}]
Show[{d[1], d[2], d[3], d[4], d[5], d[6], d[7], d[8]}, AspectRatio → 1,
 GridLines → Automatic, GridLinesStyle → Directive[Gray, Dashed], Frame → True,
 PlotRangePadding → 0, PlotRange → {{Mr + 0.01, 0}, {t - 0.05 /. ρ → 0.08, P0 /. ρ → 0.08 + .01}},
 FrameLabel → {"Rn=Mn/fc Ag h", "Kn=Pn/fc Ag"}]
Show[{d[1], d[2], d[3], d[4], d[5], d[6], d[7], d[8]}, AspectRatio → 1,
 GridLines → Automatic, GridLinesStyle → Directive[Gray, Dashed], Frame → True,
 PlotRangePadding → 0, PlotRange → {{Mr + 0.01, 0}, {0, P0 /. ρ → 0.08 + .01}},
 FrameLabel → {"Rn=Mn/fc Ag h", "Kn=Pn/fc Ag"}]
```

Out[98]=

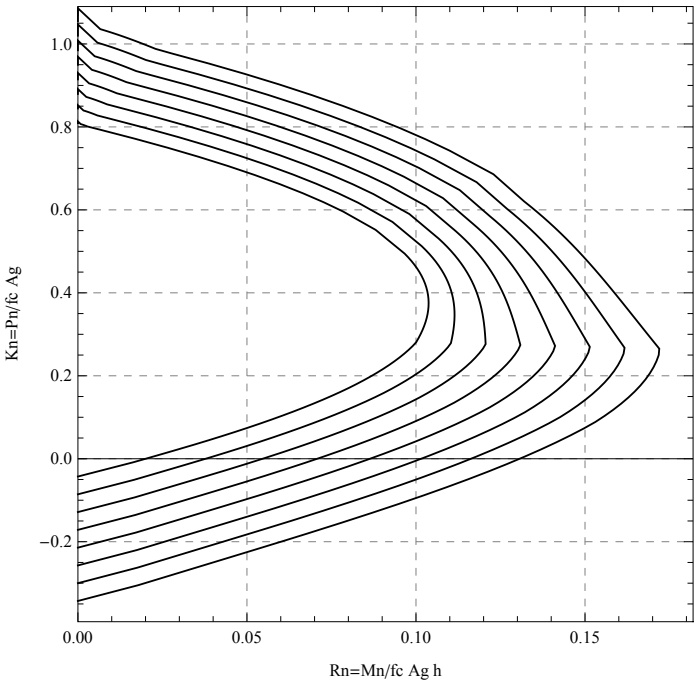

Out[99]=

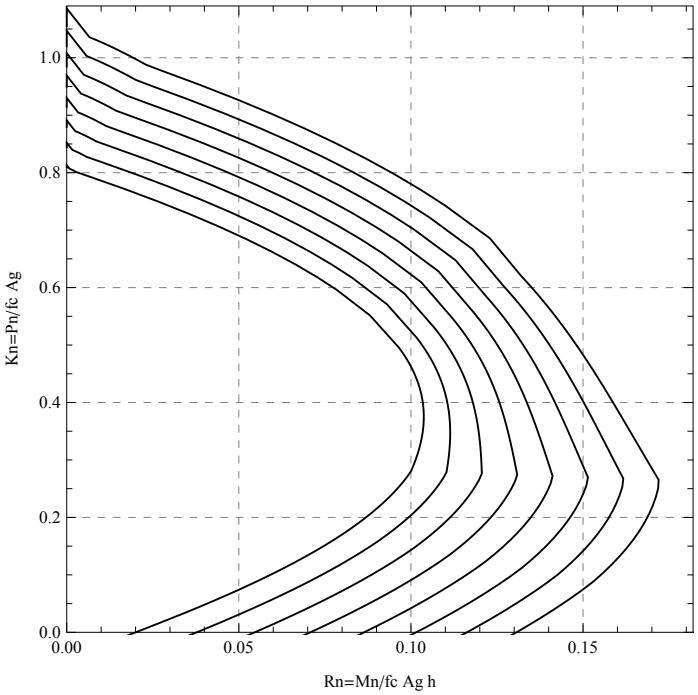

VITAE

Name : Nizar Abdul-Hamid Yousef Assi

Nationality : Palestinian

Date of Birth : 11/Jan/1990

Email : nizar97eng@hotmail.com

Address : KFUPM, Dhahran, Saudi Arabia, T.L:+966 55 494 3247

Academic Background : Civil Engineering

- Graduated from Birzeit University with B.Sc. degree in civil engineering in 2012 with **Distinction grade (86%)**, Department of Civil Engineering, West Bank, Palestine. (Received Honor Awards in most semester in BS program)
- Received a **scholarship** from Hani Qaddumi Scholarship Foundation (HQSF) in Palestine to study the BS degree at Birzeit University in 2008.
- Received a **scholarship** from King Fahd University for Petroleum and Minerals (KFUPM) in 2011 to study the MS degree at KFUPM.

- MS (Civil Engineering - Structure) from King Fahd University for Petroleum and Minerals (KFUPM), May 2015, **GPA (3.94/4)**